공학석사 학위논문

A Study on the Range Prediction and Optimization of Punch Edge Shape for the Strengthening Piercing Punches by Using 3D Printing AM Technology and the Partial Semi-Additive Method

3D 프린팅 AM 기술과 부분적 세미-적층 기법을 이용한 피어싱 펀치 강화를 위한 펀치 에지 형상의 범위 예측 및 최적화에 관한 연구

울산대학교 대학원

기계자동차공학과

왕시량

3D 프린팅 AM 기술과 부분적 세미-적층 기법을 이용한 피어싱 펀치 강화를 위한 펀치 에지 형상의 범위 예측 및 최적화에 관한 연구

지도교수 양 순 용

이 논문을 공학석사 학위 논문으로 제출함

2020 년 02 월

울산대학교 대학원

기계자동차공학과

왕시량

A Study on the Range Prediction and Optimization of Punch Edge Shape for the Strengthening Piercing Punches by Using 3D Printing AM Technology and the Partial Semi-Additive Method

Advisor: Professor Soon Yong Yang

Submitted to the Office of Graduate School of
University of Ulsan
In partial Fulfillment of the Requirements for the Degree of

Master of Science

By

SHILIANG WANG

School of Mechanical Engineering
University of Ulsan
Ulsan, Republic of Korea
February 2020

왕시량의 공학 석사학위 논문을 인준함

심사위원 염 영 진 인

심사위원 주 석 재 인

심사위원 양 순 용 인

울산대학교 대학원

2020 년 02 월

A Study on the Range Prediction and Optimization of Punch Edge Shape for the Strengthening Piercing Punches by Using 3D Printing AM Technology and the Partial Semi-Additive Method

This certifies that the master's thesis of SHILIANG WANG is approved by

Committee Chair Prof. Young Jin Yum

Committee Member Prof. Seok Jae Chu

Committee Member Prof. Soon Yong Yang

ACKNOWLEDGEMENTS

The completion of the thesis is attributed to many peoples support and encouragement.

Sincerely, I am very grateful to my professors for guidance, Prof. Young Jin Yum Prof. Yong Seok Kim Prof. Soon Yong Yang. Their conscientious academic spirit and modest, open-minded personality inspire me both in academic study and daily life.

Second, I am honored to meet the brothers in our laboratory.

Last but not least, I would like to express my special thanks to my parents(JianQiang Wang & YongMei Chen) and my wife(YuWei Zhu), whose care and support motivate me to move on and make me want to be a better person.

ABSTRACT

In this paper describe the fabrication of high strength punch molds that can be applied to ultra-high strength sheet material after processing. A method of improving the strength of the punching die by means of additive manufacturing (AM) of a high strength powder material using a metal 3D printer has been proposed. Further, a semi-additive manufacture technique has been proposed to increase the punch strength through partial additive manufacturing of local parts of the punch requiring high strength. A preprocessing process for predicting the semi-additive shape for the punch function portion is proposed for application of AM technology of the metal 3D printer to this semi-additive technique. The preprocessing process for determining the semi-additive shape consists of predicting the step of the punch strength based on the shear process of the sheet material, analyzing the stress distribution of the punch, defining the semi-additive range, designing the semi-additive shape and verifying the additive interface strength and durability of the semi-additive shape. The main factor affecting the measurement of influence during the hole process is the thickness of the plate, while the effect of material and speed (above a certain level) is unknown. During the machining process, the maximum point of reaction force appears on the sidewall of the wall, resulting in a horizontal force, which is the cause. Make sure the half sample shape (depth/height) detected in this study is in the range of 2-3 mm. The flat shape is the final shape, and the following shape shows that it has a 45 ° line shape compared to a triangle with the triangular face shape. Thus, in the case of a rectangular cross-section with the interface added vertically, separation from the

interface has been shown to cause separation by adding as many layers as possible in the depth direction of the punch. It is advantageous In selecting such a semi-additional shape, it has been confirmed that larger additional areas can lead to more slipping or separation, while complex shapes are more easily exposed to folds. It can be used to extend the life of semi-additives. The shape and the range determined in the simulation process define a semi-additive area (volume) for the 3D printing AM technique using a high-strength powder material, and a semi-additive punch was manufactured according to the defined area (volume). The semi-additive mold manufacturing technology based on a partial additive technique presented in this paper is expected to greatly benefit the maintenance of the punch by manufacturing the punch in a special field requiring high strength or by regenerating a punch mold that is discarded after a certain period of use.

Furthermore, regeneration of a high strength punch can be achieved through semi-additive techniques in a relatively low-strength punch that would have been discarded. Therefore, the proposed technology can compensate for productivity and price challenges encountered when manufacturing punching dies using AM technologies such as the current metal 3D printer. If the cost problem can be solved in the future ,this technology will be used in a wide range.

Keywords: Punch strength analysis, Punch stress distribution analysis, Semi-additive range selection, Semi-additive Shape Design, Verification the semi-additive shape strength, Semi-additive punch manufacture

CONTENTS

Chapter 1 Introduction

Nowadays, the vehicle lightweight technology requires ultrahigh strength parts that become stronger, which could maintain high safety with only a small amount of materials and minimize the manufacturing cost. It is mainly applied to the field of the vehicle body, as introduced in **Fig 1.1** [1]. At the same time, the lighter weight of vehicle components also increases fuel efficiency, which reduces emissions and protects the environment. For the lightweight of the vehicle, the ultra-high-strength steels played a leading role in the automotive production.

Fig. 1.1 High strength components of the vehicle

The post manufacturing process of an ultra-high-strength steel sheet such as a hot stamping part manufacturing process, mold damage has become the biggest problem. Mold damage can lead to inaccurate machining, In order to solve this problem, the

current factory uses a laser process. But the high cost of laser equipment and the production is low, efficiency is still a problem. Due to the laser cutting limitation of laser power and equipment volume, laser cutting can only cut medium and small thickness plates and tubes, and the cutting speed decreases significantly as the thickness of the workpiece increases. Laser cutting equipment costs a lot, one-time investment is big. Another solution is to use mold surface treatment. The cost with small burden, but the deep and strong heat treatment will cause the mold chipping, This will also affect the machining accuracy [2]. So, in view of the development of additive manufacturing technology and the existing achievements, researchers try to use different metal powders and different manufacturing methods to improve the mold's mechanical properties and wear resistance [3-5].

1.1 Hot stamping & Problems encountered

Currently, the automotive sector is in need for lighter and stronger materials. Lightweight and sturdy is now the primary technical indicator. A technical approach to this is hot stamping molding technology. Hot stamping molding is technically preferred, but there are difficulties in post-processing (piercing or trimming process), cost, time and space. This is because the post-processing of hot stamping is mostly performed by the laser process. At the production site, many efforts have been made to convert these laser processes into press processes. However, a press process that requires a strengthened post-processing mold has not yet been achieved due to technical limitations. After hot stamping, conversion from the laser process to the

press process must be accompanied by more advanced mold strengthening technology.

1.2 Hot stamping punch abrasion Cause Analysis.

In the hot stamping process, parts with increased strength cause damage to the mold due to strong reaction forces generated in the material, high stress occurs at the moment the punch starts processing, Stress is not just in the vertical direction of processing There is also large transient stress in the horizontal direction. This is one of the main reasons for the damage of the punch. thus reducing the surface quality and dimensional accuracy of the product and shortening the life of the mold, in particular, since the strength of the material increases, and excessive scratches are generated on the surface of the mold and the material, the adhesion phenomenon due to the high surface pressure applied to the mold during the molding process is called abrasion. (adhesion of high pressure on the surface, resulting in scratches) [1, 2]. Damage of the shear punch mold in the press process includes chip-ping, cracking, gross fracture, and galling. Such damage is caused by the incongruity of hardness toughness and abrasion resistance of the mold material.

1.3 Existing solution & problem.

The surface strengthening treatment method mainly used by the factory at this stage is method of applying a heat treatment or a nitriding treatment to the surface of a punch mold and then performing a surface treatment (coating) for generating a surface

layer of another element or a heat treatment is mainly applied to solve such problems. Nitriding treatment refers to a chemical heat treatment process in which nitrogen atoms are infiltrated into the surface layer of a workpiece in a certain medium at a certain temperature. The nitrided article has excellent wear resistance, fatigue resistance, corrosion resistance and high temperature resistance. Although high hardness and high wear resistance are obtained after nitriding, the hardened layer is also very brittle. The heat treatment generally does not change the shape of the workpiece and the overall chemical composition, but imparts or improves the performance of the workpiece by changing the microstructure inside the workpiece or changing the chemical composition of the surface of the workpiece. It is characterized by improved intrinsic quality of the workpiece Surface treatment is not a fundamental solution because deeper coatings require a higher cost, and deep, strong heat treatments increase the probability of chipping. these solutions are not the best, can't solve the problem completely.

1.4 Punch strengthening study using Additive manufacturing technique

Although mold strengthening technology involves various classical technologies, the field of mold strengthening has recently been revived with the advent of metal 3D printing technology [3-5]. Many studies have been carried out for metal mold manufacturing and mold reinforcement used in the cold press forming process using

metal 3D printing DED (Direct Energy Deposition) technology. Metal 3D printing DED technology Spray metal powder directly onto the focus of the laser to form a molten pool for printing.

1.5. The research process of strengthening punch with the Semi-additive technique

The research process of this study is as follows **(Fig. 2.1)**. As described in the foregoing, the methods commonly used in the post-treatment of metal parts on heat-treated factories are laser cutting and punch punching. However, the limitations of lasers are too large and the cost is high, so punching with punches is currently the solution. Then a high-strength die is required, which requires high hardness, high toughness, and high wear resistance to be used in actual production. In the design of the punch reinforcement, a metal 3D printed DED semi-additive method is used to reinforce the punched punch. The DED method has been selected among various methods of metal 3D printing. The full name of this method is direct energy deposition (the specific description will be described below). The definition of the semi-additive method is the semi-additive method is considered.

The property of a material, a multilayer additive process in which one or more materials are used to additive the desired material to the desired part with a certain thickness. With this method, a hardened layer of the punch surface and an intermediate buffer layer can be formed. It can make the punch meet the design

requirements. In the selection of punching materials, the properties of steel HWS powder with high toughness and high wear resistance are selected to meet the design requirements of punch strengthening. The punching process is then simulated to determine the stress concentration range of the stresses experienced by the punch during processing. This range is a stress distribution analysis based on the stamping strength analysis of the sheet. After determining the stress range, the design of the semi- additive shape was started, and the shape of the design was simulated, and the shape analysis was performed by various stacked shapes and simulations.

After analyzing the knot, the comparison data and the result analysis compare the differences of the respective shapes, confirm the most suitable semi- additive assembly shape, and after determining the additive shape, actually manufacture the punch using the determined shape, firstly, the additive part processing.

After the processing is completed, the additive is performed, and after the additive process is completed, the heat treatment process is performed, and after the completion of the above process, the final processing is completed to complete the manufacture of the punch. After the completion of the manufacturing, the punches and the original unreinforced punches were reinforced with a newly-made additive process for the durability test, and the results were analyzed (SKD11 punch and HWS semi- additive reinforced punch).The test results were compared after the comparison test and analyzed.

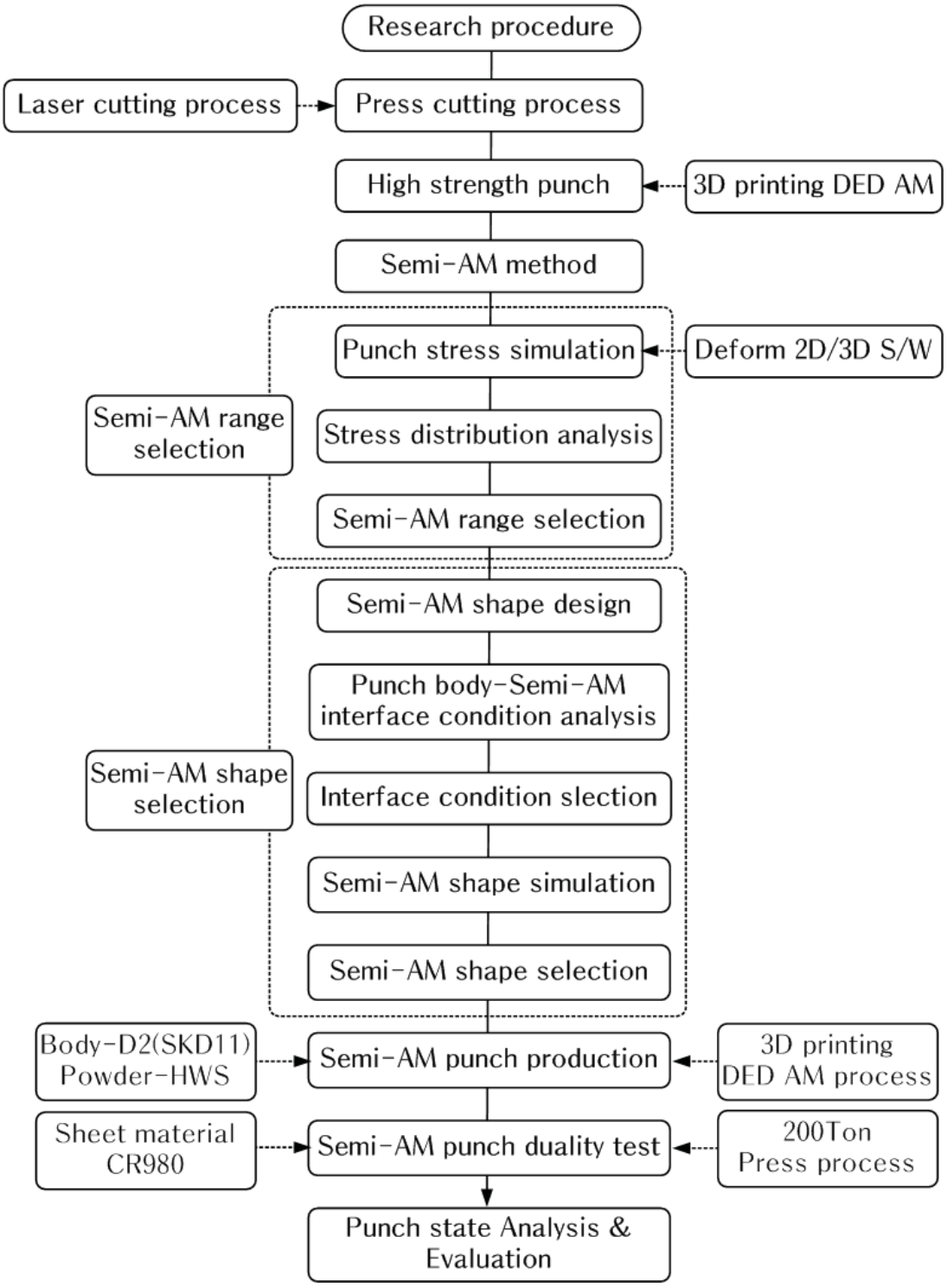

Fig. 1.2 The research process of strengthening punch with the Semi-additive technique

Chapter 2. Punch Strength Prediction and Semi-additive Shape Simulation

In this study, Determined the punch strength required for the shearing (piercing) of **CP1180** (1200MPa class) and **22MnB5** (1500MPa class) parts of high strength sheet material and the stress distribution concentrated on the punch with the intention of using partial additive (Semi-Additive) 3D printing to strengthen the punch. In other words, by predicting the width and depth of the portion where the stress is concentrated, increase the strength of the punch by predicting the shape range of the punch that affects the punch shear action. An analytical simulation for predicting punch strength was performed based on high strength sheet piercing process variables. The condition and range of the process analysis were analyzed based on previous research literature on shear mechanisms and a process analysis of the sheet material. The simulation processor for the punch, strengthening in the stress concentration part can achieve the best strengthening effect using AM technology in the smallest range.

2.1 Simulation Overview

The commercial code DEFORM 2D was used for punch shear process analysis. The DEFORM code implements the processes of shearing and propagating the material geometrically so that it is similar to a real-world scenario. When the fracture critical value at which the fracture occurs in the material is reached (as an implementation method for the shearing process), the elements of the sheared portion

are deleted. This requires defining the number of elements required for visual processing and knowing the ductile fracture value at which shear (fracture) occurs, which is a characteristic of the material. To realize a precise shearing mechanism that is close to the actual one, it is necessary to generate a dense mesh in the shear portion, and a high level of software expertise is required. Previous studies have shown that these values (element number, ductile fracture value, mesh density) are difficult to generalize depending on the material and are determined by experimental values and repeated analytical values. Therefore, optimization of these values requires a process of finding the required value by comparing the experimental and numerical values based on the shape of the specimen, and then repeating the analysis for different target materials [15].

However, in the present study, the fracture critical value (critical damage value) for high-strength sheet materials was selected from previous literature [25-26]. Fracture critical values based on Cockcroft and Latham for sheet materials CP1180 and 22MnB5 were 1.1 (cold work) and 0.48 (cold work)/2.28 (hot work), respectively.

In addition, The DEFORM code uses plastic flow data as the basis of the simulation, so that the flow stress curve data for the target sheet material is required. These flow stress data can be collected from a variety of sources, but are provided only as reference data, so material testing is essential to obtain data on specific application fields. The s-s curve data obtained from the test must be compensated for when apply it to the simulation analysis [14].

2.2 Simulation process

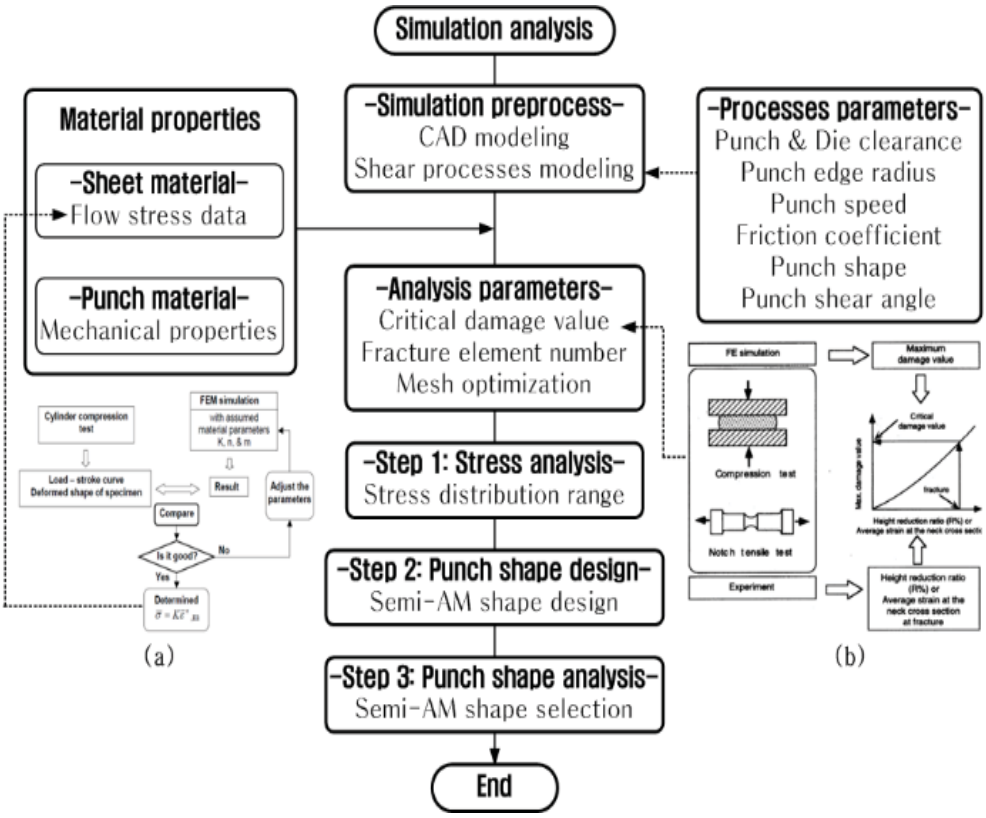

Fig. 2.1. Simulation processor for punch strength prediction: (a) Interpolation of flow stress data [14], (b) calculation of the critical damage value [15].

In this study, determined the punch strength required for the shearing (piercing) of CP1180 (1200MPa class) and 22MnB5 (1500MPa class) parts of high strength sheet material and the stress distribution concentrated on the punch with the intention of using partial additive (semi-additive) 3D printing to strengthen the punch. In other words, by predicting the width and depth of the portion where the stress is concentrated, increase the strength of the punch by predicting the shape range of the punch that affects the punch shear action. An analytical simulation for predicting punch strength was performed based on high strength sheet piercing process variables. The condition and

range of the process analysis were analyzed based on previous research literature on shear mechanisms and a process analysis of the sheet material. The simulation processor for the punch strength required for the high-strength part piercing process introduced in this study is shown in **Fig. 2.1.**

The process parameters affecting the results of the piercing analysis are sheet material thickness, punch diameter, punch corner radius, holder diameter, die diameter, stripper force, punch speed, friction coefficient, and punch and die clearance. The main process variable is the clearance between the punch and the die. Long industry experience has shown that the clearance between punch and die should be 5% of the sheet material lateral thickness. However, the clearance is determined by the thickness of the sheet material, the tensile strength and the material type. It is also determined by the requirements of a specific operation. In this study, the process parameters were analyzed and selected from the literature related to high-strength sheet material shear analysis [16, 27]. The clearance for high-strength sheet material **CP1180** is reported to be 10-18% of the sheet thickness, a punch speed of 50 mm/sec, and a punch corner radius of 0.005-0.03 mm.

2.2 Simulation object punch spec

Specification the top die's thickness is 8mm, the total length of the punch is 50mm, the upper and lower clamps of the plate are 5mm thick, thickness of the sheet is 1.2mm, the working part of the punch (actually involved in the punching part) is a cylinder with a radius of 5 mm and a length of 13 mm. The head of the punch has a chamfer R Above this part is a cylinder with a radius of 6.5mm and a length of 28.429mm. The upper and lower parts of this part are R 10mm and 0.5mm round.

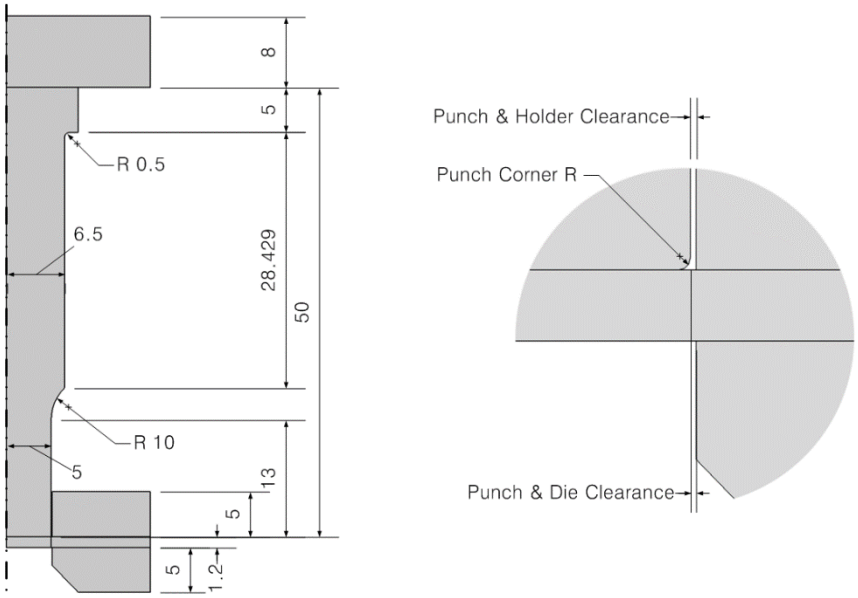

Fig. 2.2 Punch specification for simulation analysis

There will be clearance between the punch and the holder & die of the plate. If the clearance is too large, the burr of the stamped workpiece is relatively large, and the punching quality is poor. If the clearance is small, although the quality of the punching is good, the wear of the mold is serious, the service life of the mold is greatly reduced, and the break of the punch is easily caused. If the clearance is too large or too small, it is easy to cause adhesion on the punch material, thereby causing the material to be taken during the stamping. Too small a clearance easily creates a vacuum between the bottom surface of the punch and the sheet material and a scraping of the scrap occurs. Reasonable clearance can extend the life of the mold, good discharge effect, reduce burrs and flanging, keep the plate clean, hole diameter will not scratch the plate, reduce the number of sharpening, keep the plate straight, and accurately punch the hole.

2.3 Selection of piercing process parameters

A Two-Dimensional plane strain model was used for this piercing process analysis, and the conceptual parameter schematic for piercing process analysis are shown in **Fig. 2.2** Sheet materials required for the process analysis had a tensile strength of 1200 MPa (**CP1180**: Complex Phase steel) and a 1500 MPa grade (**22MnB5**: Boron steel). The sheet material thickness was 1.2 mm.

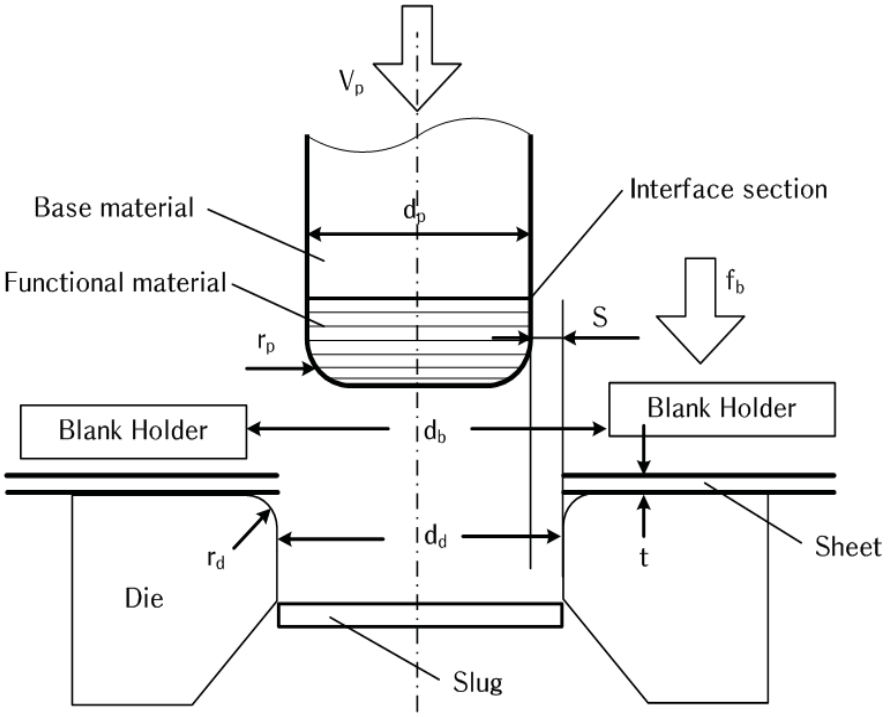

Fig. 2.2 Two-Dimensional schematic of the piercing process

The punching process analysis was performed based on the above description. The process analysis results showed that the optimal process parameters required for punch strength prediction simulation was selected, and these process parameters are summarized in **Table 2.1** In addition, a simulation analysis of piercing strength required for the piercing shear of high strength sheet materials CP1180 and 22MnB5 was performed using the simulation analysis processor and the selected piercing

process analysis conditions for predicting the piercing punch strength.

Table 2.1 Process parameters selected for punch strength prediction simulation

Parameter		Value
Sheet material	Material	CP1180/ 22MnB5 Boron steel
	Thickness 't'	1.2 mm
	Flow stress curve data	$\bar{\sigma} = 1605 \cdot \epsilon^{0.07}$ MPa $\bar{\sigma} = 2178.2 \cdot \epsilon^{0.103}$ MPa
	Fracture critical value	1.1
Punch diameter 'd_P'		10.0 mm
Punch corner radius 'r_P'		0.01~0.02 mm
Stripper diameter 'd_b'		10.06 mm
Die diameter 'd_d'		10.12 mm ($dp + 2S$)
Die corner radius 'γ_d'		0.01~0.02 mm
Stripper pressure ('f_b' /area)		Various conditions MPa
Punch base material		SKD11(D2)
Punch functional material		HWS, M4, CPM4
Punch velocity 'v_p'		50 mm/sec
Coefficient of friction		0.12 Shear Friction
Punch & die clearance 'S'		0.02mm (7%t)

2.4 Material properties

The punch material was applied to the substrate material of the general cold material SKD11 (D2) punch, and the mechanical properties of the sheet material for the process analysis applied to it were analyzed using previous research documents, as summarized

in Table 2.2. The physical properties of the sheet material differ depending on the source and literature. This means that material testing and interpretation must be performed together for accurate interpretation.

Required value by comparing the experimental and numerical values based on the shape of the specimen, and then repeating the analysis for different target materials [15].

Table 2.2 Mechanical properties of sheet and punch materials for analysis simulation

Material	YM(E) [GPa]	YS [MPa]	TS [MPa]	PR	CDV	Remark [Ref]
Sheet CP1180	210.0	951.51	1241.99	-	1.1(cold)	[16]-[18]
Sheet 22MnB5	212.0	1010.0	1500.0	-	2.28(hot) 0.48(cold)	[19]-[24]
Punch SKD11	207.0		2181.0	0.29	-	Experiment
Punch HWS	198.0	2303.0	2715.0	0.298	-	Experiment
Punch M4	214.0	-	-	0.3	-	MatWeb

However, in the present study, the fracture critical value (critical damage value) for high-strength sheet materials was selected from previous literature [25-26]. Fracture critical values based on Cockcroft and Latham for sheet materials CP1180 and 22MnB5 were 1.1 (cold work) and 0.48 (cold work)/2.28 (hot work), respectively. In addition, the DEFORM code uses plastic flow data as the basis of the simulation, so that the flow

stress curve data for the target sheet material is required. These flow stress data can be collected from a variety of sources, but are provided only as reference data, so material testing is essential to obtain data on specific application fields. The s-s curve data obtained from the test must be compensated for when apply it to the simulation analysis [14].

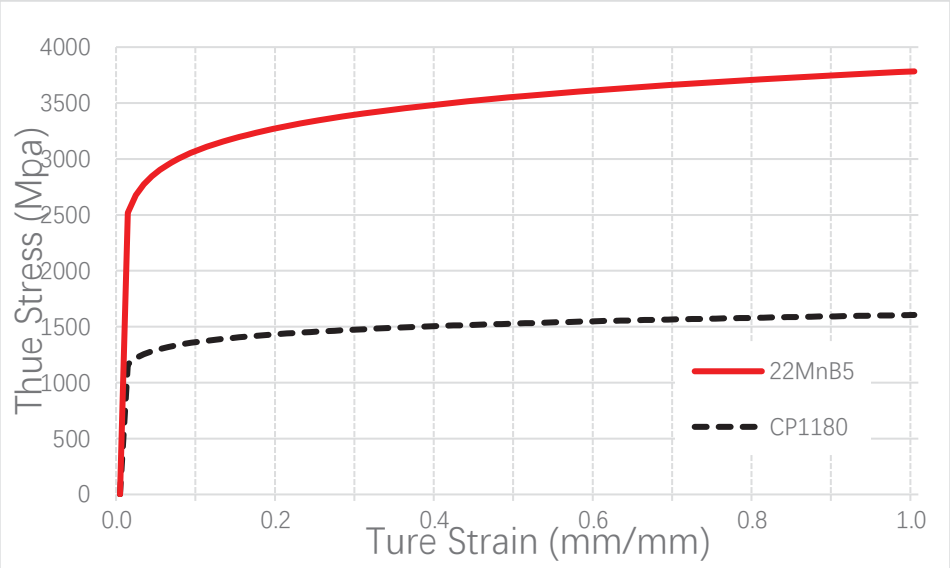

Fig. 2.3 Flow stress curve of sheet material CP1180 and 22NmB5

In this paper, the flow stress curves for sheet materials were analyzed and selected from previous literature [16], [25-26]. The Hollomon models of the flow stress data curves for the selected sheet materials **CP1180** and **22MnB5** were $\bar{\sigma} = \mathbf{1605} \cdot \epsilon^{\mathbf{0.07}}$ and $\bar{\sigma} = \mathbf{2178.2} \cdot \epsilon^{\mathbf{0.103}}$, respectively, and the data curves are shown in **Fig. 2.3 .**

Chapter 3 Simulation and Results Analysis

3.1 Semi-additive range prediction simulation

The analytical model for this punch strength prediction simulation is shown in **Fig. 3.1 (a)** shows a 2D flattening model for punch strength prediction simula tion, and **Fig. 3.1 (b)** represents the elastic and plastic bodies at which deform ation occurs in the analysis process. **Fig. 3.1 (c)** shows the finite element mod el for analysis, and **Fig. 3.1 (d)** is the CAD model showing the three-dimensio nal representation of the 2D analysis model.

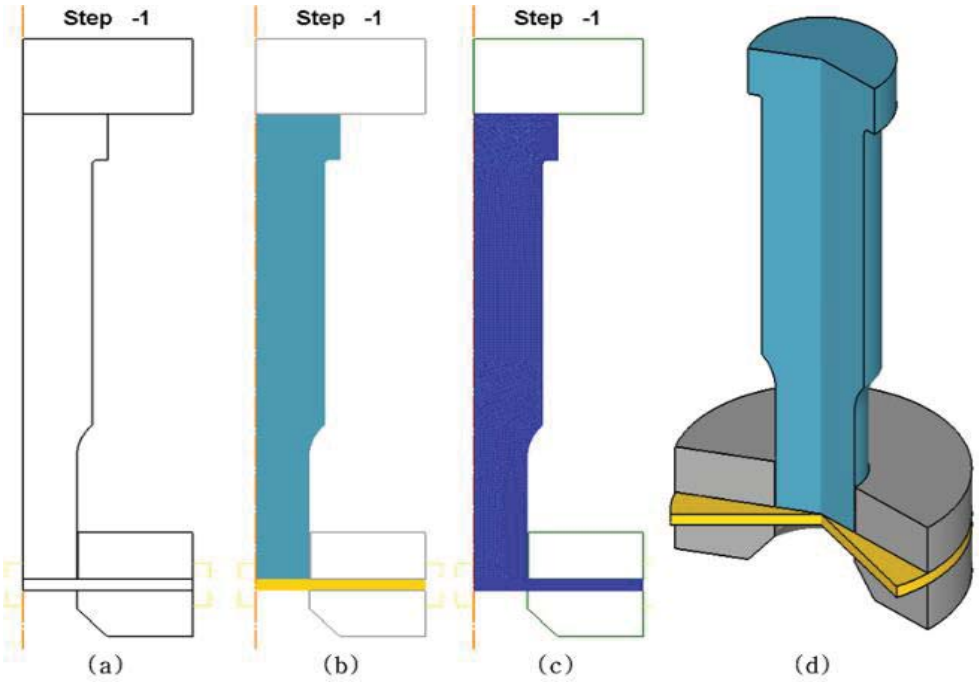

Fig 3.1 Analyze models and boundary conditions

It can be seen from Figure 3.1 that in the Piercing process, the punch and the plate are axisymmetric. Therefore, in 2D simulation, only half of the simulation can be performed to obtain the complete result. This saves time and computing resources, and reduces the overall amount of calculations, allowing you to build smaller grids and more precise calculations.

The results of the stamping strength prediction simulation are shown in **Fig. 3.2 (a)** of **Fig. 3.2** shows the maximum stress and stroke generated in the punc h, and **Fig. 3.2 (b)** shows the state of the maximum stress generated in the side of the punch during the shearing process. **Fig. 3.2 (c)** shows the trend of the p unch load according to the stroke of the punch, and **Fig. 3.2 (d)** shows the out line of the stress distribution when the maximum stress occurs in the punch. It is also found in **Fig. 3.2 (b)** that the maximum point of the punch stress appe ars on the sidewall of the punch during the machining process, and a horizont al force appears, which is one of the causes of the damage of the punch.

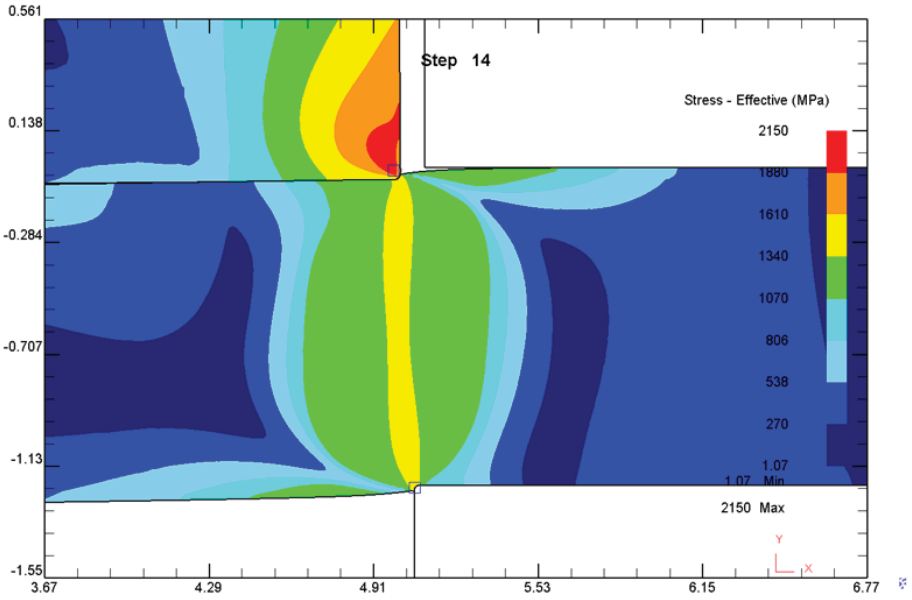
Step 14
Stress - Effective (MPa)
2150
1880
1610
1340
1070
806
538
270
1.07
1.07 Min
2150 Max
0.561
0.138
-0.284
-0.707
-1.13
-1.55
3.67
4.29
4.91
5.53
6.15
6.77

(a)

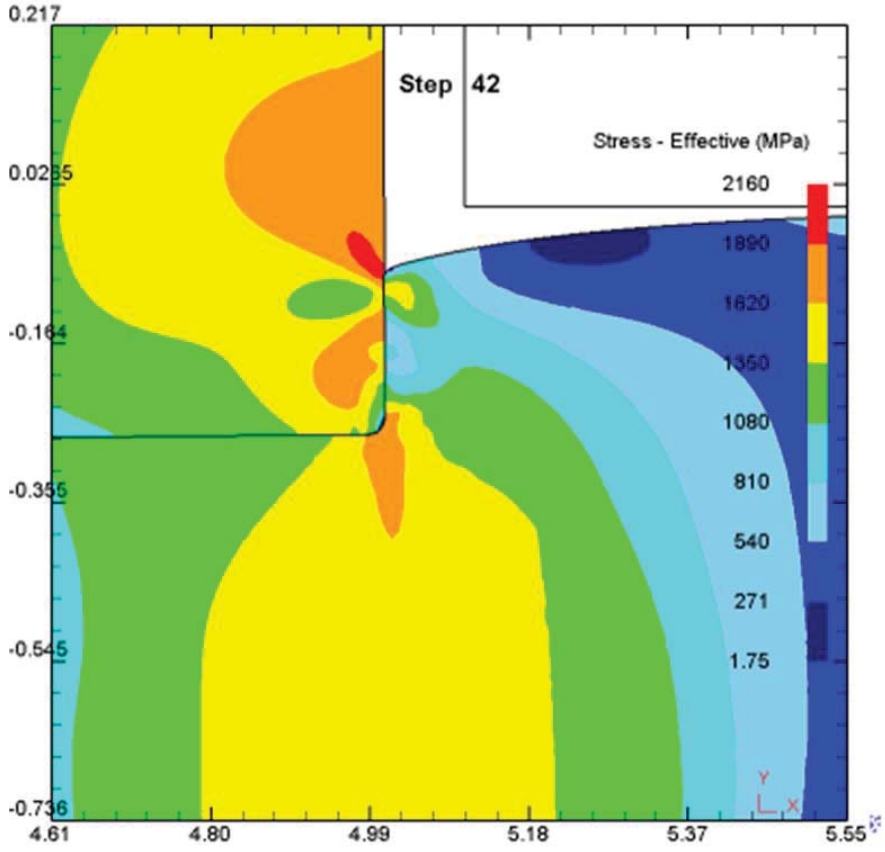
Step 42
Stress - Effective (MPa)
2160
1890
1620
1350
1080
810
540
271
1.75
0.217
0.0285
-0.164
-0.355
-0.545
-0.736
4.61
4.80
4.99
5.18
5.37
5.55

(b)

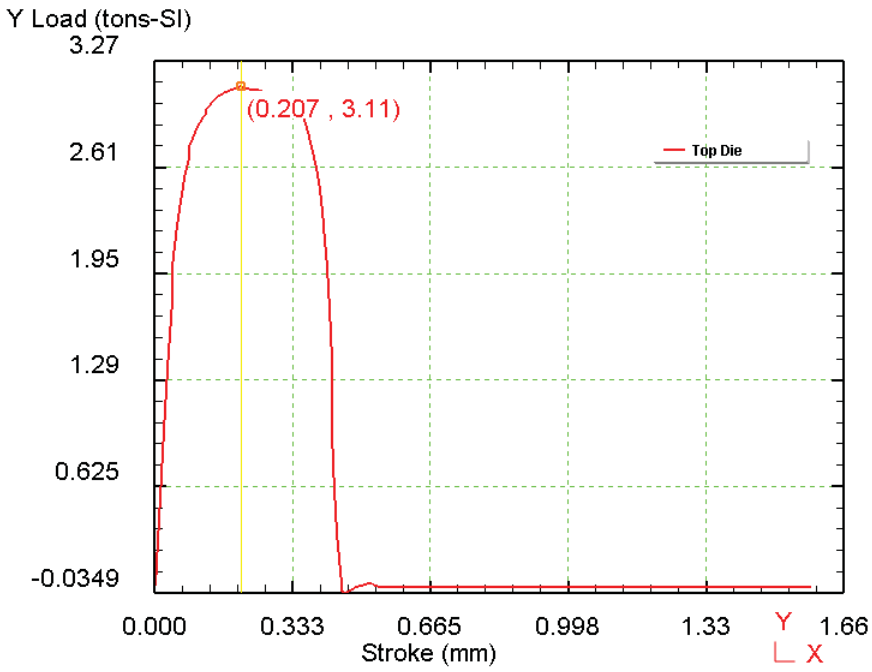

(c)

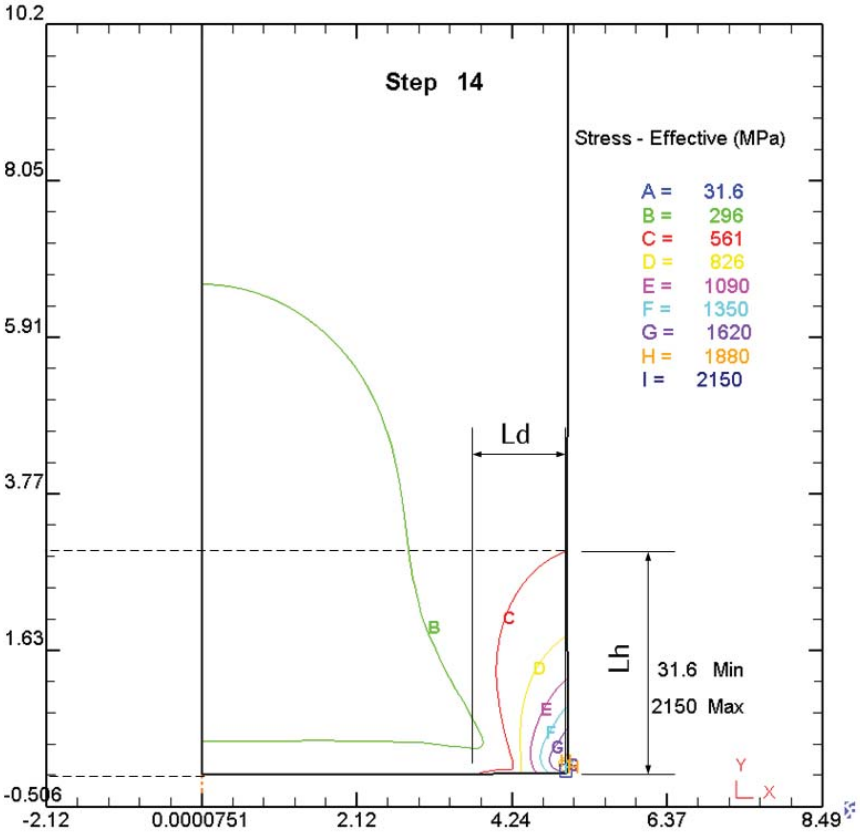

(d)

Fig. 3.2 Simulation results for predicting punch strength

Table 3.1 Prediction simulation results of punch stress distribution

Punch & die Clearance (t ×[%])	Punch concentration stress distribution				Punch maximum stress [MPa]	
	Depth (L_d) [mm]		Height(L_h) [mm]			
	R=0.01	R=0.02	R=0.01	R=0.02	R=0.01	R=0.02
2%	1.05	1.25	2.55	2.65	2,270	2,200
3%	1.30	1.45	2.65	2.95	2,210	2,130
5%	1.00	1.25	2.65	2.65	2,230	2,260
7%	1.20	1.25	2.50	2.75	2,290	2,220
8%	1.25	1.15	2.75	2.55	2,240	2,330
10%	1.25	1.05	2.70	2.50	2,230	2,300
13%	1.25	1.25	2.65	2.65	2,270	2,250
17%	1.30	1.10	2.60	2.45	2,240	2,380
20%	1.25	1.10	2.65	2.40	2,220	2,340
Average	**1.21**	**1.21**	**2.63**	**2.62**	**2,244**	**2,268**

Table 3.1 lists the stress distributions when the maximum stress occurs in th e punch. Analyze the outline of **Fig. 3.1 (d)** and measure and arrange the dept h and height of the punch shape. During the perforation of the high-strength s heet CP1180, the average maximum stress acting on the punch was 2256 MPa.

Table 3.1 shows the simulated stamping strength prediction results for the ma ximum stamping stress and stress distribution range of this high-strength sheet (CP1180).

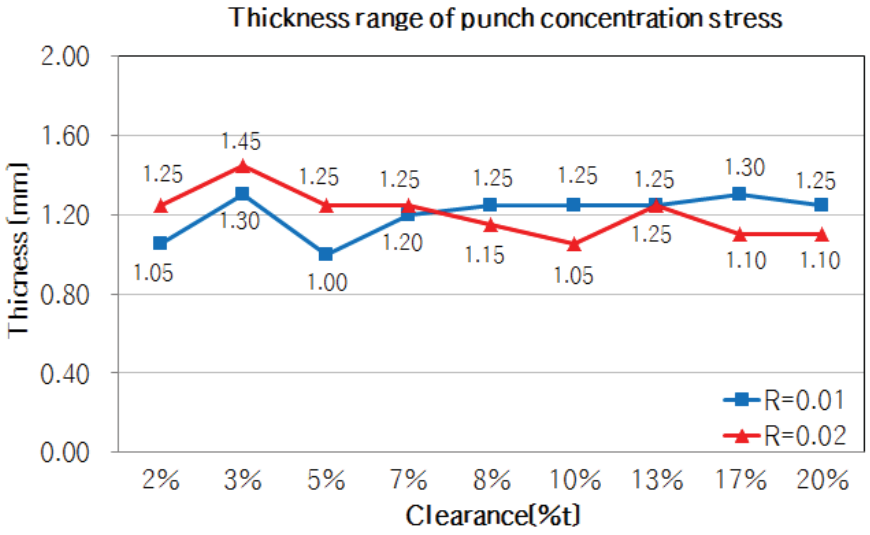
Thickness range of punch concentration stress
Thicness [mm]
2.00
1.60
1.20
0.80
0.40
0.00
1.25
1.45
1.25
1.25
1.25
1.25
1.25
1.30
1.25
1.05
1.30
1.00
1.20
1.15
1.05
1.25
1.10
1.10
R=0.01
R=0.02
2%
3%
5%
7%
8%
10%
13%
17%
20%
Clearance[%t]

(a)

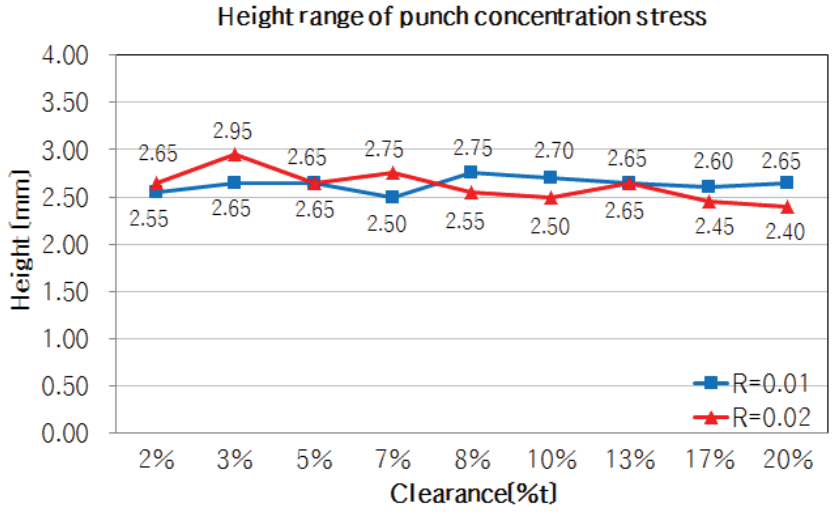
Height range of punch concentration stress
Height [mm]
4.00
3.50
3.00
2.50
2.00
1.50
1.00
0.50
0.00
2.65
2.95
2.65
2.75
2.75
2.70
2.65
2.60
2.65
2.55
2.65
2.65
2.50
2.55
2.50
2.65
2.45
2.40
R=0.01
R=0.02
2%
3%
5%
7%
8%
10%
13%
17%
20%
Clearance[%t]

(b)

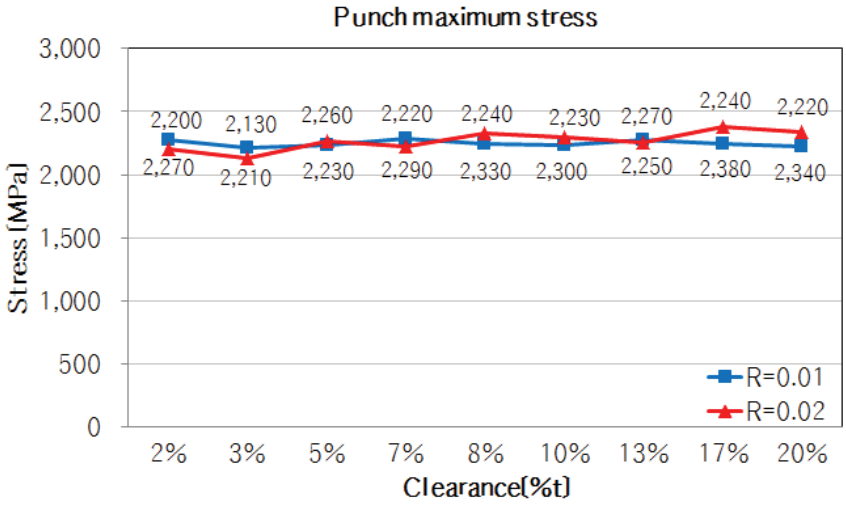
Punch maximum stress
Stress [MPa]
3,000
2,500
2,000
1,500
1,000
500
0
2,200
2,130
2,260
2,220
2,240
2,230
2,270
2,240
2,220
2,270
2,210
2,230
2,290
2,330
2,300
2,250
2,380
2,340
R=0.01
R=0.02
2%
3%
5%
7%
8%
10%
13%
17%
20%
Clearance[%t]

(c)

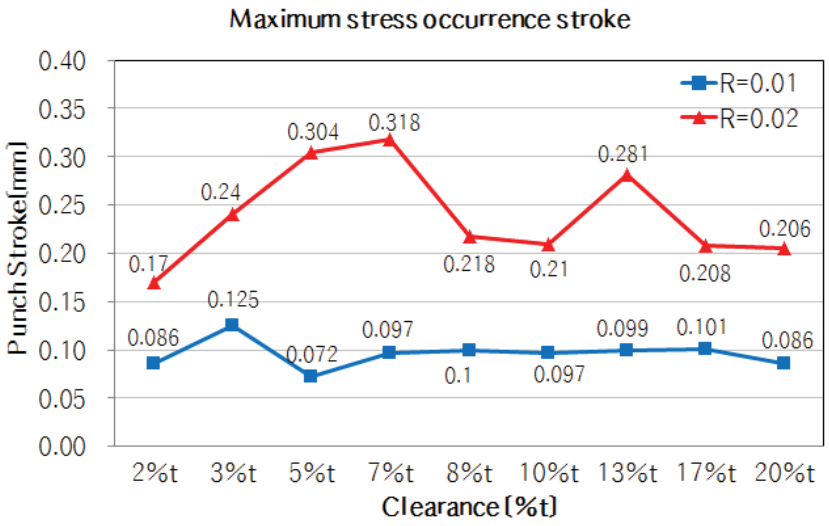

(d)

Fig. 3.3 Maximum stress and stress distribution in punching process

Fig. 3.3 is shown. **Fig. 3.3 (a)** and **Fig. 3.3 (b)** are graphs showing the depth and height of the punch shape according to the punch and die gap and the p unch corner radius, respectively. **Fig. 3.3 (c)** and **Fig. 3.3 (d)** show the maxim um stress and maximum stress generation strokes, respectively, based on the pu nch and die gap and the corner radius of the punch. The figure shows the sha pe range of the punch, where the maximum stress and the stress acting on the punch during the punching process. As shown in **Fig. 3.3 (a)** and **Fig. 3.3 (b).** There is almost no relationship between the punch corner radius and the d ie gap. However, when R = 0.01, the maximum stress occurs at 0.096 mm, an d when R = 0.02, the maximum stroke is 0.2394 mm.

In order to observe the punch strength according to the punch speed, different punch materials and plates were simulated and analyzed. **Fig. 3.4 (a)** shows the punch stress according to the punch material and the sheet, and **Fig. 3.4 (b)** sh ows the punch stress distribution according to the punch speed of the punch m

aterial HWS and the sheet material **22MnB5**. **Fig. 3.4 (c)** shows the stress distr ibution depending on the punch stress of the sheet, and **Fig. 3.4 (d)** shows the stress distribution on the punch when the sheet is 22MnB5.

As shown in **Fig. 3.4 (a),** the punch stress is minimally affected by the punch material (HWS, M4, D2), and is mainly affected by the sheets (CP1180, 22Mn B5). In addition, it was found that the critical fracture damage value (CDV) h ad no effect on the punch stress and had an effect on the shear time of the s heet. As shown in **Fig. 3.4 (b)**, the large change in the value at which the pu nch stress drops sharply is a phenomenon occurring during the shearing proces s due to software re-meshing and density change of the mesh. . This phenome non was found to be caused by unevenness. In addition, the sharp increase in punch stress during the shearing process is caused by pressing the sheared she et against the micro-region on the punch side, and it is analyzed that the punc h is worn and scratched in the actual punching operation. As shown in **Fig. 3. 4 (c).** The punching speed (50 to 400 mm / sec) does not seem to affect the change in the punching stress. If the punching speed is not very slow and has a certain speed (50 mm/sec), it does not seem to significantly affect the punch ing stress.

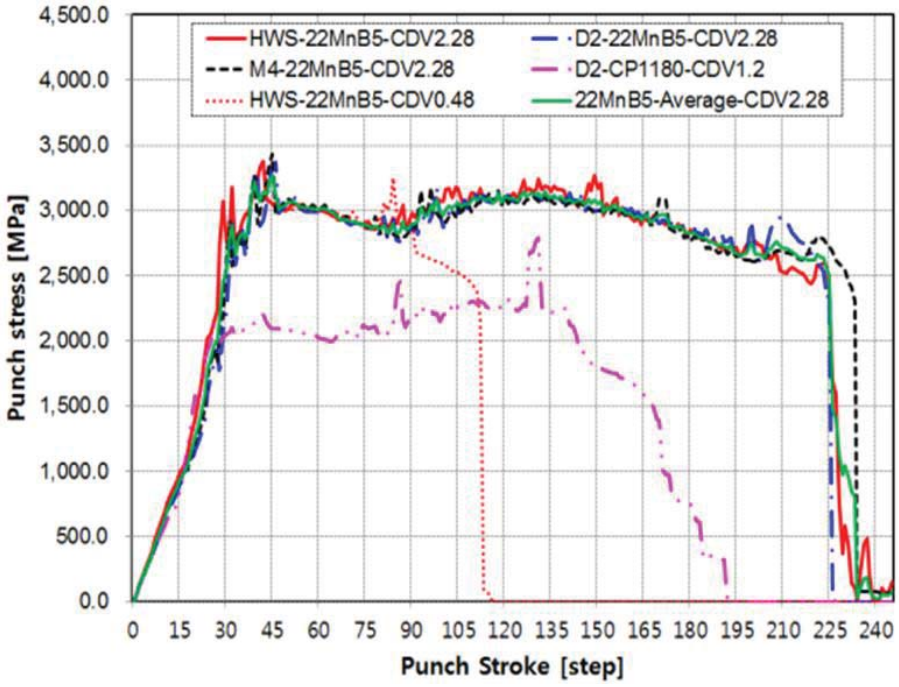
HWS-22MnB5-CDV2.28
D2-22MnB5-CDV2.28
M4-22MnB5-CDV2.28
D2-CP1180-CDV1.2
HWS-22MnB5-CDV0.48
22MnB5-Average-CDV2.28
Punch stress [MPa]
4,500.0
4,000.0
3,500.0
3,000.0
2,500.0
2,000.0
1,500.0
1,000.0
500.0
0.0
0 15 30 45 60 75 90 105 120 135 150 165 180 195 210 225 240
Punch Stroke [step]

(a)

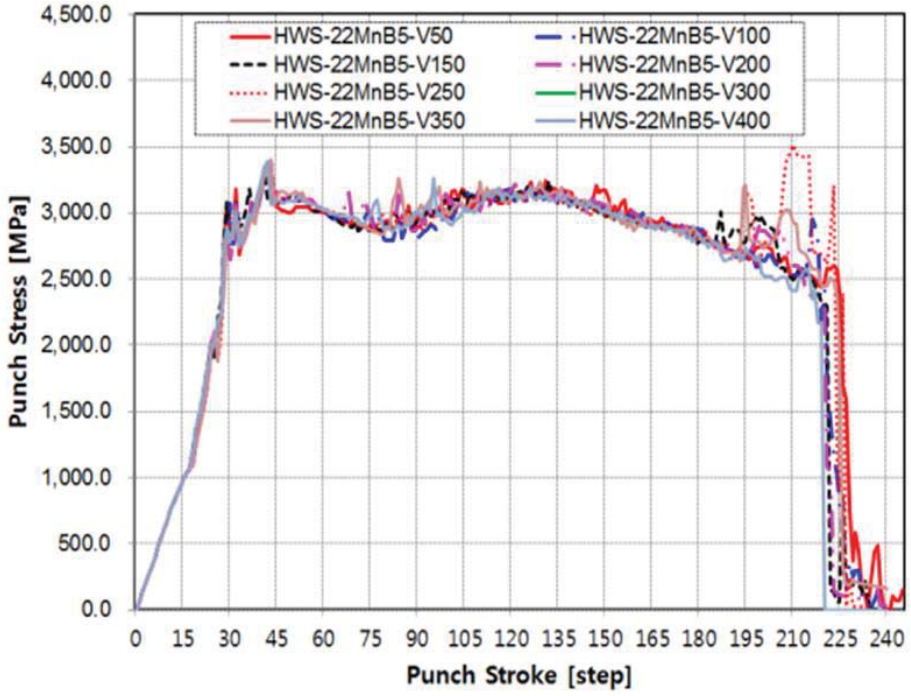
HWS-22MnB5-V50
HWS-22MnB5-V100
HWS-22MnB5-V150
HWS-22MnB5-V200
HWS-22MnB5-V250
HWS-22MnB5-V300
HWS-22MnB5-V350
HWS-22MnB5-V400
Punch Stress [MPa]
4,500.0
4,000.0
3,500.0
3,000.0
2,500.0
2,000.0
1,500.0
1,000.0
500.0
0.0
0 15 30 45 60 75 90 105 120 135 150 165 180 195 210 225 240
Punch Stroke [step]

(b)

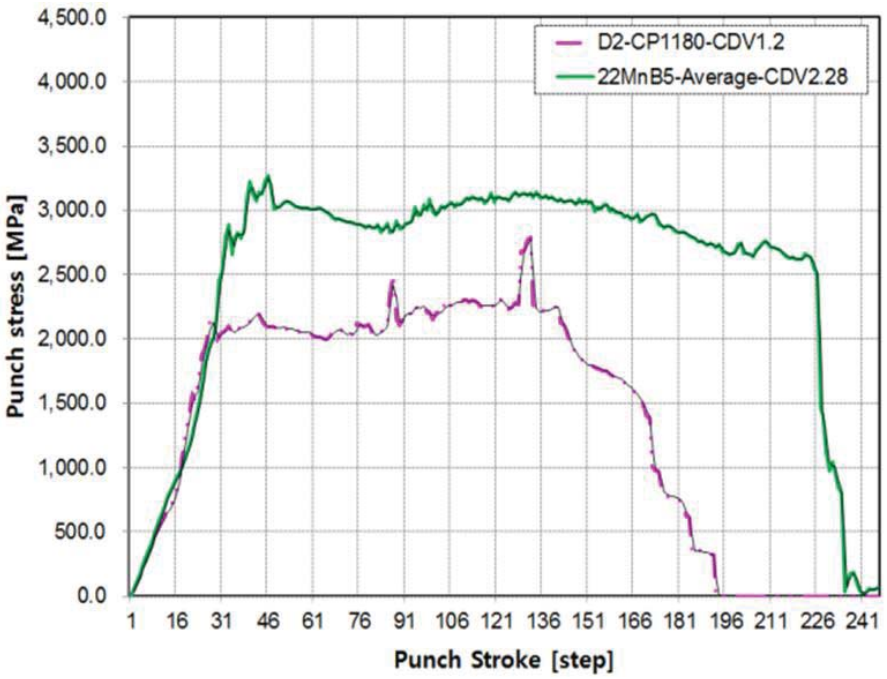

(c)

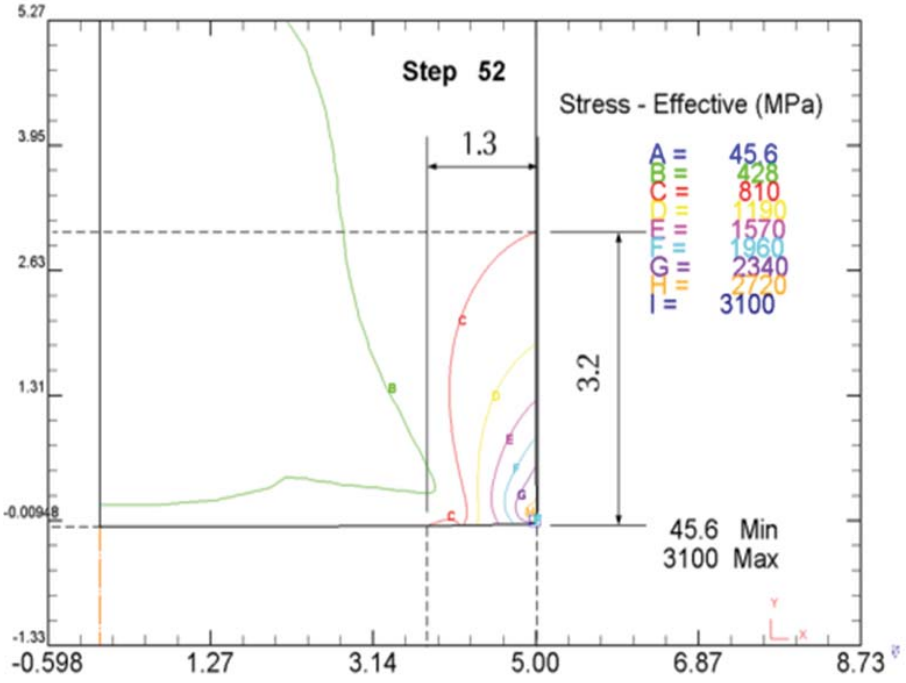

(d)

Fig. 3.4 Punch stress in cording to punch speed

Fig. 3.4 (d) shows the stress distribution profile generated in the punch accord ing to the shearing force of the sheet 22MnB5, and the depth and width of th

e stress action are analyzed to be 1.3 mm and 3.2 mm, respectively. The maxi mum stress of the punch was observed to be 3,267 MPa. The shape range of the semi-additive can be determined from the punch stress distribution accordin g to the punch and the die gap and according to the punch speed and the pun ch stress distribution of the sheet. Therefore, the shape range for the semi-addi tive is 1.21 mm for the sheet CP1180, and is 2.32 mm for the sheet 22MnB5 of 1.3 mm and 3.2 mm.

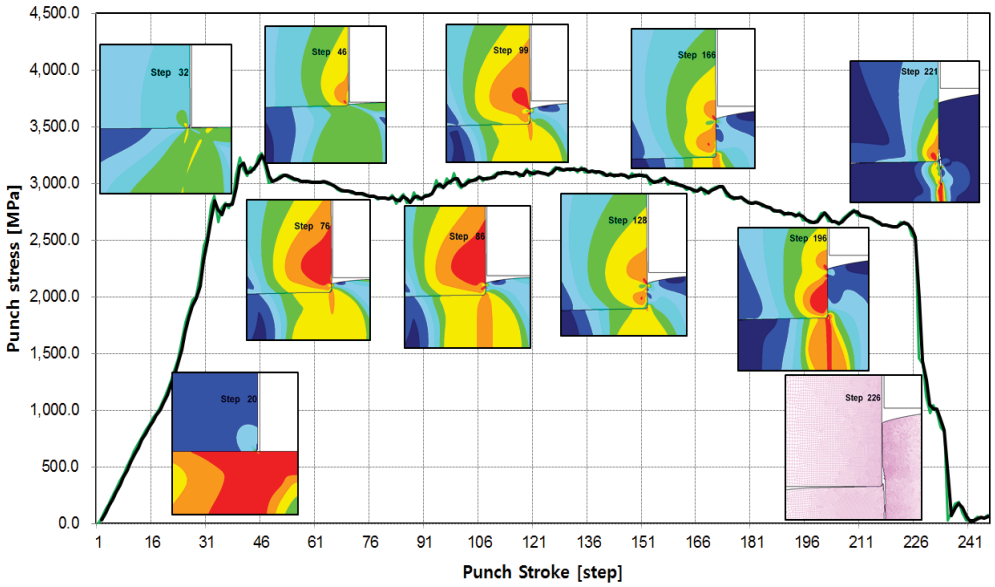

Fig. 3.5 Punch Stress Distribution in Shear Process

The punch stress distribution in shear process shows on **Fig. 3.5.** At the begi nning of the machining, the stress on the punch rapid increase, the stress distri bution during processing can be seen from the results, where the stress is mai nly distributed at the bottom of the punch. It's worth noting that at the same t ime, not only the maximum concentration point of the stress at the bottom of the punch, but also the stress and the focus on the side of the punch, which a

lso indicates that during the machining process the side of the punch is subject to irregular forces, which is one of the main causes of damage to the punch.

3.2 Semi-additive shape selection & simulation

Semi-additive punch shape design depending on the shape and extent of th e punched edge. Design the shape of the edge portion of the punch to reinforc e the punch into any shape and then select the best shape through process ana lysis The range of the shape by the edge of the punch is defined as the semi-additive range selected above , it shows on **Table. 3.2** and **Fig. 3.6** and **Fig. 3. 7** and **Table. 3.2** shows the 3D printed shape and name of the design.

Table 3.2 Semi-additive punch shape size range

Shape type	Diameter (d)	Additive thickness (L_t)	Additive Height (L_h)	Additive depth (L_d)	Punch radius (R)
Flat type	10	2.0	-	-	0.02
Ring type	10	1.2	2.5	-	0.02
		0.6	2.5		
Cap type	10	0.5	2.5	-	
Cap-Ring type	10	0.5	2.5		
Straight-Edge Type	10	1.2	3.0	-	
Edge S-Lug type	10	1.2	3.0		
Edge R-Lug type	10	1.2	3.0		
Half-Cap type	10	0.5	2.5	1.5	
Round-Edge type	10	1.2	3.0	R=4.35	

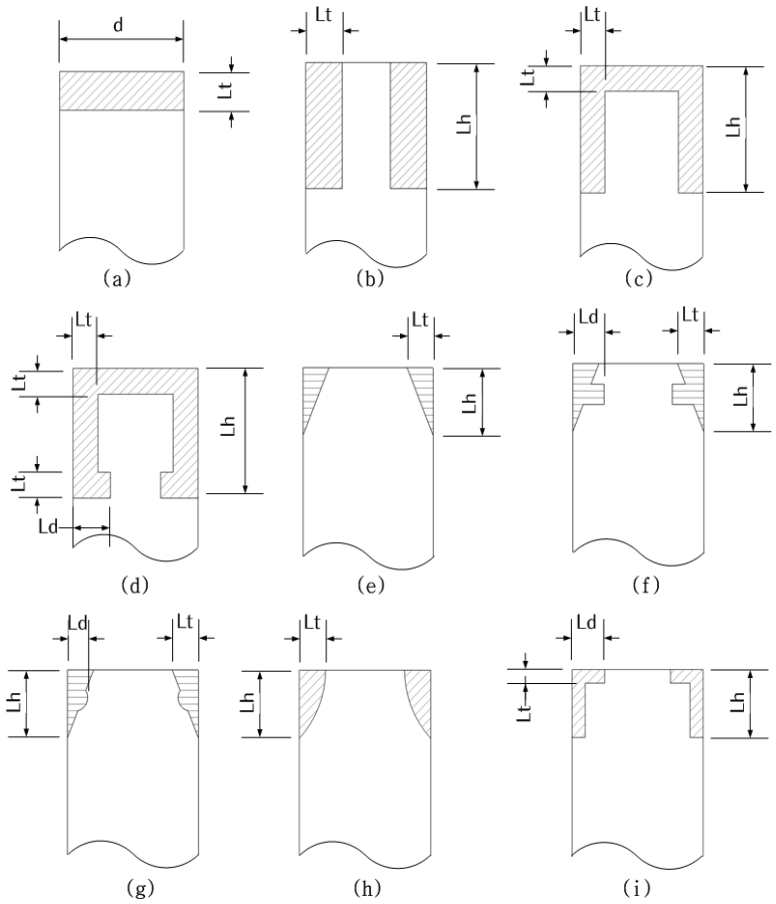

Fig. 3.6 Semi-additive shape design

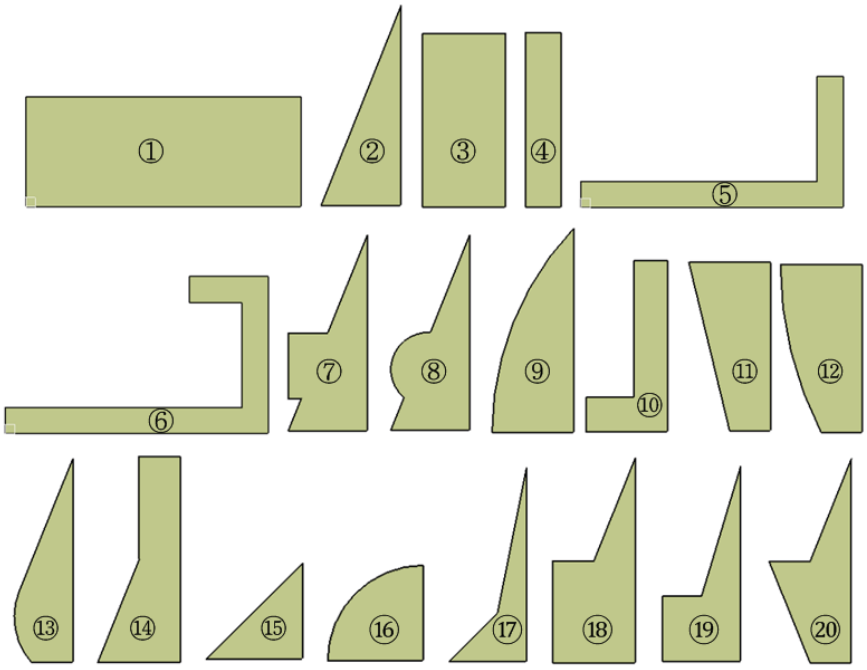

Fig. 3.7 Shape of semi-additive geometry

Table 3.2 Name of semi-additive geometry

1. Flat type	2. Thick-ring type
3. Thin-ring type	4. Cap type
5. Half-cap type	6. Ring lug-cap type
7. Straight-edge type	8. Straight-edge-S-lug type
9. Straight-edge-R-lug type	10. Top Triangle-Bottom Square-Big Type
11. Top Triangle-Bottom Square-Small Type	12. Round-edge type
13. Inverse-ladder type	14. Inverse-round ladder type
15. Top triangle-round-edge type	16. Top square-edge type
17. Regular triangle-edge type	18. Sector edge type
19. Gull shape-edge type	20. Top triangle-bottom ladder type

Proactive execution to characterize the analysis software to optimize the geom etry of the semi-additive to enhance the perforation function. The selected inter face friction conditions were applied to the verification analysis of the semi-ad ditive shapes of various designs by analyzing the analysis of software character istics. The boundary contact conditions are defined as follows. Software contact conditions: Shear Friction(Sticking), Coulomb Friction(Sliding), Hybrid Friction, Tau Friction

About the Shear Friction: Constant shear (fixed) friction is most commonly used for batch molding simulations. Typical values (using constant shear only): (0.08-0.1) for cold forming processes；(0.2) for warm forming processes；(0.2 t o 0.3) for lubricated hot forming processes；(0.7-0.9) for unlubricated surfaces

Coulomb Friction: Coulomb (sliding) friction for sheet metal forming operatio

ns

Tau Friction: Tau friction is used when the user needs to distribute shear str ess to the surface.

The analysis model settings are shown in **Fig. 3.8**. Different colors indicate different contact conditions

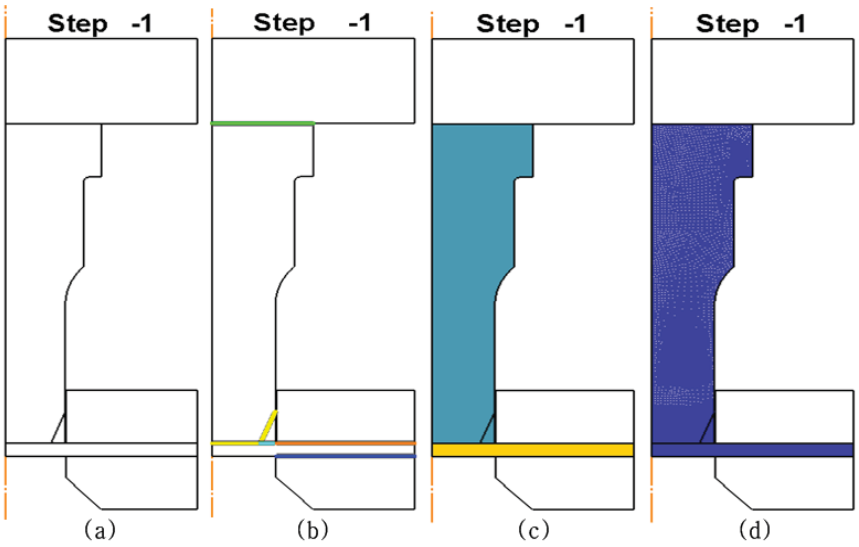

Fig. 3.8 Analyze models and boundary conditions

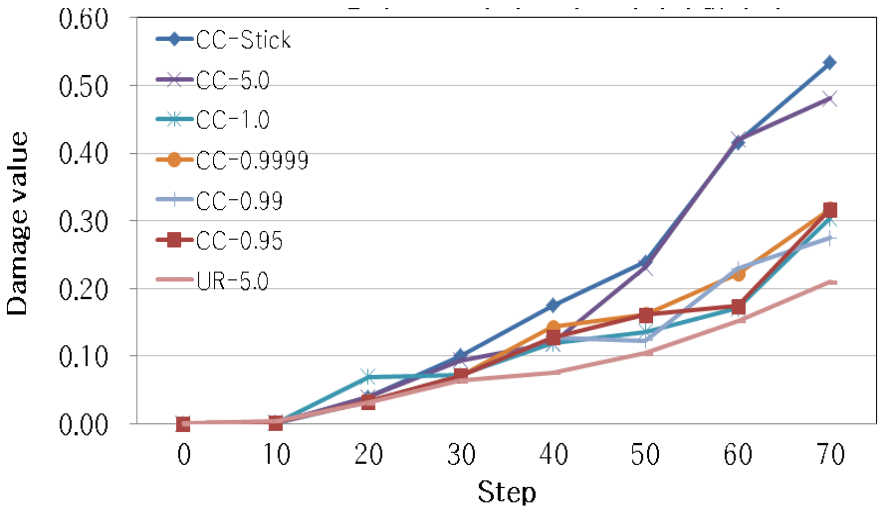

Fig. 3.9 Comparison of fracture damage values under combined Coulomb fricti on conditions

In Coulomb Frictional even under mixed friction conditions, joint slippage occurs slightly from step 30 under adhesion conditions and coefficient of friction (HC). Under mixed friction conditions, the damage values were similar except for the adhesion conditions and the coefficient of friction (HC)5. The data is shown in **Fig. 3. 9.**

The mixed friction condition showed a smaller damage value than other frictional conditions, but showed a clear tendency by adjusting the friction coefficient (HC).

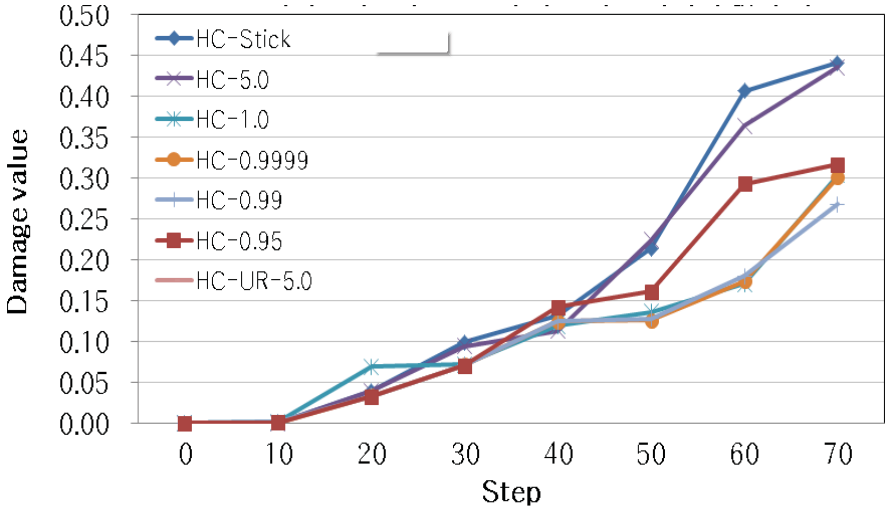

Fig. 3.10 Comparison of fracture damage values under mixed surface friction

In Hybrid Frictional (**Fig. 3.10**) Even under mixed friction conditions, joint s lippage occurs slightly from step 30 under adhesion conditions and coefficient of friction (HC).Under mixed friction conditions, the damage values were simil ar except for the adhesion conditions and the coefficient of friction (HC)5. The mixed friction condition showed a smaller damage value than other frictional conditions, but showed a clear tendency by adjusting the friction coefficient (H

C).

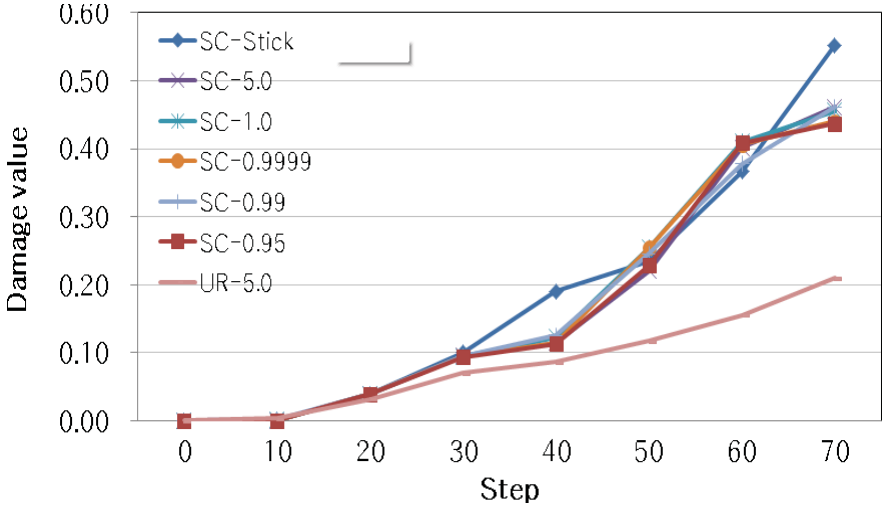

Fig. 3.11 Comparison of fracture damage values according to shear friction co nditions

In Shear Frictional (**Fig. 3.11)** under shear friction conditions, in addition to t he viscous conditions, the joint will slip slightly from the 30th step and above. Damage values other than viscous conditions showed similar trends with little difference. User rutin conditions cannot be analyzed due to large slippage.

In Constant Tau(**Fig. 3.11**) Under the tau friction condition, the joint sliding p henomenon is large except for the step 10 and above in the adhesive state. In the tau rubbing state, the damage value between the stuck state and the statio nary state shows a large difference. Due to the lack of distinction, the applicat ion of tau friction conditions in analysis is negligible

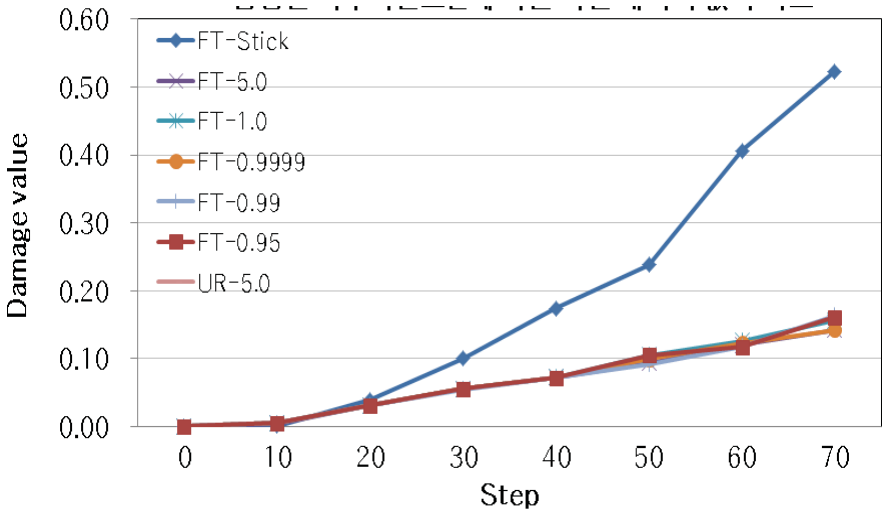

Fig 3.12 Comparison of fracture damage values based on Tau friction condition s on the joint surface

Under the friction (**Fig. 3.12**) conditions other than the tau friction condition, the viscous damage value and the friction coefficient of each friction type wer e 1 and 5, respectively, showing a similar tendency. There is a clear differenc e between when 1 and 5. As described above, the mixed friction condition me ans that the condition can be controlled on the joint surface in accordance wit h a user-defined friction coefficient value. Therefore, the friction conditions for the process analysis for optimizing the semi-additive shape to enhance the punc hing function were applied to the mixing type with a coefficient of friction of 5.0.3.3 simulation results and discussion

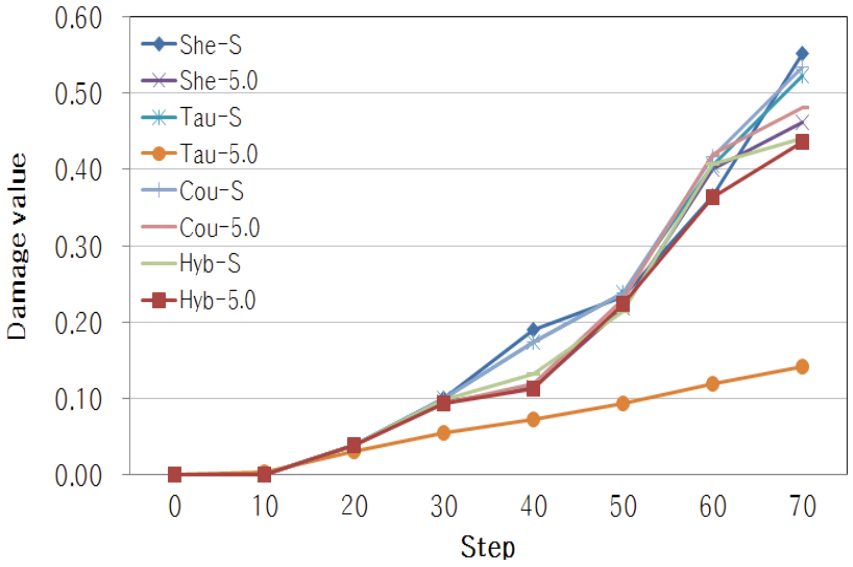

Fig. 3.12 Compare the fracture damage value according to the type of friction (when t he condition is 5 and the friction coefficient is 5)

As a preliminary simulation analysis of each semi-additive shape, the friction conditions of the semi-additive joint boundaries of the dissimilar materials were analyzed. This was done to proactively characterize the analysis software to optimize the analysis of the semi-additive shape. In this analysis, the software interface boundary conditions are divided into shearing force, sliding force, mixed friction and Tau friction. Here, shear and Coulomb friction conditions provide information about the additive and slip at the joint interface during analysis, while tau friction conditions provide information on shear stress on the surface. In addition, the mixed friction condition means that shearing and coulomb conditions are simultaneously applied, and peeling and sliding phenomena can be simultaneously observed at the joint surface boundary. Therefore, in this analysis, it is defined as a technique for selecting

boundary conditions, focusing on the fact that changes such as fixation, slip, and peeling occur at the boundary of dissimilar materials depending on the friction conditions and affect the damage of the shear material value.

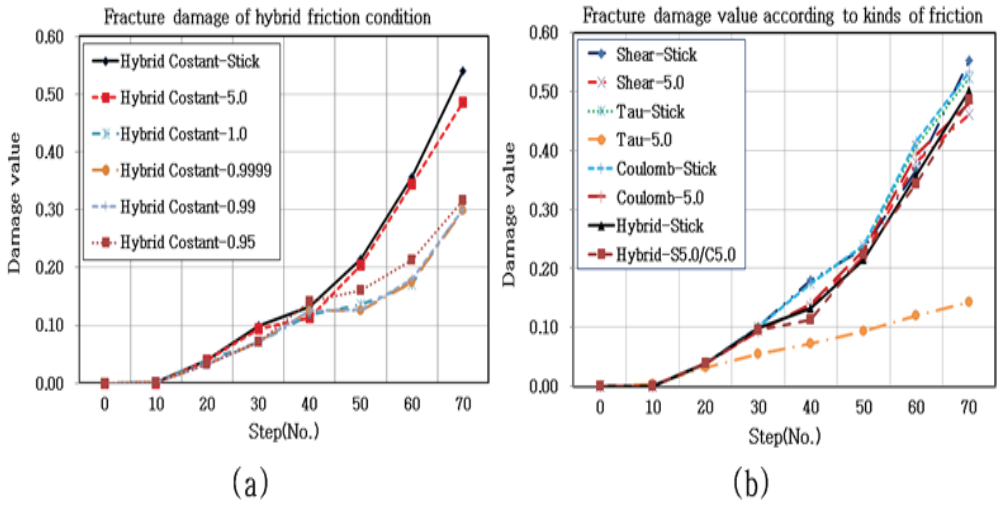

Fig. 3.13 Compare the fracture damage value according to the type of friction (when the condition is 5 and the friction coefficient is 5)

Fig. 3.13 shows a comparison of the damage values according to the magnitude of the mixed friction conditions, and **Fig. 3.13 (b)** shows a comparison of the damage values according to the type of the friction conditions.

If a gap of more than 0.001 mm occurs under the connection condition between the two objects, the contact is marked as dropped. In other words, when the contact condition is less than 0.001 mm, it is marked as a bond.

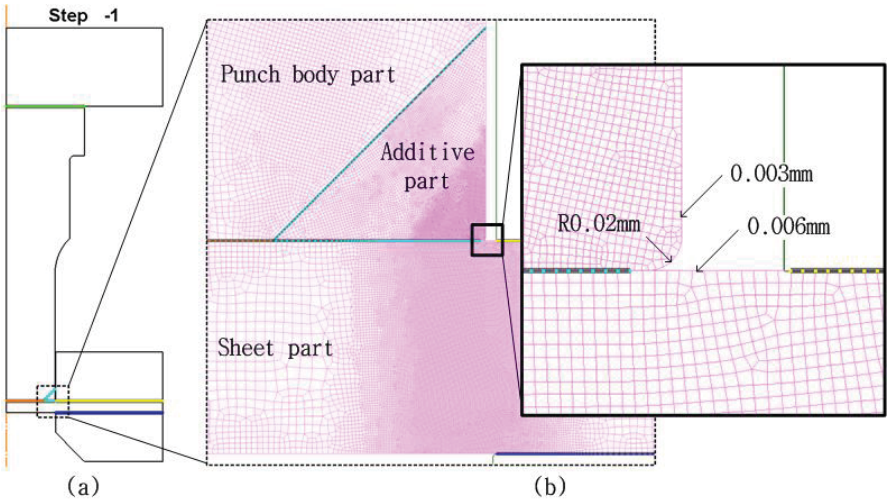

Fig. 3.14 Mesh size composition for microstructure analysis

Meshing is performed before the simulation, because the approximate stress concentration range has been determined, and in order to make the simulation operation more efficient, a method of partitioning different density meshes is adopted. The specific mesh size is shown on **Fig. 3.14** .The mesh unit size of the punch is 0.003mm, and the mesh size of the plate is 0.006mm.

This can make the simulation of the stress concentration area more detailed, and use a larger size mesh in the area where the stress cannot reach, which can reduce the unnecessary calculation amount tereby obtaining a more accurate result in a short time.

The goal is to minimize and overcome it. However, if the additive range is not as large as the punch and the mold reinforcement range is small, the cost of machining and additive complex shaped punch inserts is higher than the advantage of gold reinforcement.

In particular, when the high strength cold work die steel powder HWS material found in the present invention is applied, there is no limitation on the additive range, and

there is an advantage that additive can be performed within a desired range.

The result of analysis from the results of various shape designs is that as shapes become more complex, these shapes are designed to absorb the impact forces acting on the punch and are therefore more susceptible to impact.

A common phenomenon caused by the analysis of various stacked shapes is the edge of the punch and the side of the punch, where stress is concentrated at the edge of the punch and the side of the punch at the beginning of the shear.

The purpose of the semi- additive shape is to minimize the additive ability of the expensive high-strength powder and to shorten the additive time, but the additive range is limited due to the limitation of the additive range of the high-strength mold steel (high-speed steel) metal powder.

Therefore, taking this into account when stacking semi-additive will also increase the life of the punch. The punch depends on the worksheet material. When **22MnB5** boron steel was used in the same worksheet, the punch bars of **M4** and **D2** showed almost the same trend according to HWS. When the punching material is **D2** and the worksheet material is **22MnB5** boron steel (1500 MPa) and **CP1180** (1200 MPa), the punching rods have a large difference. The break point of the worksheet material depends on the CDV (severe damage value). In the case where the working material is 22MnB5, when CDV 2.28 (hot), the breakpoint is shown as step 195, and in step 82, the breakpoint that occur

s when CDV is 0.48 (cold) can be seen(**Fig. 3.15**).

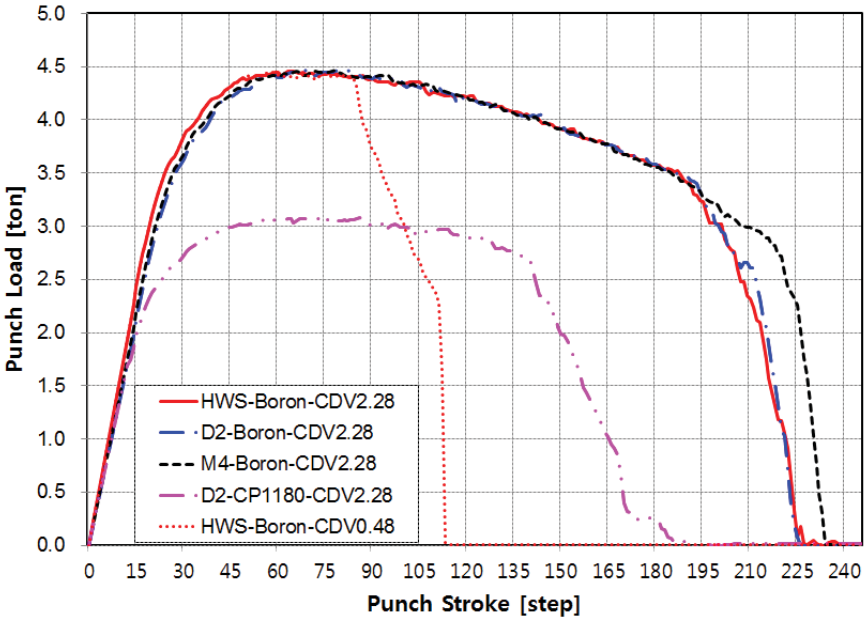

Fig. 3.15 Punch load according to punch material and CDV value

3.3 Simulation results and discussion

In the simulation analysis for such a semi-additive shape selection, the stability of the joint is indirectly judged by comparing the damage values acting on the sheet according to the shape analysis of the design. The range of stress distribution, the slip and separation state at the interface, the size of the additive range, and the difficulty in manufacturing the additive are all defined as criteria for shape selection. **Fig. 3.16** and **Table 3.3** shows a comparison of the damage values caused by the semi-superimposed shape analysis of the design.

Table. 3.3 damage values based on semi-additive geometries

Step / Shape	10	20	30	40	50	60	70	80	90	100	110	120	130	140	150
① Flat type	0.00292	0.0489	0.102	0.157	0.25	0.481	0.482	0.574	0.663	0.946	1.05	1.1	2.48	2.01	1.17
② Thick-ring type	0.00416	0.0410	0.0695	0.118	0.196	0.323	0.455	0.606	0.754	0.852	1.09	1.44	1.91	1.11	1.32
③ Thin-ring type	0.00224	0.037	0.0761	0.129	0.261	0.585	0.481	0.551	0.638	0.783	1.59	1.59	1.1	1.28	1.12
④ Cap type	0.00371	0.0471	0.101	0.152	0.253	0.363	0.486	0.644	0.849	0.895	1.1	1.82	1.66	1.1	1.71
⑤ Half-cap type	0.00179	0.0385	0.0872	0.143	0.260	0.380	0.502	0.599	0.798	0.835	1.0	1.09	1.12	1.15	1.25
⑥ Ring lug-cap type	0.00312	0.0437	0.101	0.171	0.324	0.499	0.526	0.648	0.860	0.903	1.10	2.76	1.88	1.12	1.40
⑦ Straight-edge type	0.000923	0.0318	0.0809	0.131	0.208	0.340	0.464	0.591	0.773	0.824	0.923	1.10	1.61	1.22	1.66
⑧ Straight-edge-S-lug type	0.00107	0.0373	0.0694	0.139	0.207	0.344	0.442	0.630	0.811	0.921	1.13	1.10	1.16	1.70	1.25
⑨ Straight-edge -R-lug type	0.00243	0.0407	0.0724	0.130	0.237	0.393	0.461	0.680	0.780	0.850	1.03	1.31	2.21	2.10	1.21
⑩ Top Triangle-Bottom Square-Big Type	0.00288	0.0506	0.0782	0.140	0.229	0.369	0.540	0.656	0.731	0.850	0.933	1.50	2.98	2.66	1.31
⑪ Top Triangle-Bottom Square -Small Type	0.00317	0.0494	0.0832	0.155	0.255	0.398	0.465	0.582	0.757	0.929	1.01	1.15	1.21	3.44	1.59

⑫ Round-edge type	0.0002	0.0396	0.0699	0.116	0.241	0.378	0.428	0.664	0.702	0.801	0.916	1.06	1.28	1.25	1.13
⑬ Inverse-ladder type	0.00277	0.0525	0.106	0.163	0.372	0.467	0.872	0.526	0.812	0.757	1.08	1.20	3.69	5.0	4.18
⑭ Inverse-round-ladder type	0.00159	0.0392	0.0941	0.164	0.245	0.372	0.517	0.647	0.732	0.879	1.01	1.13	1.4		
⑮ Top triangle-round-edge type	0.000964	0.0446	0.0985	0.124	0.232	0.381	0.472	0.628	0.772	0.937	2.28	1.09			
⑯ Top square-edge type	0.00265	0.038	0.102	0.141	0.250	0.406	0.492	0.675	0.788	1.00	1.44	1.35	1.67	1.81	1.25
⑰ Regular triangle-edge type	0.000843	0.0318	0.101	0.132	0.231	0.346	0.511	0.621	0.835	0.992	1.07	1.14	3.01	2.45	1.18
⑱ Sector edge type	0.0000195	0.0374	0.0749	0.119	0.278	0.394	0.591	0.655	0.895	1.07	1.11	1.09	2.66	1.22	1.14
⑲ Gull shape-edge type	0.000765	0.038	0.111	0.13	0.265	0.404	0.485	0.68	0.947	0.979	1.03	1.1	4.81	1.13	
⑳ Top triangle-bottom	0.00124	0.0432	0.37	0.367	0.438	0.562	1.74	2.36	1.48	1.35	1.08	1.9	2.68	3,22	1.14

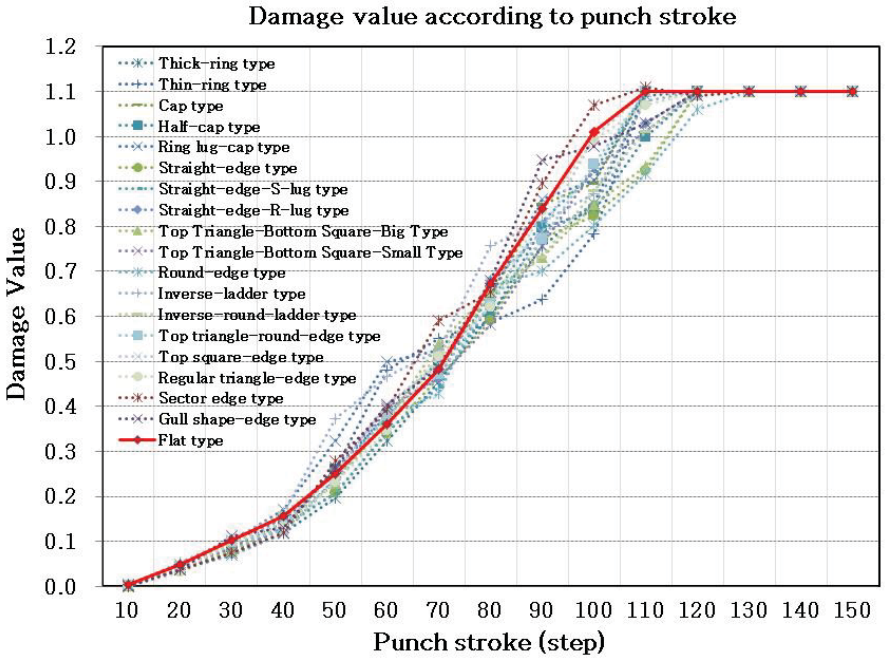

Fig. 3.16 Damage value according to the punch stroke

Planar geometry seems to be the most stable. Next, the shape is stable. In th e semi-additive geometry, the interface was found to have a 45 degree sloped boundary instead of vertical and acute angles. That is, it is shown that the equ ilateral triangle is more stable than the triangle. In addition, the interface comp osed of pure straight lines seems to be more stable than the interface including the circular curve. As the boundary surface is away from the punch blade, th e peeling phenomenon becomes large, and when the boundary surface tilt angle is greater than 45 degrees, the slip occurs at 45 degrees. In the case of a rin g, slippage does not occur but peeling occurs. As shown by the ring, thin addi tive in the depth direction of the punch body, if possible, seems to help reduc e peeling.

There is no slip or peel at the interface between the different materials, and t he shear force of the punch is stably transmitted to the material, so the stress

distribution tends to be the same as the shape of the punch of the same mater ial.

Peeling and slipping occur at the interface of all the different materials in wh ich the edges of the punch are partially machined or stacked.

In particular, the peeling occurs in a shape having a boundary in the vicinity of the vertical, and the slip occurs when the angle of the diagonal inclination approaches an acute angle.

Therefore, the formation of an additive interface in the same direction as the application of the perforated rods when additive between different materials sho uld be avoided. It is desirable to stack only in the same shape as the punch. Although the purpose of designing the partial semi- additive shape is to minim ize the additive ability of the expensive high-strength powder and to shorten th e additive time, additive is limited due to the limitation of the additive range of the high-strength mold steel (high-speed steel) metal powder the scope is li mited.

Chapter 4 Prototype Production and Testing

4.1 Additive Manufacturing Method

4.1.1 Additive manufacturing DED Method and Equipment

Metal 3D printing direct energy deposition (ADDD) additive manufacturing (AMD) technology uses a high power laser to completely melt and deposit metal powder. This results in a complete fusion between the materials, resulting in a high quality additive.

In addition, since the additive quality has a dense structure, there is an advantage that it is suitable for manufacturing a tool such as a mold. So far, the laser is expensive, the manufacturing time is very long, and the output surface is rough, which requires post processing. In recent years, research has been actively carried out on the use of DED technology to reinforce mold parts to improve the life of high-strength steel molds.

In addition, due to the compact structure and excellent mechanical properties, applications in the mold industry (such as mold/mold surface hardening, mold reshaping and mold repair) are also increasing. Generally, the stack thickness of the DED method is stacked by adding one layer in the range of 100-300 μm. Most of the heat sources used as heat sources use a CO_2 laser beam, and the beam oscillated by the laser beam engine has a diameter of about 0.8 to 1.0 mm. In the DED method, the powder material mainly uses a spherical powder in the range of 40 to 140 μm. Generally, the closer the shape of the powder material is, the more uniform the particle composition is, and the better the fluidity at the time of supply. The DED type

of equipment used in this study used DMT's (Direct Metal Tool) MX3 metal printer and demonstrated the concept of device configuration and stacking. **Fig. 4.1**. the unit is equipped with a 4kW CO2 laser supply system for use as a large heat source, a five-axis CNC machine, a powder supply consisting of three hoppers, a coaxial powder nozzle and one consisting of MX-CAM software. In particular, the coaxial powder supply nozzle tip is a symmetrical supply of powder and forms a laser to form a uniform molten pool that is supplied to the coaxial shielding gas for preventing oxidation of the molten pool. At this time, the Shield gas mainly uses an inert gas.

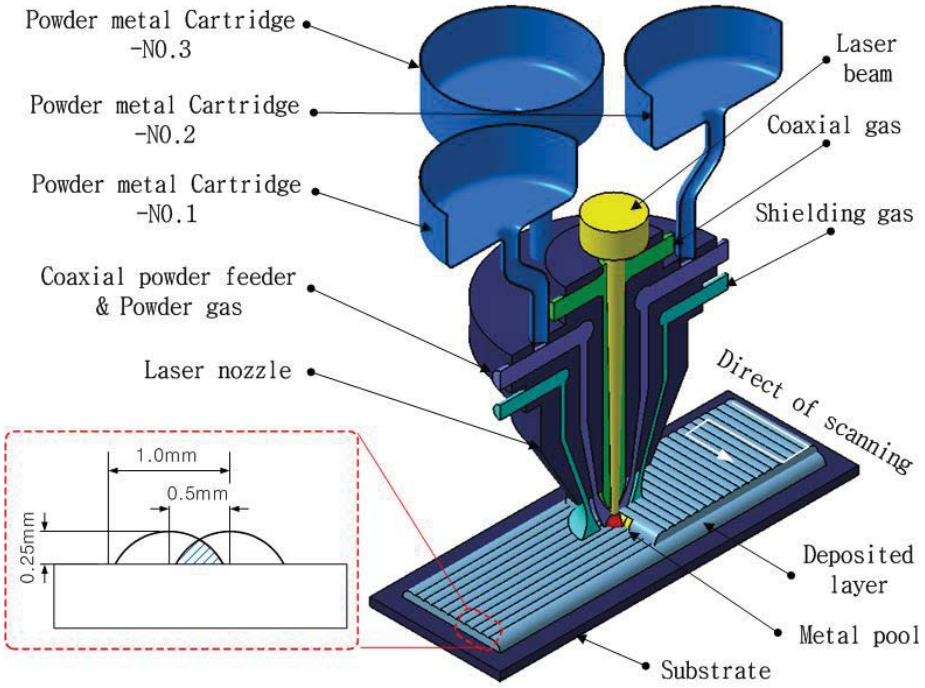

Fig. 4.1 Device configuration and additive layer concepts in DED AM systems

4.1.2 Powder material & Punch parameter

The high wear resistant steel (HWS) used in this study is a high toughness, high wear resistant cold work tool steel material specifically designed for hard cutting high

strength steel (AHS). HWS materials not only form difficult working conditions, such as cutting, deep drawing and bending dies, but also difficult to shape materials (such as high strength, high elongation CP, DP, TRIP and Mart materials with high work hardenability). It is also used for tool applications. To achieve these mechanical properties, like most tools and other specialty steels, HWS has heat treatment properties that allow for optimal mechanical and physical properties through heat treatment prior to final processing [28]. HWS powder is a CPM (powder metallurgy) series powder with high wear resistance, hardness and toughness. HWS powder contains alloying elements such as chromium (Cr), molybdenum (Mo), tungsten (W), vanadium (V), manganese (Mn), silicon (Si) and nickel (Ni) to form various carbide high carbons. The chemical composition of the alloy steel balls is shown in Table 4.1 The manufacturer did not provide a quantitative estimate of the chemical composition of the HWS powder, but the composition range was shown by a manufacturer-defined chart [29]. Therefore, the chemical composition of the HWS powder material shown in **Table 4.1** is the data of the research results obtained from the analytical study.

Table. 4.1 Chemical composition of the HWS powder material

Materials used	Element (wt %)										
	C	Si	Mn	P	S	Ni	Cr	Mo	Cu	V	W
HWS(powder)	1.08	1.38	0.34	-	-	-	7.80	1.86	-	2.66	1.73

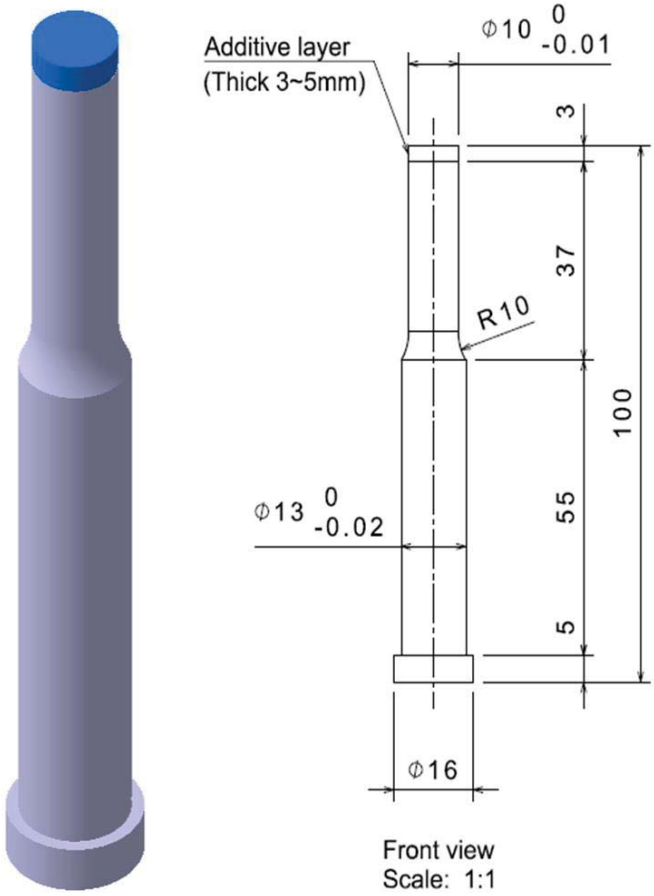

Fig. 4.2 Shape and specification of semi-additive piercing punch

The Shape and specification of semi-additive piercing punch is shown in **Fig 4.2.** The punch is 100mm in length. The punch consists of three parts. The uppermost fixed part is a cylinder with a diameter of 16mm and a length of 5mm. There is 0.5 at the joint with the middle part. Chamfer rounded corners.

In the middle is an excessive part of 55 mm in length, and the bottom part is the main working part composed of a cylinder of 10 mm in diameter and 40 mm in length. When stamping, the fixed part is fixed on the stamping upper mold. As the mold moves up and down, the working part contacts the stamped sheet to complete the stamping process.

4.1.3 Process parameters in DED method additive manufacturing

The main process parameters of metal 3D printing DED include laser power, powder feeding speed, track scanning interval and laser scanning speed. Different combinations of these parameters may have different effects on the shape and mechanical/metal properties of the additive (ie roughness, hardness and microstructure) [27]. The mechanical and metallurgical properties of the final additive can be affected by process variables. High power laser energy increases the melt rate and convection of the melt, thereby increasing the height and width of the additive beads. That is, as the laser power increases, the height, width, and dilution of the beads (between the interface/substrate and the stack) gradually increase. Increasing the powder feed rate has no effect on the bead width and dilution depth, but it does affect the rapid increase in bead height. Due to the rapid increase in the height of the bead, excessive feed of the powder can also result in excessive additive, which ultimately affects the geometric accuracy of the part.

As the scanning speed of the nozzle head feeding the laser beam and the powder increases, the height of the beads is greatly reduced, and the width and dilution depth of the beads are slightly lowered. This means that as the scanning speed increases, the powder feed rate and laser beam energy will shorten the melting time, while the specific energy density per unit volume and the powder feed density will also decrease, thereby reducing the size of the overall stacked beads. The metal powder is transported by gravity and supplied with gas through a nozzle. At this time, the powder gas is used to supply the powder for generating the molten pool on the surface of the substrate, and the coaxial gas prevents oxidation in the molten pool by injecting the processing gas around the laser beam. Increasing the powder gas flow increases

the bead height and does not affect the bead width and dilution depth. The concentration of particles in the powder stream increases as the flow rate of the powder gas increases, but the increase in the flow rate of the coaxial gas affects the amount of powder delivered to the bath [28].

As described above, it is necessary to grasp the effects of the additive process conditions by combining the process conditions, and to change the conditions according to the selected powder materials. This is because this is the process of obtaining the optimum process conditions for manufacturing high quality parts through DED technology. In particular, as described in this study, the most important factor in the heterogeneous material semi- additive technique using the DED method is the perfect bond between the substrate and the additive. In other words, the substrate material is melted by an organic combination of various process conditions, and at the same time the flowing powder material is completely melted by perfect chemical and metal bonding to form a third interface material. In the additive process, not only the interface portion where the substrate material and the powder material are combined, but also during the additive of the same powder material, the additive must be remelted, and the incoming powder material must also be melted to satisfy Combination of chemistry and metallurgy.

Therefore, the additive process conditions between heterogeneous materials do not mean that only one part is satisfied, and it is important to find a key point that can be fully satisfied between the applied materials.

So, the process for optimizing process conditions between dissimilar materials need a lot of repeated explains. **Table 4.2** lists the semi- additive process conditions

between the substrate D2 and the dissimilar materials of the powder materials HWS and P21 obtained in this study.

Table. 4.2 Process parameters for powder additive

Metal powder	Laser beam power (W)	Slicing layer height (mm)	Overlap width (mm)	Powder flow rate (g/min)	Laser traverse speed (mm/min)	Powder gas (l/min)	Coaxial gas (l/min)
P21	900	0.25	0.5	5	850	2.5	8.0

4.2 Semi-additive punch production

After fabrication, the punch and the original unreinforced punch were reinforced with a new additive process for durability testing and analysis of the results SKD11 punch(**Fig. 4.3 (a))** and HWS semi-additive reinforcing punch(**Fig. 4.3 (b)**) Multiple samples were completed during the manufacturing process for subsequent durability testing

And after determining the additive shape, the punch is actually fabricated using the determined shape, first, the additive part is machined. After the completion of the treatment, additive is performed, and after the additive process is completed, the heat treatment process is performed, and after the above process is completed, the final treatment is completed to complete the manufacture of the punch.

(a) **(b)**

Fig. 4.3 (a) SKD11 Punch, (b) HWS semi-additive reinforcing punch

4.3 Durability test

Test mechanism was Daegu Machinery Parts Research Institute .Testing equipment was 200 tons stamping die set(**Fig. 4.4 / Fig. 4.5**) test machine parameters is show in **Table. 4.3** repair mold (automatic cutting machine not available) the sheet material was CR980, 1.2mm, Width 57mm (only two punches can be used at the same time). This test uses the automatic feeding device (**Fig. 4.4 (b))** to automatically transport the metal material (**CR980**) into the punching machine. After each punching, it will be forwarded in conjunction with the automatic feeding device for automatic repeated testing.

(a) (b)

Fig. 4.4 (a) Test material, (b) Automatic feeding machine

(a) (b) (c)

Fig. 4.5 (a) Test device, (b) (c) Punching machine

Table. 4.3 Test machine parameters

Tonnage	200 ton
Bolster Size	1400mm * 840mm
Stoker Per Minute (CONTINUE)	0-40 SPM
Stroke	250 mm
Die Height	480 mm

Slide Adjustment	120 mm
Main Motor	Torque Servo Motor

The test Punch was SKD11 Bulk Punch / HWS powder half-additive punch, the test speed was 30 SPM (stroke per minute), The test method was observed after every 100 shots punch and sheet (**Fig. 4.6)**.

The test will be end when an abnormality occurs in the punch during this period, the punching machine was used to test the punch. After the stamping parameters were set, the auto feeding and the press were synchronized, the test was started. Each 1000 stamped sheets were marked during the test, and remove the punch for comparison. Every 1000 times were found in the later observation.

(a) (b)

Fig. 4.6 (a) microscope, (b) Taking pictures with the help of the staff

4.4 Analysis and consideration of test result

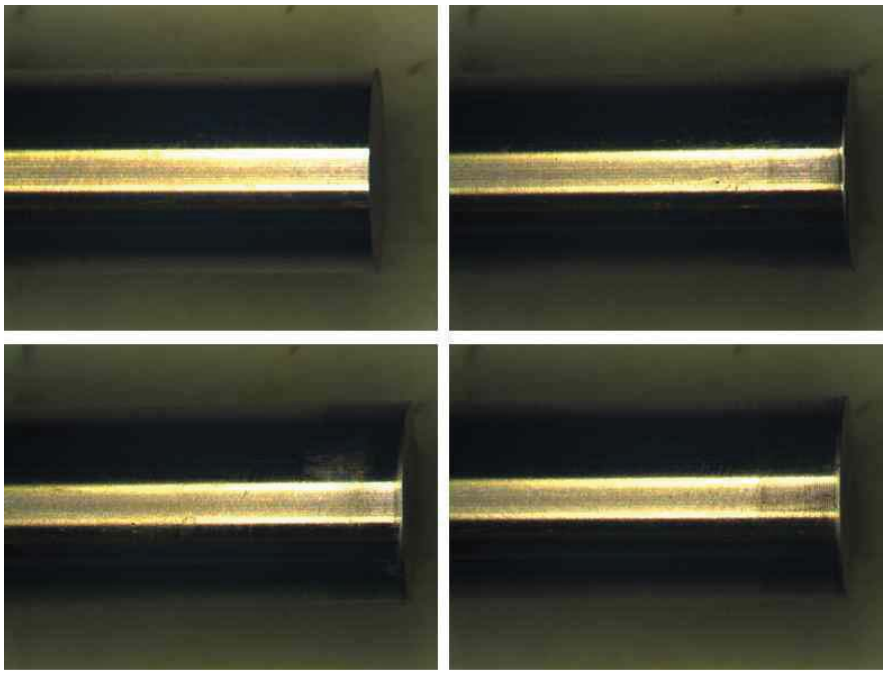

Fig. 4.7 Status after HWS powder material semi-additive punch test: 1000 Times

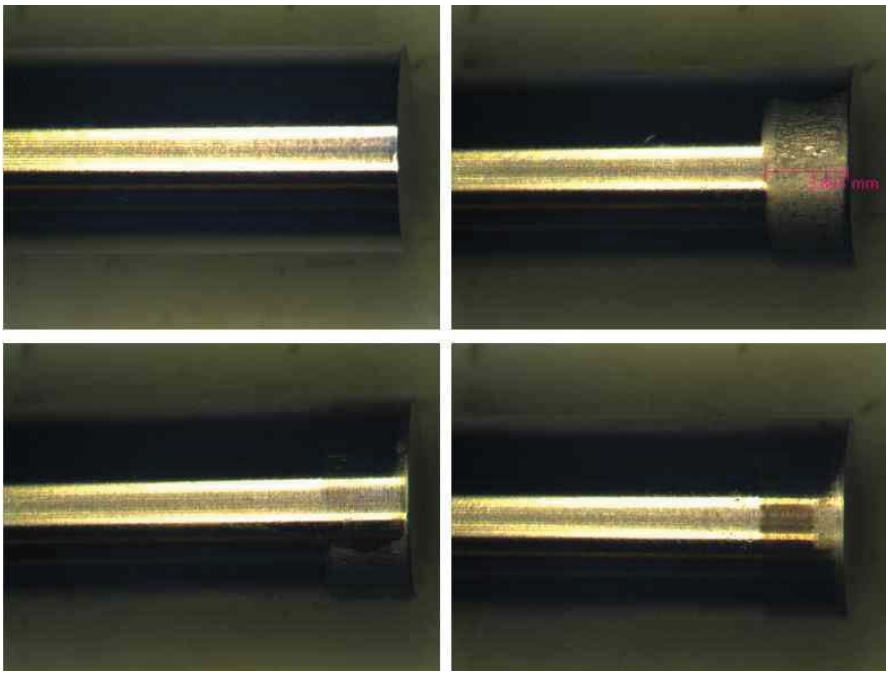

Fig. 4.8 SKD11 Bulk Material Punch Test Status: 1000 Other Tests

HWS compared with the SKD11 bulk punch, the wear performance is good. In order to be more accurate and meaningful, more stamping tests must be performed. There is a slight difference in the incision of the stamped sheet, which is the image of the durability of the different punches. (**Fig. 4.7 & Fig. 4.8**), judging from the appearance, after the same number of processing, the HWS punch still retains the basic punch shape, but the SKD11 punch has obvious visible damage to the head, which will inevitably affect the subsequent processing accuracy, and easy damaged punches continue to process and may produce more damage faster

But SKD11 bulk punch and HWS additive punch After 100(**Fig. 4.9**) strokes, 500 strokes(**Fig. 4.10**) and 1000 strokes(**Fig. 4.11**), The peculiarity of burrs in the postural observation is Unrolled but rollover slightly increased Indicates a state. In the SKD11 bulk punch, the turning of the perforations is larger than in the HWS stacking punch, which seems to affect the slight wear of the punch. Piercing punch can be greatly reduced, resulting in improved punch life. The hole machining quality of the HWS in the stamped sheet is better than that of the SKD11 hole, which also proves that the durability of the HWS punch is better.

Fig. 4.9 SKD11 bulk punch HWS Multilayer punch seat specimen hole state after 100 strokes

.

Fig. 4.10 Sheet specimen hole state after SKD11 bulk punch HWS Semi-additive punch 500 strokes

Fig. 4.11 SKD11 bulk punch HWS Multilayer punch seat specimen hole state after 1000 strokes

Chapter 5 Conclusion

5.1 Research results

In this paper, a simulation analysis was performed for the purpose of choosing a shape for using the partial semi-additive technique as a strengthening method for piercing punches. As a preliminary process, the punch strength required for the piercing process of high-strength sheet material was predicted through a process simulation analysis based on process variables. The range of the shape of the punch affecting the shear action was measured from the predicted results of punch strength. A semi-additive volume was defined based on the measured punch shape range, and various semi-additive shapes were employed. The simulation analysis for the semi-additive shape verification was performed using the friction characteristics of the interface boundary condition for the designed semi-additive shape. The following results were obtained from the simulation analysis of the semi-additive shape used for strengthening a piercing punch:

1) The main factor affecting the punch stress prediction in the piercing process is the sheet material strength, while the effect of the punch material and the punch speed (above a certain level) were insignificant.
2) The average maximum stress acting on the punches in the piercing process of the high-strength sheet material 22MnB5 was 3,267 MPa, and the depth and height of the punch shape in which stress was concentrated were estimated to be 1.3 mm and 3.2 mm, respectively.

3) The average maximum stress acting on the punches in the punching process of the CP1180 high-strength sheet material was 2,256 MPa, and the depth and height of the punch shape where the stress was concentrated were estimated to be 1.21 mm and 2.625 mm, respectively.

4) Confirmed that the range of semi-additive shape (depth / height) predicted in this study was within the range of 2 to 3 mm, which is a possible range for additive manufacture high-strength metal mold powder material by 3D printing.

5) A flat type shape was the most stable shape to add, while the next best shape was an edge having a triangular sectional shape. This shows that in the semi-additive shape, an interface with a 45 degree and pure line is more stable than the case with a curve, a perpendicular shape or an acute angle.

6) In the case of a rectangular cross section having a vertical additive interface, separation occurred as the interface moved away from the punch edge. Therefore, it has been shown that it is advantageous to prevent the separation phenomenon by adding as thin a layer as possible in the depth direction of the punch body.

7) In this semi-additive shape selection, con-firmed that more complicated shapes are more susceptible to impact, and larger additive areas result in more slip or separation. In addition, confirmed that additive interfaces with a thin, low, simple shape can be used for improving the lifetime of a semi-additive punch.

8) The maximum point of the punch stress appeared in the sidewall of the punch during the machining process, and a horizontal force appeared which is one of the causes punch damage.

9) In the durability test, the damage of SKD11 punch is greater than that of HWS punch under the same number of punching times, which will affect the quality of punching resulting in improved punch life. The punch durability of HWS powder is higher than that before unreinforced, and it can be used longer in processing.

5.2 Future research topics

In the post-treatment process of the heat treated sheet parts, not only the piercing process but also the trimming process is very difficult. Moreover, the trimming process for the post-treatment of the hot stamping is more difficult. The trimming process for the post-treatment of hot stamping is almost identical to the piercing process. Therefore, the research method for the piercing process studied in this paper can be applied to trimming process for the future research also.

In the future work, analyze the range of maximum stress that the punch of the trim ming process receives during processing, and then will be determine the strengthening area of the trimming punch based on the range of maximum stress. And, the strength ening portion shape design of trimming punch, simulation test to determine the final metal 3D printing shape, And practically, the trimming punches will be manufactured and tested for durability.

REFRERNCE

[1] Z. Wang, H. Kubota, D. Xue, Q. Lin, M. Okamura, Galling Behavior in Square Cup Drawing of High-tensile-strength Steel, *J. Jpn. Soc. Technol. Plast*., 47 (549) (2006) 988~992.

[2] H. S. Choi, S. G. Kim, B. M. Kim, D. C. Ko, Quantitative Evaluation of Scratch Related Tool Life for Stamping of UHSS Using Pin-on-Flat Surface Test, *Trans. Mater. Process*., 22 (2) (2013) 86~92.

[3] G. Y. Baek, D. S. Shim, J. S. Seo, M. H. Kim, Hardfacing of Piercing mold using DED technique, *Conference of The Korean Society For Technology of Plasticity*, (2016) 122-122.

[4] Y. S. Kim, R. Li, V. T. Hoang, J. W. Kum, Y. J. Yum, S. Y. Yang, "A Study on the Production of Full-Additive Manufacturing Punch fabricated of High-Strength Mold Steel Powder Materials Using 3DP Technique", *21st International Conference on Mechatronics Technology*, (2017) 366-371.

[5] Y. S. Kim, R. Li, V. T. Hoang, J. W. Kum, Y. J. Yum, S. Y. Yang, A Study on Mechanical Properties of HWS (High Wear resistance Steel) Powder Material using the Additive Manufacturing (AM) DED (Directed Energy Deposition) Process by Metal 3D Printing, *The 13th International Forum on Strategic Technology*, (2018) 22-22.

[6] E. M. Lee, G. W. Shin, K. Y. Lee, H. S. Yoon, D. S. Shim, Study of High Speed Steel AISI M4 Powder Deposition using Direct Energy Deposition Process, *The Korean Society For Technology of Plasticity, Transactions of Materials Processing*, 25 (6) (2016) 353-358

[7] G. Y. Baek, G. Y. Shin, E. M. Lee, D. S. Shim, K. Y. Lee, H. S. Yoon, M. H. Kim, Mechanical Characteristics of a Tool Steel Layer Deposited by Using Direct Energy Deposition, *Met. Mater. Int*., 23 (4) (2017) 770~777.

[8] D. S. Shim, G. Y. Baek, E. M. Lee, Effect of substrate preheating by induction heater on direct energy deposition of AISI M4 powder, *Materials Science & Engineering* A 682 (2017) 550–562.

[9] E. M. Lee, G. Y. Shin, H. S. Yoon, D. S. Shim, Study of the effects of process parameters on deposited single track of M4 powder based direct energy deposition, *Journal of Mechanical Science and Technology* 31 (7) (2017) 3411~3418

[10] R. Li, V. T. Hoang, Y. S. Kim, Y. J. Yum, S. Y. Yang, J. W. Kim, A Study on Analytical Prediction of Punch Strength Required for Ultra High Strength Parts in Piercing Process after Hot Stamping, *12th International Forum On Strategic Technology*, (2017) 71~71

[11] R. Li, V. T. Hoang, J. W. Kim, Y. S. Kim, Y. J. Yum, S. Y. Yang, A Study Prediction of Punch Shape Range for Improving Punch Strength by Partial Semi-Additive Method Using Metal 3D Printing Technique, *21st International Conference on Mechatronics Technology*, (2017) 350~354

[12] R. Li, V. T. Hoang, J. W. Kim, Y. S. Kim, Y. J. Yum, S. Y. Yang, A Study on the Semi-Additive Shape Design for Strengthening Metal Molds of Functional part by Using High Alloy Tool Steel (High Speed Steel) Powder and Metal 3D Printing Technique. *2017 KSAE Annual Autumn Conference and Exhibition*, (2017) 119~119

[13] S. L. Wang, R. Li, V. T. Hoang, W. J. Kim, Y. S. Kim, Y. J. Yum, S. Y. Yang, A Study on the Optimization of Punch Edges Shape for Enhancing Functional Part of Piercing Punch, *Proceedings of the KSME Spring Annual Meeting*, (2018)

[14] Manas Shirgaokar, Hyunjoong Cho, Taylan Altan, New Developments in FEM Based Process Simulation to Predict and Eliminate Material Failure in Cold Extrusion, *Engineering Research Center for Net Shape Manufacturing (ERC/NSM),* The Ohio State University, 339 Baker Systems, 1971 Neil Avenue, Columbus, Ohio-USA.

[15] H. K Kim and M. Yamanaka, Prediction and elimination of ductile fracture in cold forgings using FEM simulation, Engineering Reseach Center for Net shape Manufacturing, *Columbus, Ohio*, USA, SFTC REF #103

[16] D. Y Kim, H. I. Park, J. W. Lee, J. H. Kim, M. G. Lee and Y. S. Lee, Experimental study on forming behavior of high-strength steel sheets under electromagnetic pressure, *Proc IMechE Part B: Journal Engineering Manufacture 229 (4)*, (2015) 670–81

[17] S. H. Cha, M. S. Ahn, J. D. Nam, P. K. Seo, K. W. Won, B. M. Kim, Development of the Trimming Die for the Automotive Sill Side Part with Advanced High Strength Steel of CP1180, *The Korean Society for Technology of Plasticity 2012 Fall Conference*, (2012) 211-214

[18] H. S. Choi, J. W. Lee, S. G. Kim, D. C. Ko, P. K. Seo, B. M. Kim, The Effect of Process Parameters on The Characteristic of Sheared Edge in Trimming of DP980, *The Korean Society for Technology of Plasticity 2012 Fall Conference* , (2012), 542-545

[19] Bardelcik, Alexander, "High Strain Rate Behaviour of Hot Formed Boron Steel with Tailored Properties", *University of Waterloo, Mechanical and Mechatronics Engineering Theses*, 2013.

[20] H. S. Choi, B. M. Kim, D. H. Kim, D. C. Ko, Application of mechanical trimming to hot stamped 22MnB5 parts for energy saving", *International Journal of Precision Engineering and Manufacturing* 15 (6) (2014) 1087~1093

[21] Xin Wu and Hamed Bahmanpour, Characterization of Mechanically Sheared Edges of Dual Phase Steels, *Department of Mechanical Engineering, Wayne State University*, Detroit, MI 48202

[22] Hyun-Woo Lee, Jung-Bok Hwang, Sun-Ung Kim, Won-Hyuck Kim, Seung-Jo Yoo, Hyun-Woo Lim , Young-Jin Yum, "Construction of Vehicle Door Impact Beam Using Hot Stamping Technology," *The Transactions of the Korean Society of*

Mechanical Engineers A, 34 (6) (2010) 797~803.

[23] A. Yanagida, and A. Azushima, CIRP Annals-Manufacturing Technology 58 (1), (2009) 247-250

[24] B. Shapiro, “Using ls-dyna for hot stamping”, *in 7th European LS-DYNA Conference*, Stuttgart, Germany, 2009.

[25] S. H. Cha, M. S. Ahn, J. D. Nam, P. K. Seo, K. W. Won, B. M. Kim, Development of the Trimming Die for the Automotive Sill Side Part with Advanced High Strength Steel of CP1180, *The Korean Society for Technology of Plasticity 2012 Fall Conference*, (2012) 211-214

[26] H. S. Choi, J. W. Lee, S. G. Kim, D. C. Ko, P. K. Seo, B. M. Kim, The Effect of Process Parameters on The Characteristic of Sheared Edge in Trimming of DP980), *Proceedings of the Korean Society for Technology of Plasticity*, (2012) 542-545.

[27] Anthony J. Smith, B.S., Procedure And Results For Constitutive Equations For Advanced High Strength Steels Incorporating Strain, Strain Rate, And Temperature, *THESIS for the Degree Master of Science in the Graduate School of The Ohio State University*, (2012) 10~34.

[28] R. Li, V. T. Hoang, J. W. Kim, Y. S. Kim, Y. J. Yum, S. Y. Yang, Additive manufacturing (AM) of piercing punches by the PBF method of metal 3D printing using mold steel powder materials, *Journal of Mechanical Science and Technology 33 (2) (2019) 1~8*

[29] ORSA Endüstriyel Malzemeler Web site, http://www.orsa-ltd.com/upload/files/katalog/Rovalma/ORSA-HWS-soguk-is-toz-metal.pdf

[30] ROVALMA S.A, "Quality Control Protocol of HWS metal powder," Rovalma′s reference: 171402C02001, Date of delivery note: 21/02/2017.

[31] Young Jin Yum, Soon Yong Yang, Yong Seok Kim, Hoang Van Tho, Jin Young Kim, Seong Woong Choi and Jong Won Kum, "A Study on the Fabrication of

Punch for the Post Processing of Ultra High Strength Part by Hot Stamping Using 3D Printing Technology," Proceedings of KSME Conference, Vol.2017, 307-308, (2017)

[32] N. R. Park, D. G. Ahn., "Wear Characteristics of Stellite6 and NOREM02 Hardfaced SKD61 Hot Working Tool Steel at the Elevated Temperature", International Journal of Precision Engineering and Manufacturing, Vol.15, No. 12, pp.2549-2558, 2014.

[33] S. H. Wang, J.-Y. Chen, and L. Xue., "A study of the abrasive wear behaviour of laser-clad tool steel coatings", Surface and Coatings Technology, Vol.200, 3446-3458, (2006).

[34] J. S. Park, M.-G. Lee, Y.-J. Cho, J. H. Sung, M.-S. Jeong, D. H. Kim, et al., "Effect of heat treatment on the characteristics of tool steel deposited by the directed energy deposition process", Metals and Materials International, Vol.22, 143-147, (2016).

[35] M. Pleterski, T. Muhičč, B. Podgornik, and J. Tuššek., "Blanking punch life improvement by laser cladding," Engineering Failure Analysis, Vol.18, 1527-1537, (2011).

[36] Y. Chew and J. H. L. Pang., "Fatigue life prediction model for laser clad AISI 4340 specimens with multiple surface cracks, "International Journal of Fatigue, Vol.87, 235-244, (2016).

[37] J. H. Jang, B. D. Joo, S. M. Mun, M. Y. Sung, and Y. H. Moon., "Application of direct laser melting to restore damaged steel dies," Metals and Materials International, Vol.17, 167-174, (2011).

[38] Lee, S. H., Lee, J.W., Sung, J.H., "The application of Conformal Cooling Channel in Injection Molding," Proceeding of Autumn Symposium of the Korean Society for Technology of Plasticity, 2012, 40~43 (in Korean)

[39] Woo-Sung Kim, Myung-Pyo Hong, Jun-Seok Park, Yun-Soon Lee, Kyoung Je Cha, Ji-Hyun Sung, Min-Wha Jung, Ye-Hwan Lee, "Case Studies on Applications of Conformal Cooling Channel Based On DMT Technology," Journal of the

Korean Society of Manufacturing Process Engineers, Vol.14 No.3, pp.9~14(2015.6)

[40] Woo-sung Kim, Myungpyo Hong, Yanggon Kim, Chang Hee Suh, Jongwon Lee, Sunghee Lee, Ji Hyun Sung, "Effects and Application Cases of Injection Molds by using DED type Additive Manufacturing Process," Journal of The Korean Welding & Joining Society 32(4), 2014.8, 10-14 (5 pages)

[41] M. P. Hong, J. H. Sung, D. C. Ahn, Y. S. Kim, "A Study on Three-Dimensional Molding Technology Mold Directly How to Repair," Proceedings of KSCE 2014 Spring Conference, 2014.5, 247-249.

[42] Rui Li, Yong Seok Kim, Hoang Van Tho, Young Jin Yum, Won Jun Kim. and Soon Yong Yang., "Additive manufacturing (AM) of piercing punches by the PBF method of metal 3D printing using mold steel powder materials," Journal of Mechanical Science and Technology, Vol.33, pp809-817, (2019)

[43] M.-P. Hong, J.-H. Sung, K.-J. Cha, W.-s. Kim, Y.-S. Lee, M.-G. Lee, Y.-S. Kwak, H.-S. Kim and Y.-S. Kim, "A Study on the Manufacturing Technology of High Strength Steel Trimming Die of 780MPa Class by using Dissimilar Material Additive Manufacturing Technology", Proceedings of KSPE Conference, Vol.2017 No.5, (2017)

[44] M. P. Hong, J. H. Sung, W. S. Kim, Y. S. Lee, J.W. Lee, G. J. Cha and K. M. Bae, "Study on Hot Stamping Die Manufacturing using AM(Additive Manufacturing) Technology," Proceedings of KSPE Conference, Vol.2016 No.5, (2016)

[45] S. Y. Lee, S. K. Lee, I. K. Lee, M. S. Jeong, J. H. Sung, J. W. Lee, D. H. Kim, Y. J. Cho and D. C. Ko, "Evaluation of Wear Characteristics of Porthole Extrusion Die Material Repaired by Metal Additive Manufacturing Process," Proceedings of KSTP Conference, Vol.2016 No.4, (2016)

[46] S. Y. Lee, S. K. Lee, I. K. Lee, M. S. Jung, J. H. Sung, D. H. Kim, Y. J. Cho, K. J. Cha and D. C. KO, "Evaluation of Wear Characteristics for Repaired STD61 by 3D Printing Process," Proceedings of KSPE Conference, Vol.2016 No.5, (2016)

[47] W.H. Kim, B.H. Jung, I.D. Park, M.H. Oh, S.W. Choi and D.M. Kang, ″Surface

hardness as a function of laser metal deposition parameters," Transactions of Materials Processing, 24(4), 272–279, (2015)

[48] Gyeong Yun Baek, Gwang Yong Shin, Eun Mi Lee, Do Sik Shim, Ki Yong Lee, Hi-Seak Yoon, and Myoung Ho Kim., "Mechanical Characteristics of a Tool Steel Layer Deposited by Using Direct Energy Deposition," Metals and Materials International, Vol. 23, No. 4, pp. 770~777, (2017)

[49] E. M. Lee, G. W. Shin, K. Y. Lee, H. S. Yoon and D. S. Shim, "Study of High Speed Steel AISI M4 Powder Deposition using Direct Energy Deposition Process," Transactions of Materials Processing, Vol.25(6),pp353-358, (2016)

[50] Do-Sik Shim,∗, Gyeong-Yun Baek and Eun-Mi Lee, "Effect of substrate preheating by induction heater on direct energy deposition of AISI M4 powder," Materials Science & Engineering: A, Vol.682, pp.550–562,(2017)

[51] G. Y. Baek, K. Y. Lee, G. Y. Shin, J. Y. Seo and D. S. Shim, "Study on the deposition of CPM15V and M4 powder on SKD11 substrate using Direct energy deposition(DED)," Proceedings of KSPE Conference 2017.5, pp.776-776. (2017)

【Appendix1: 20 shapes designed Simulation】

1:Flat type

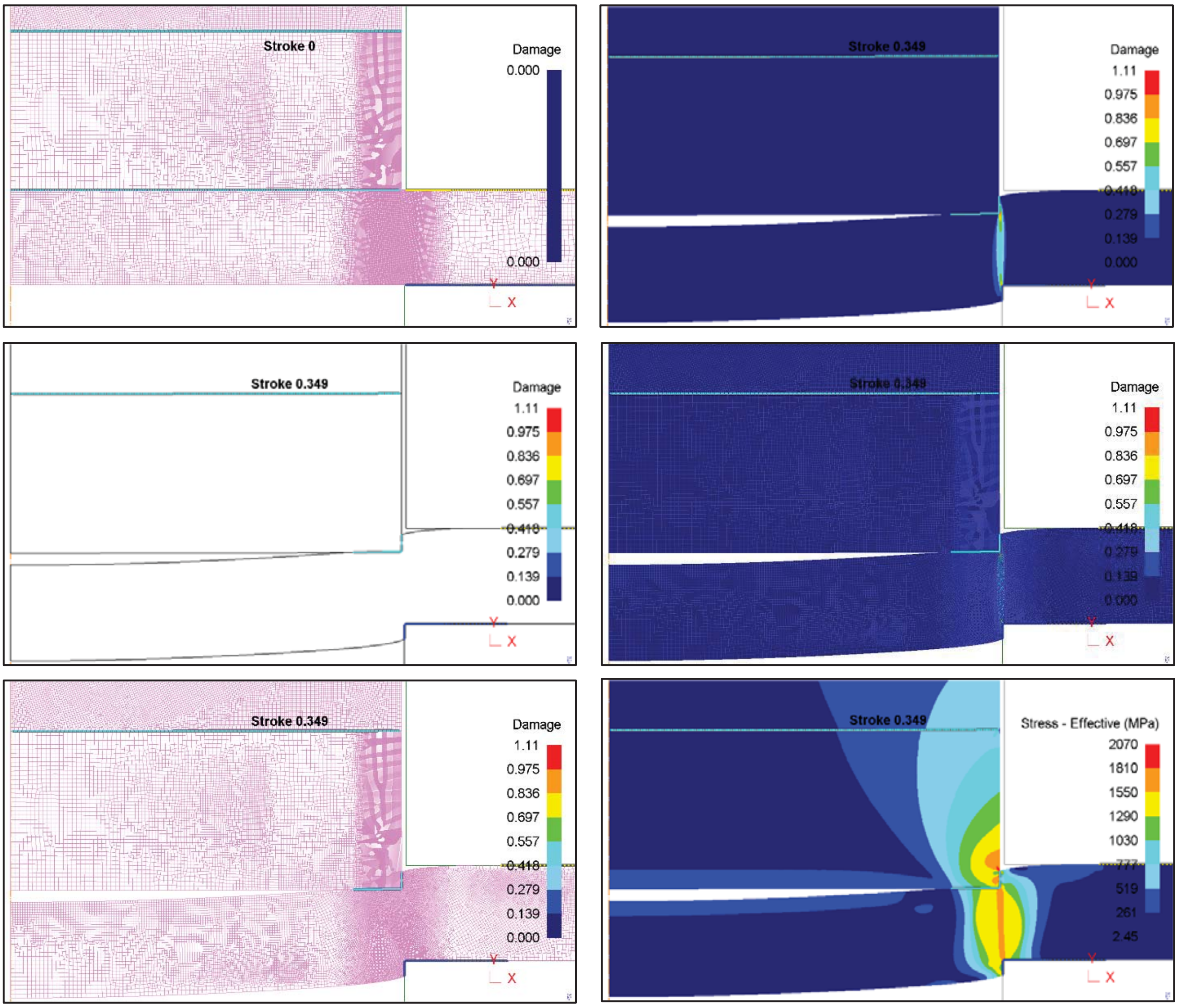

2. Thick-ring type

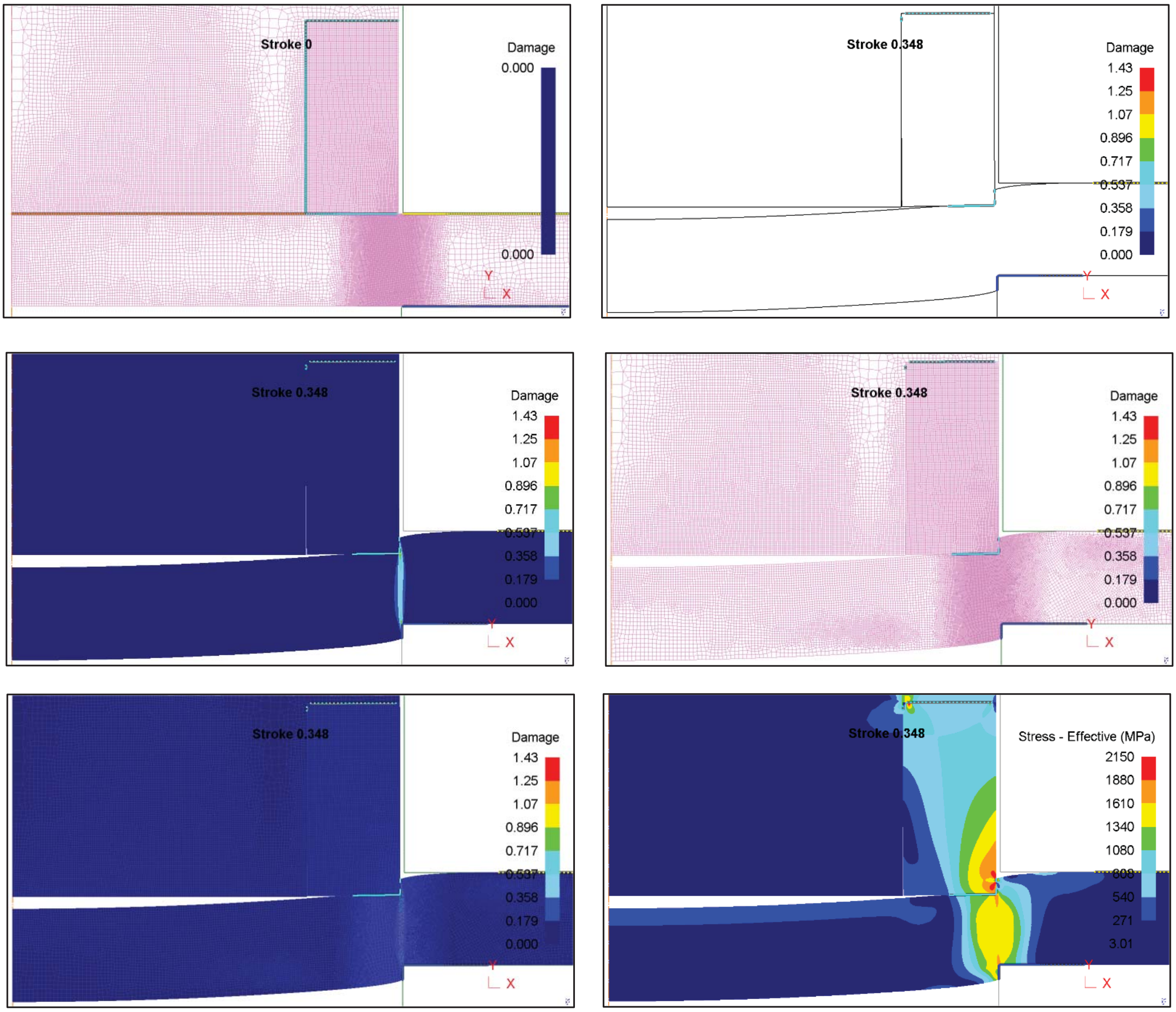

3. Thin-ring type

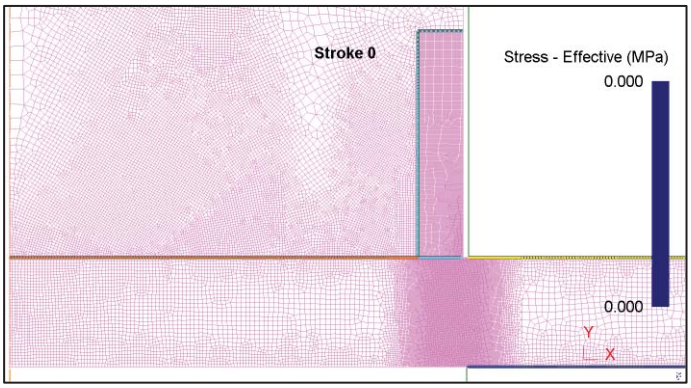

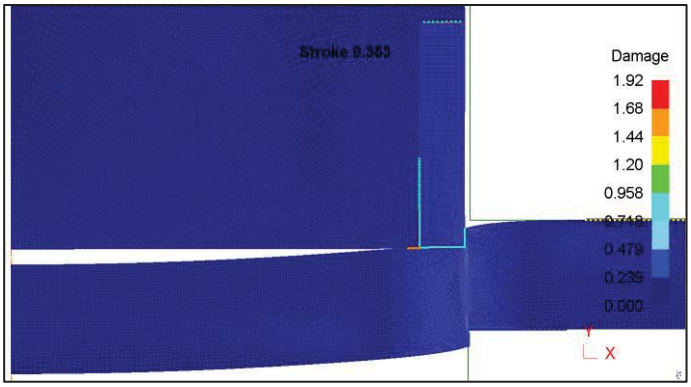

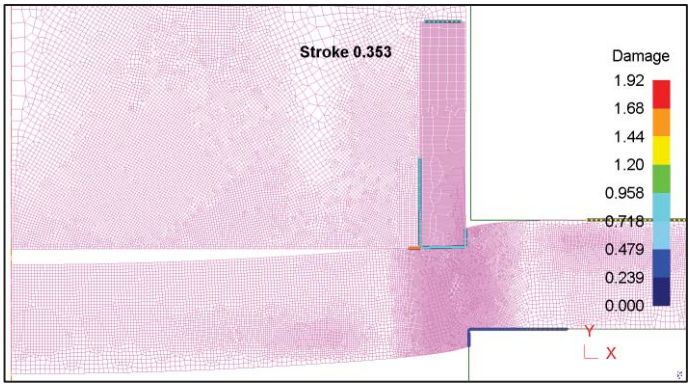

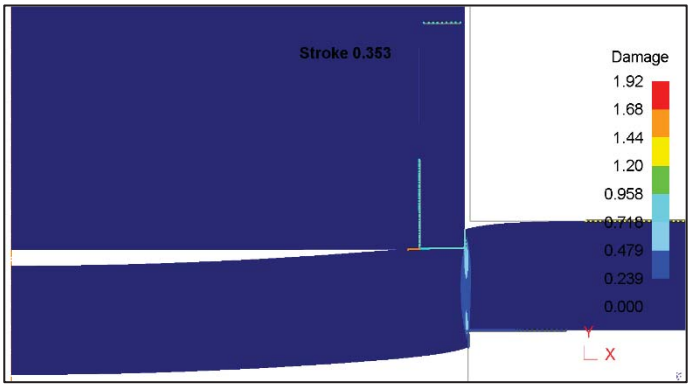

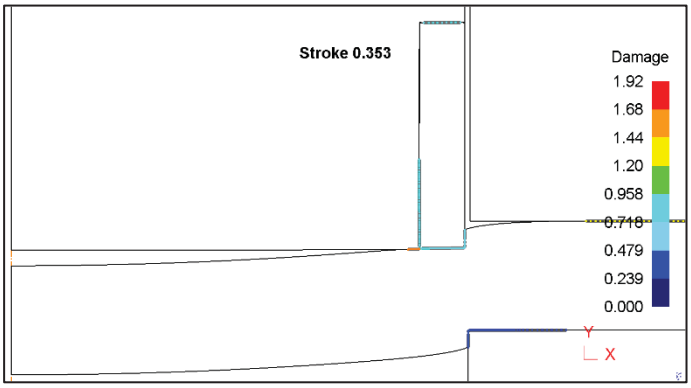

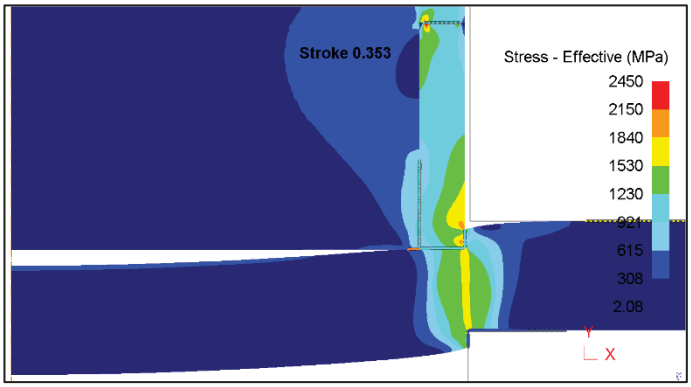

4. Cap type

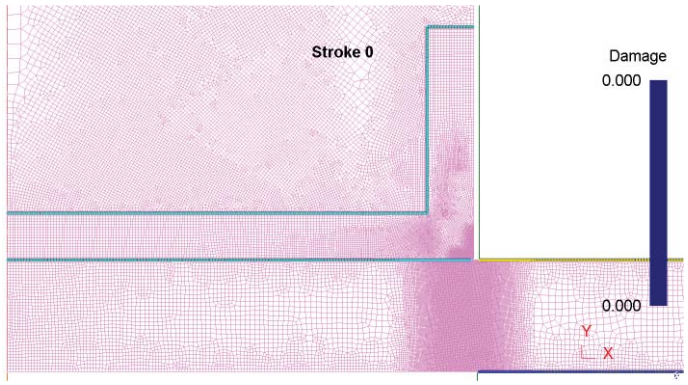
Stroke 0
Damage
0.000
0.000
Y
X

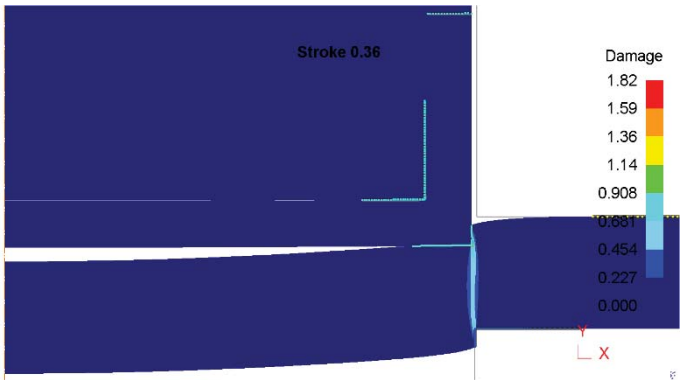
Stroke 0.36
Damage
1.82
1.59
1.36
1.14
0.908
0.681
0.454
0.227
0.000
X


Stroke 0.36
Damage
1.82
1.59
1.36
1.14
0.908
0.681
0.454
0.227
0.000
Y
X

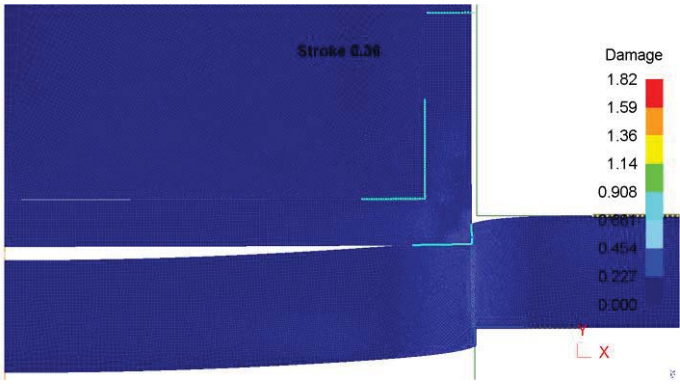
Stroke 0.36
Damage
1.82
1.59
1.36
1.14
0.908
0.454
0.227
0.000
X

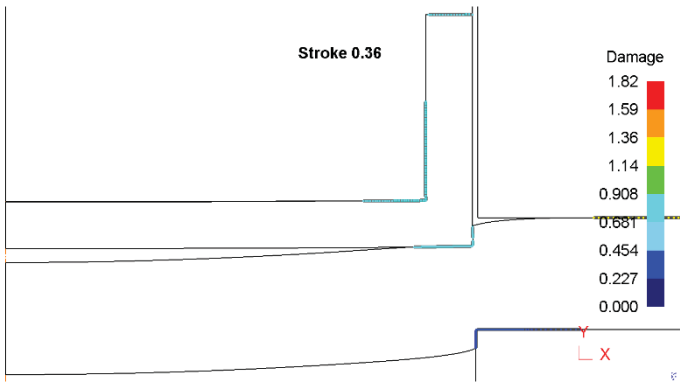
Stroke 0.36
Damage
1.82
1.59
1.36
1.14
0.908
0.681
0.454
0.227
0.000
Y
X

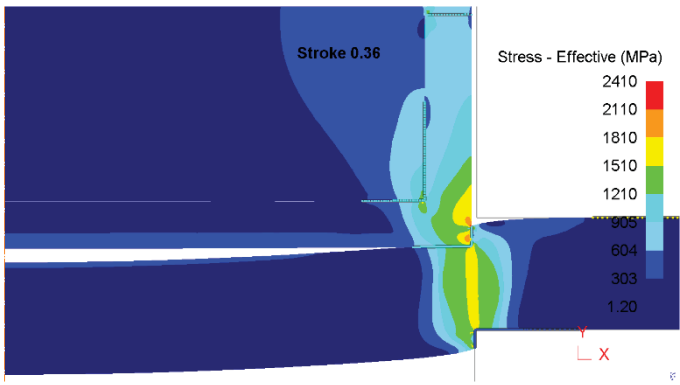
Stroke 0.36
Stress - Effective (MPa)
2410
2110
1810
1510
1210
905
604
303
1.20
X

5. Half-cap type

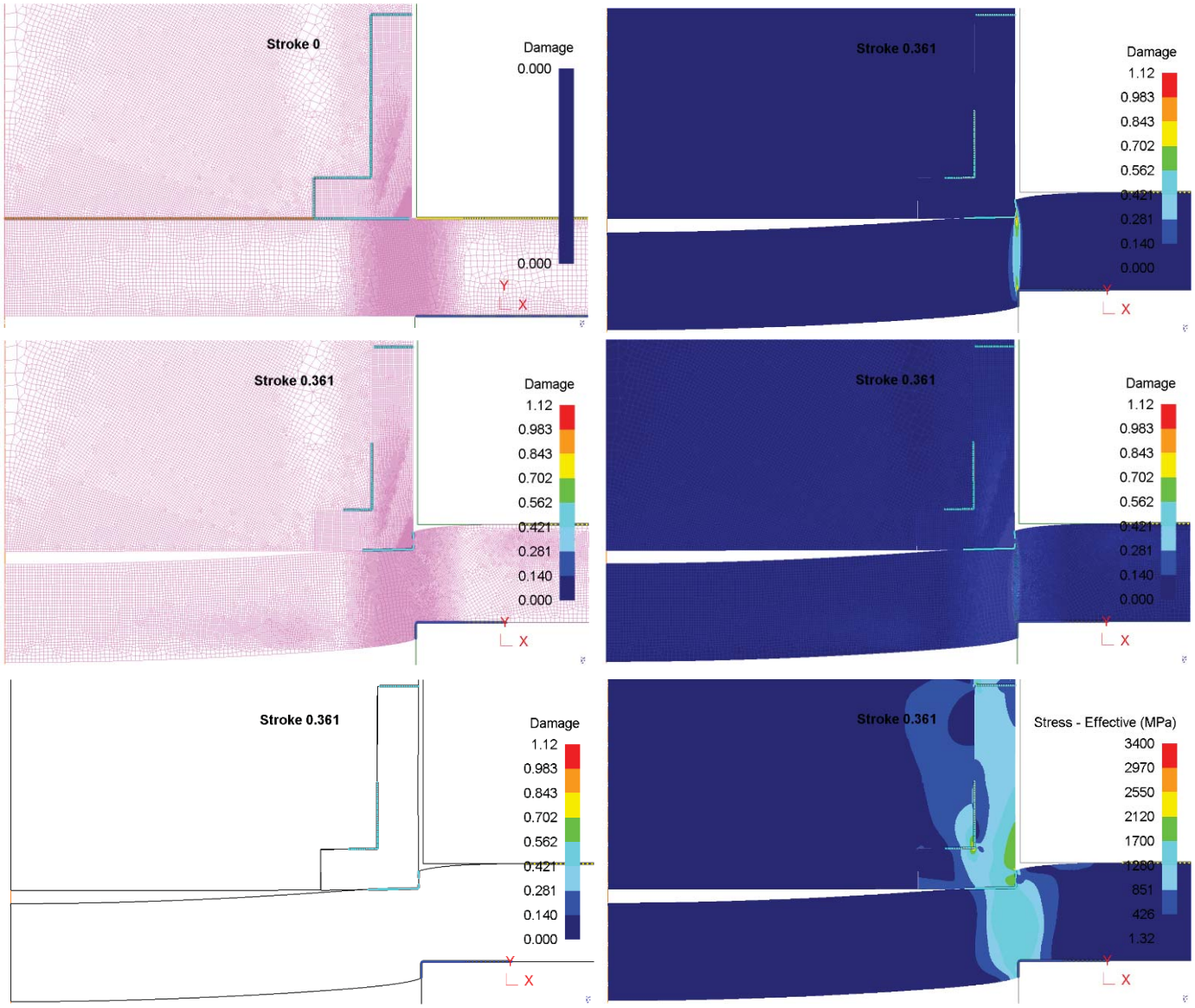

6. Ring lug-cap type

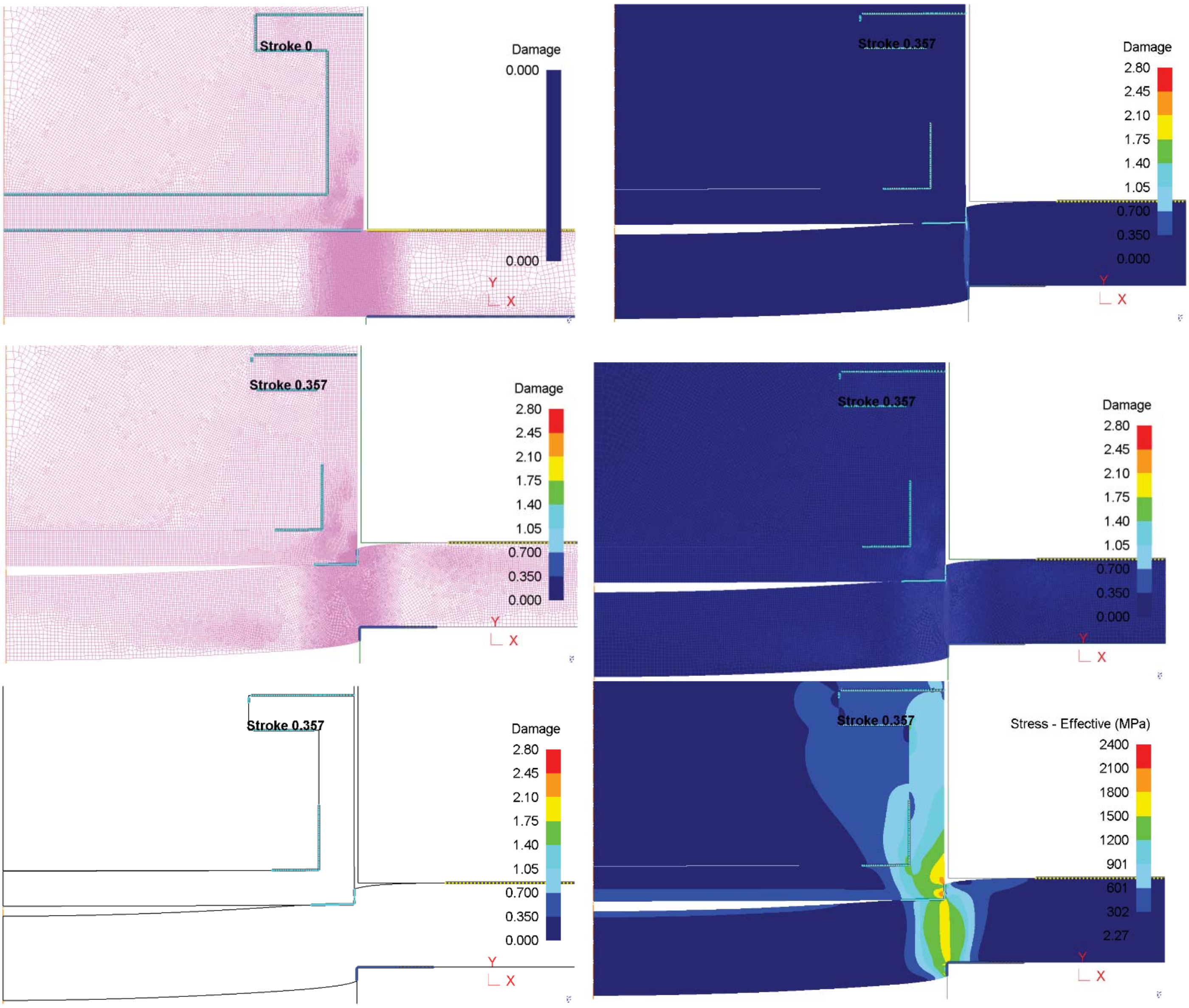

7. Straight-edge type

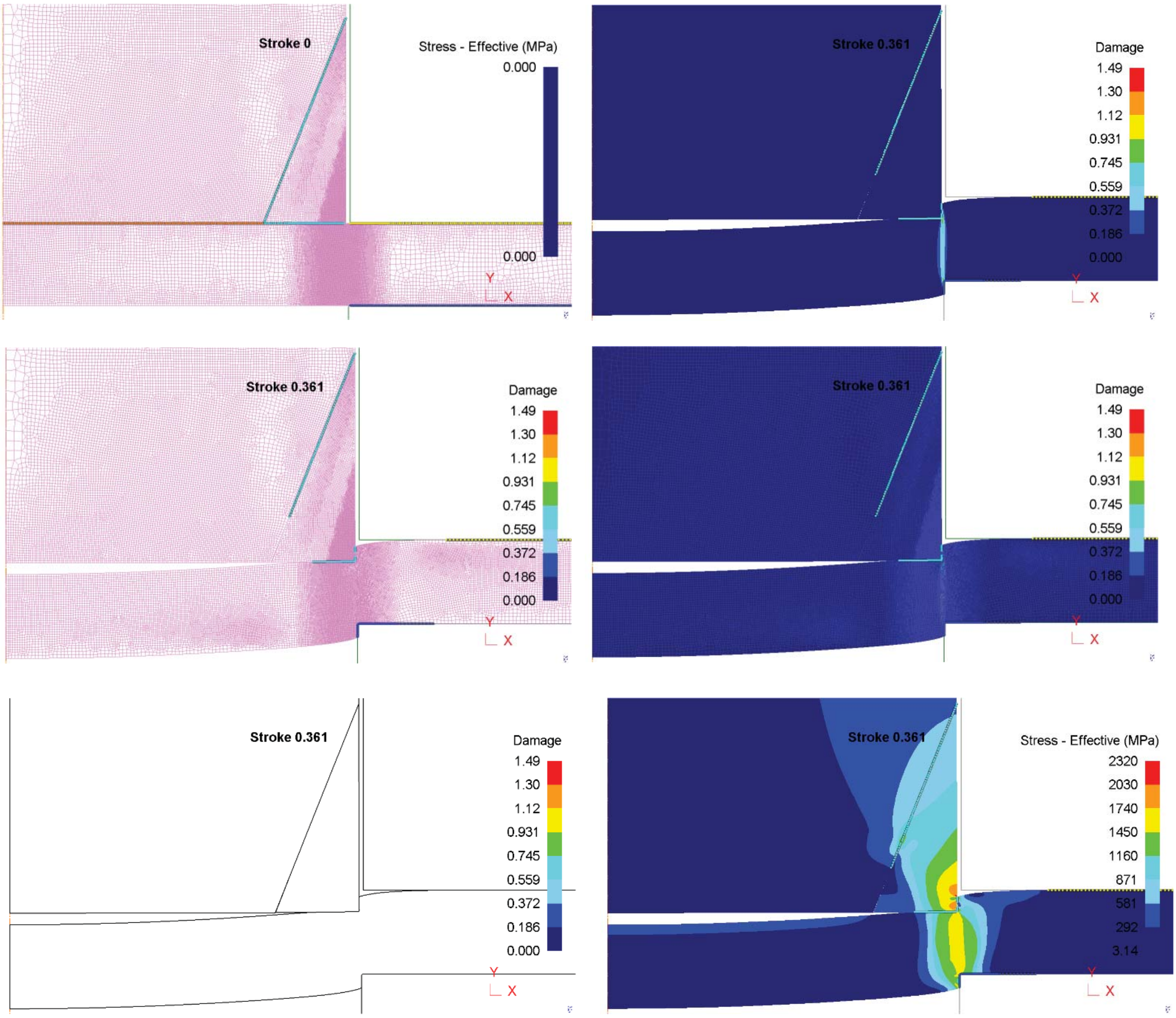

8. Straight-edge-S-lug type

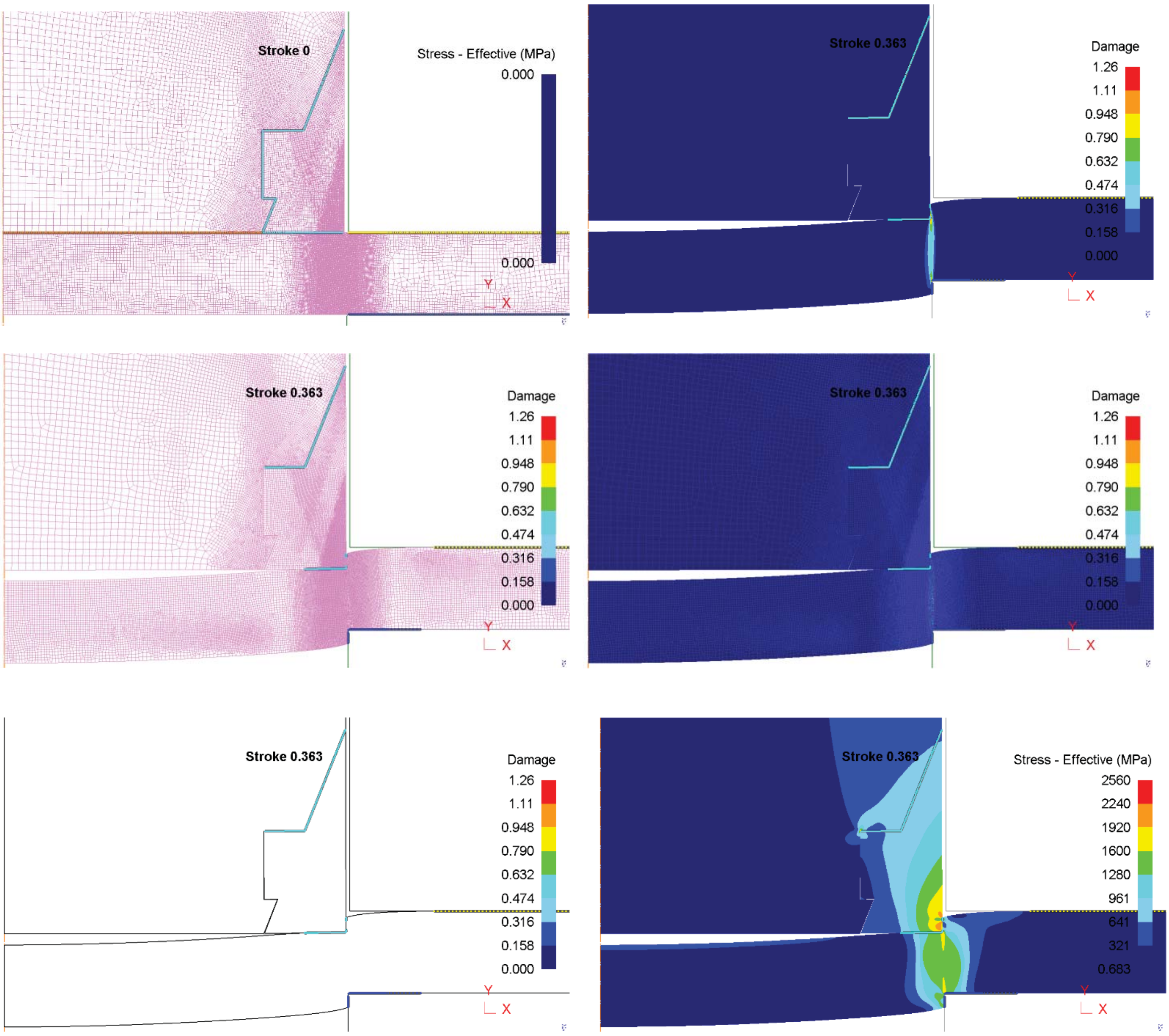

9. Straight-edge-R-lug type

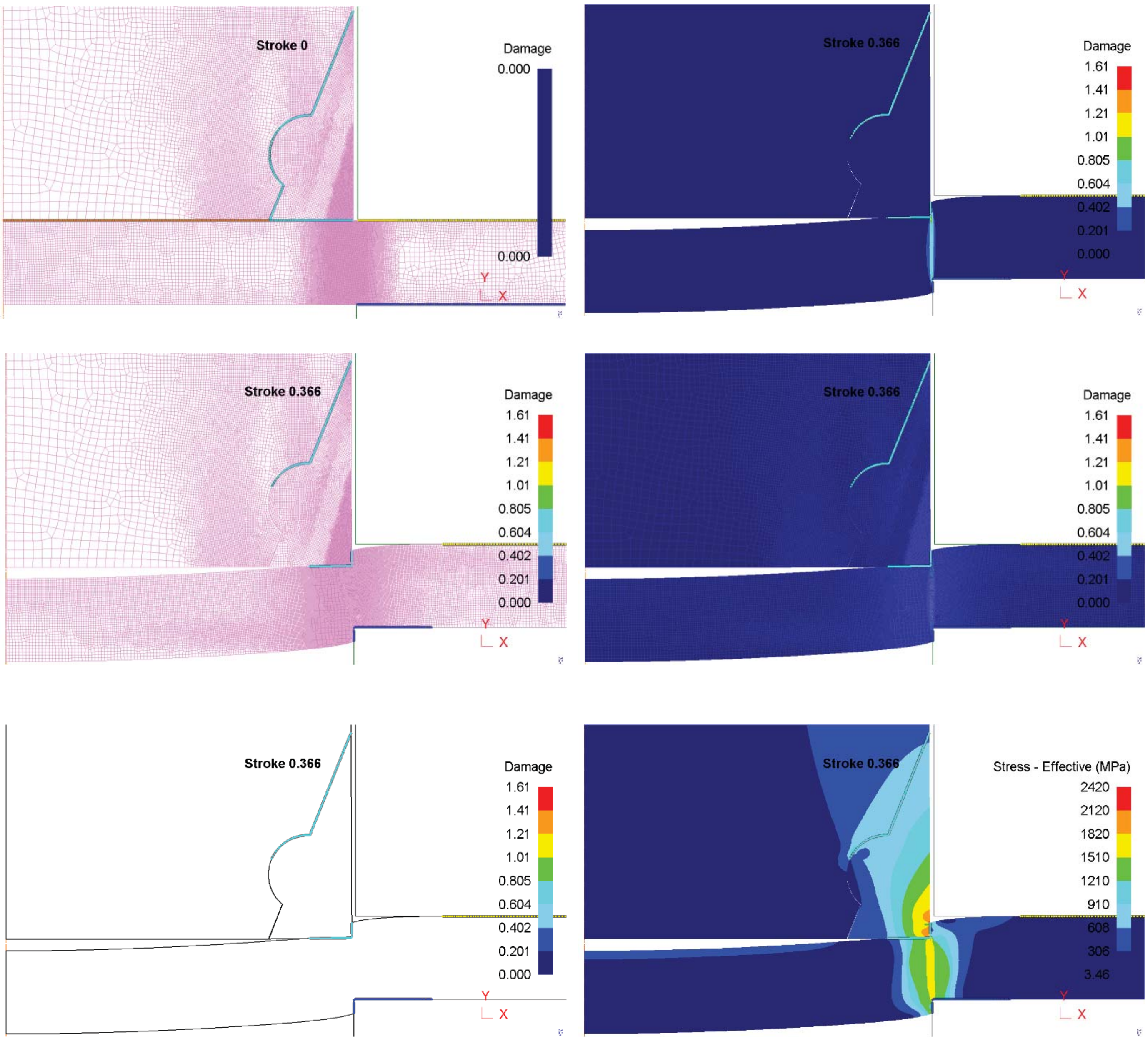

10. Top Triangle-Bottom Square-Big Type

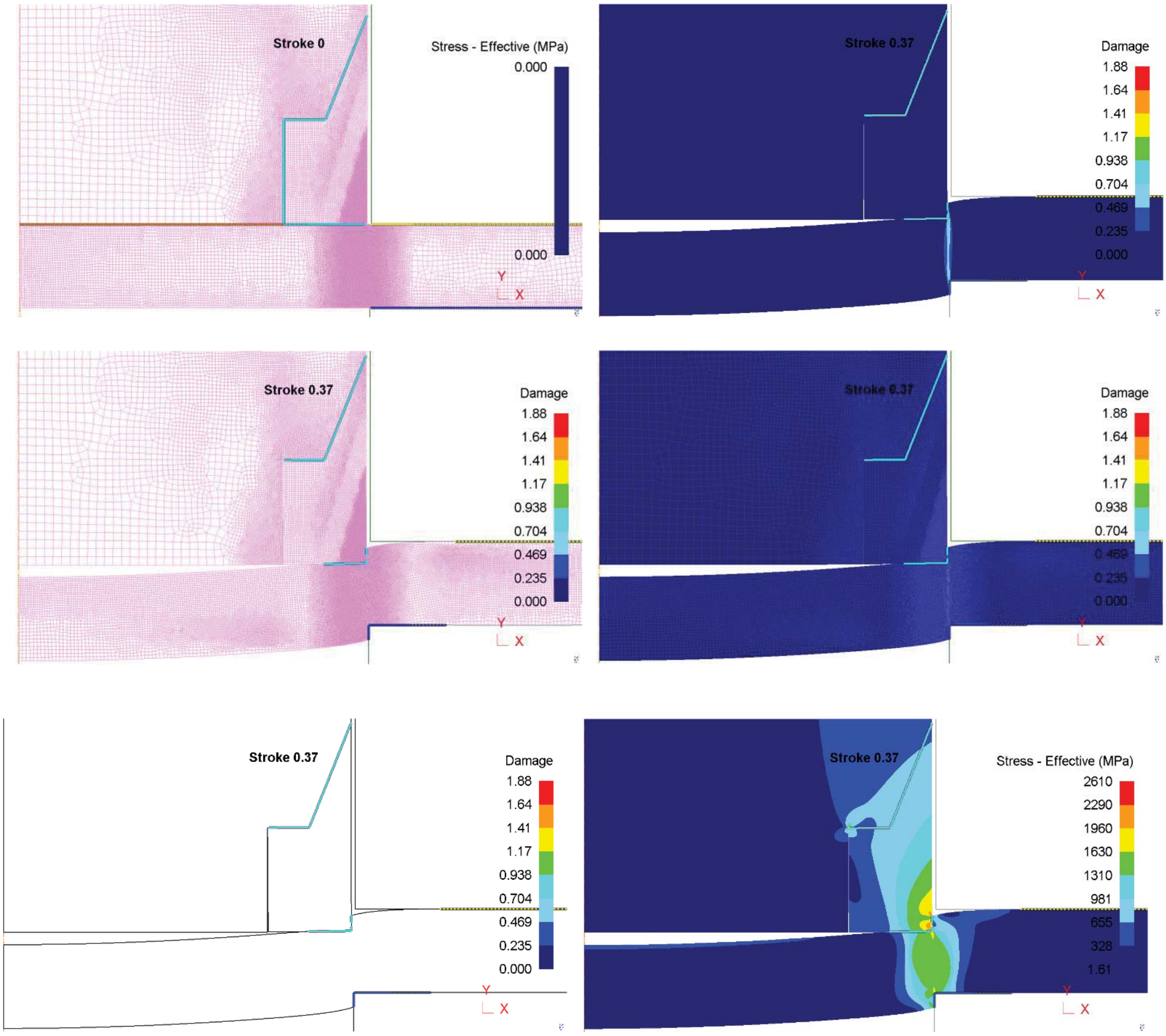

11. Top Triangle-Bottom Square-Small Type

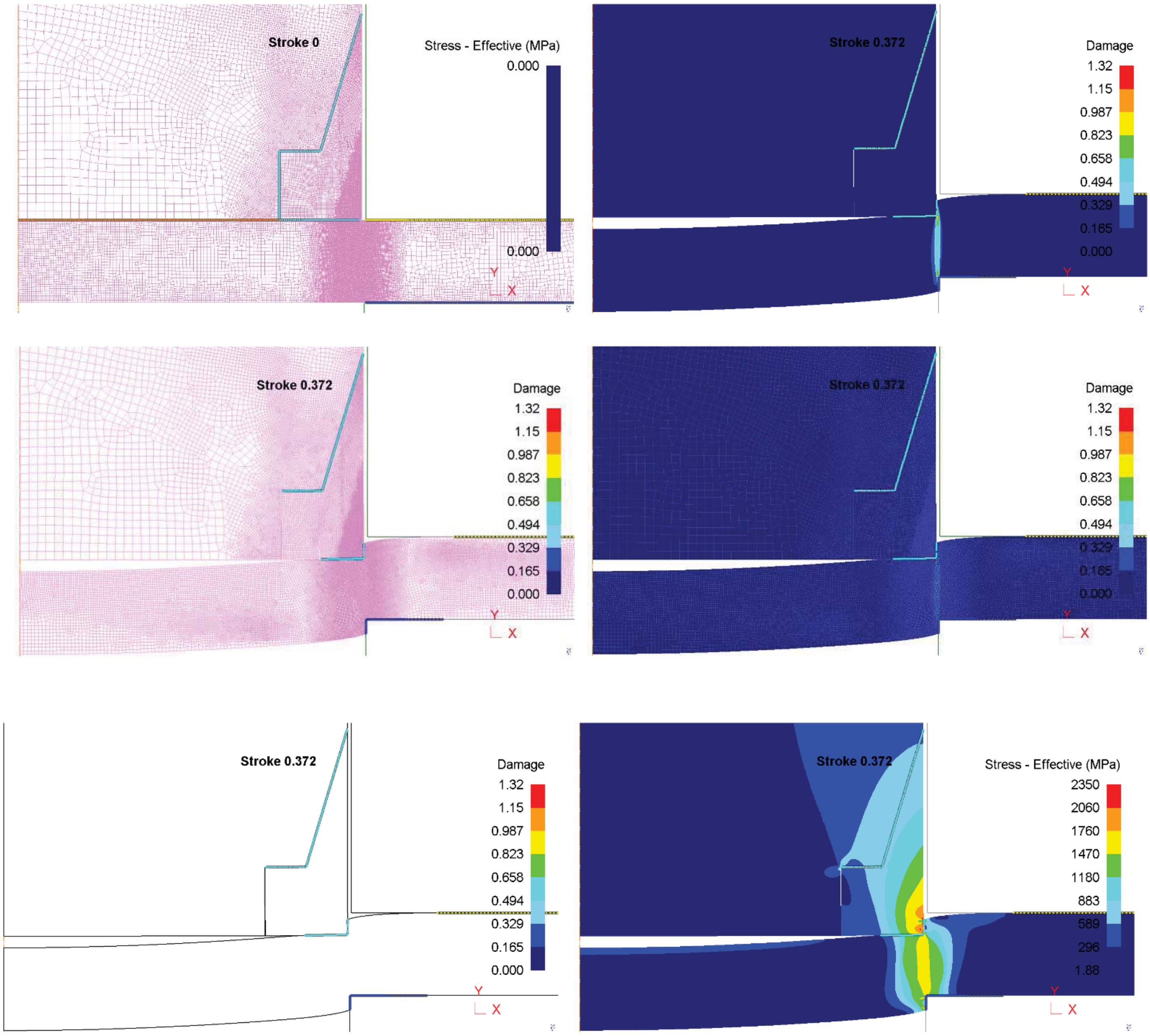

12. Round-edge type

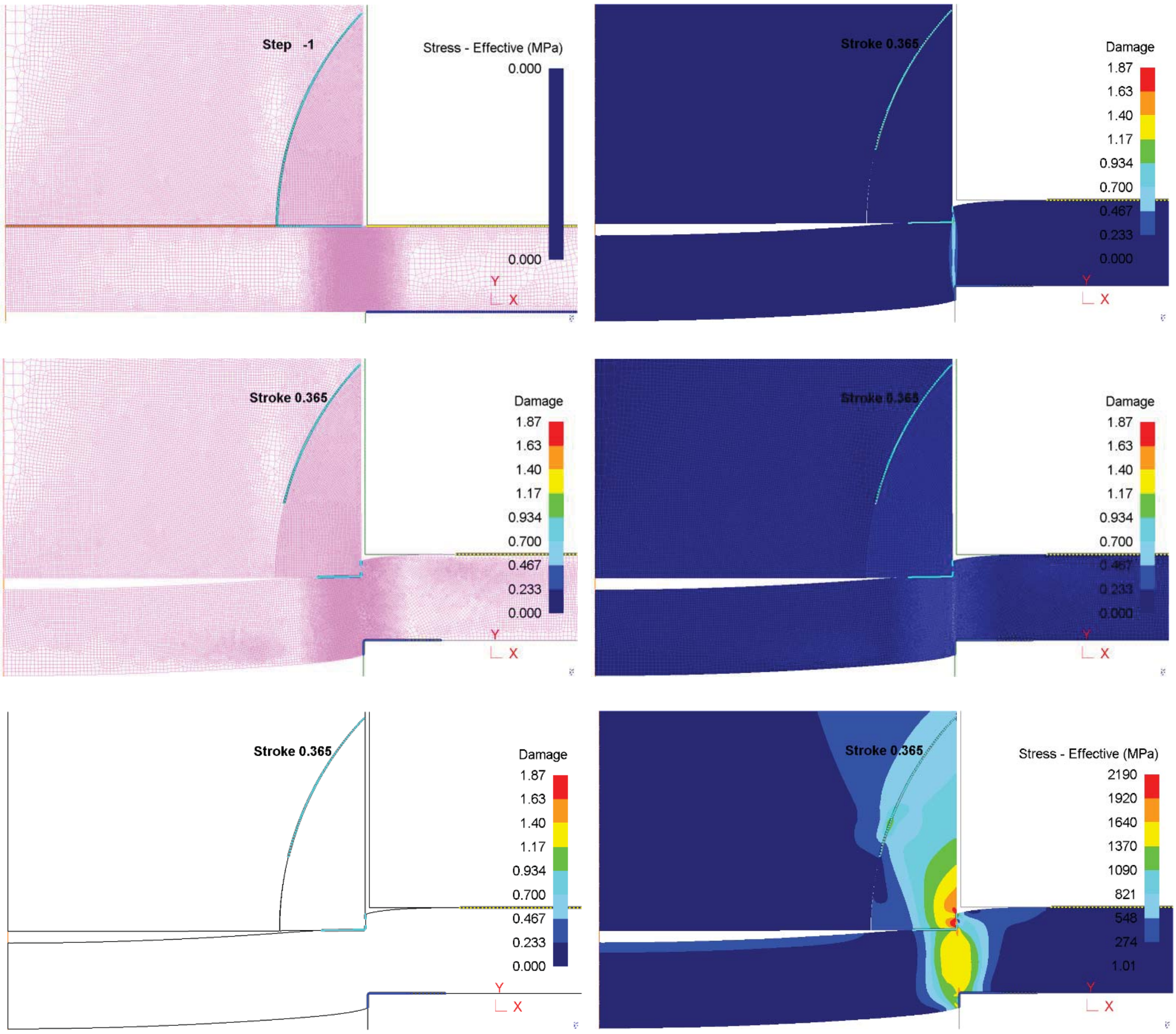

13. Inverse-ladder type

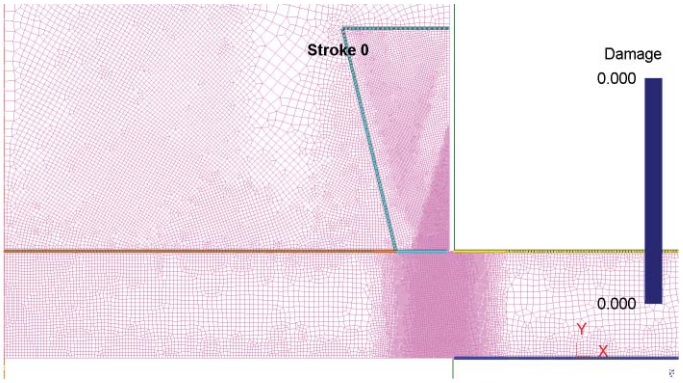

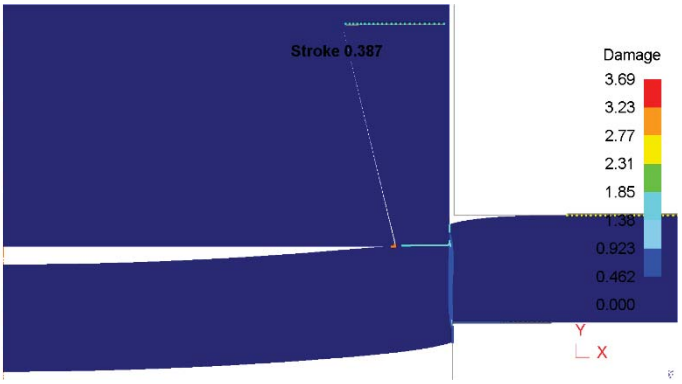

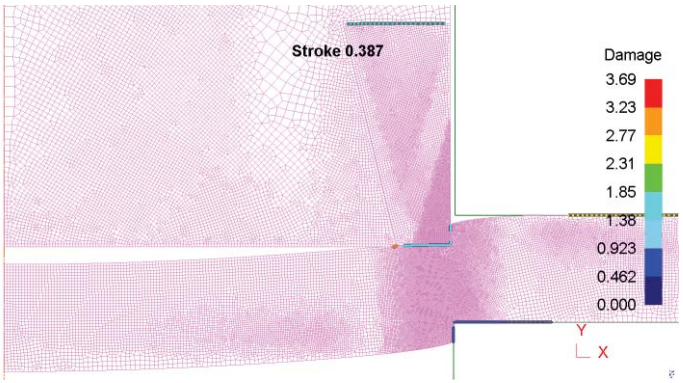

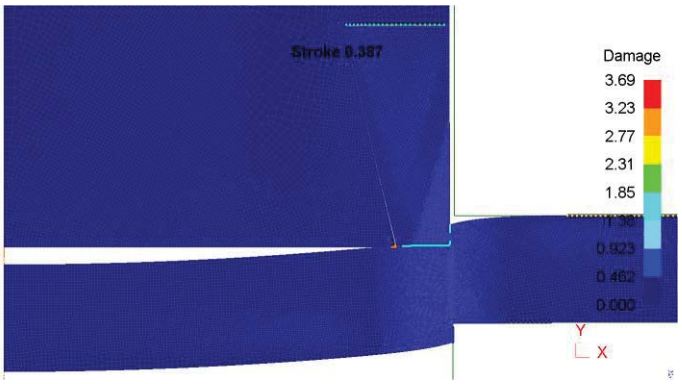

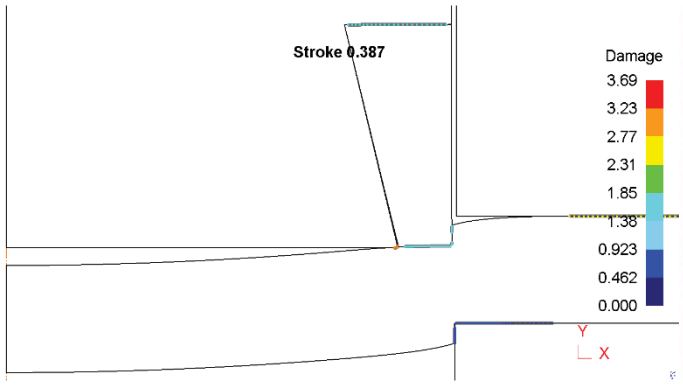

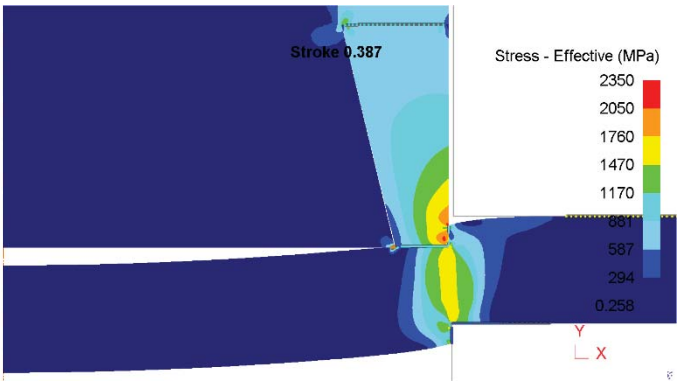

14. Inverse-round ladder type

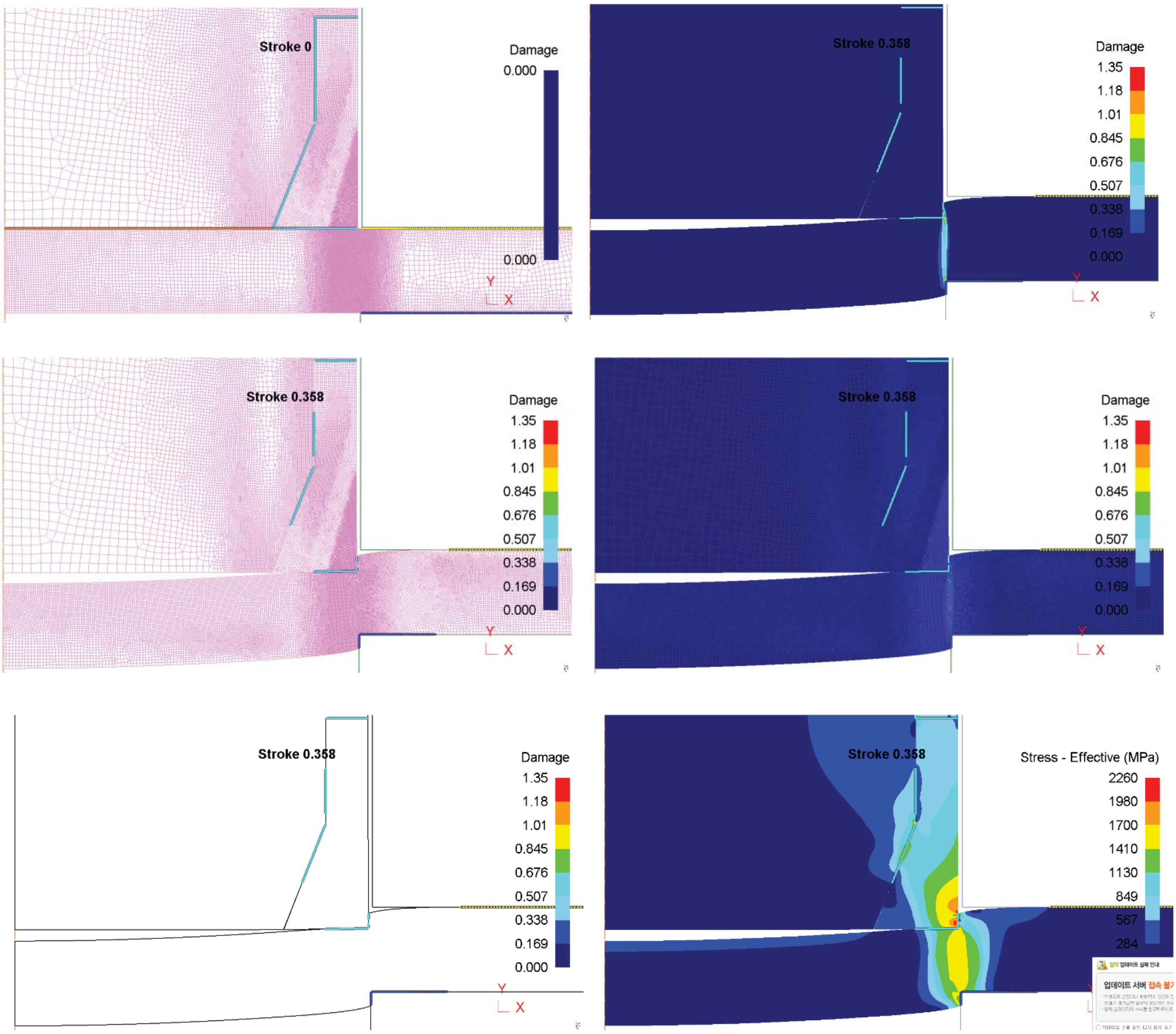

15. Top triangle-round-edge type

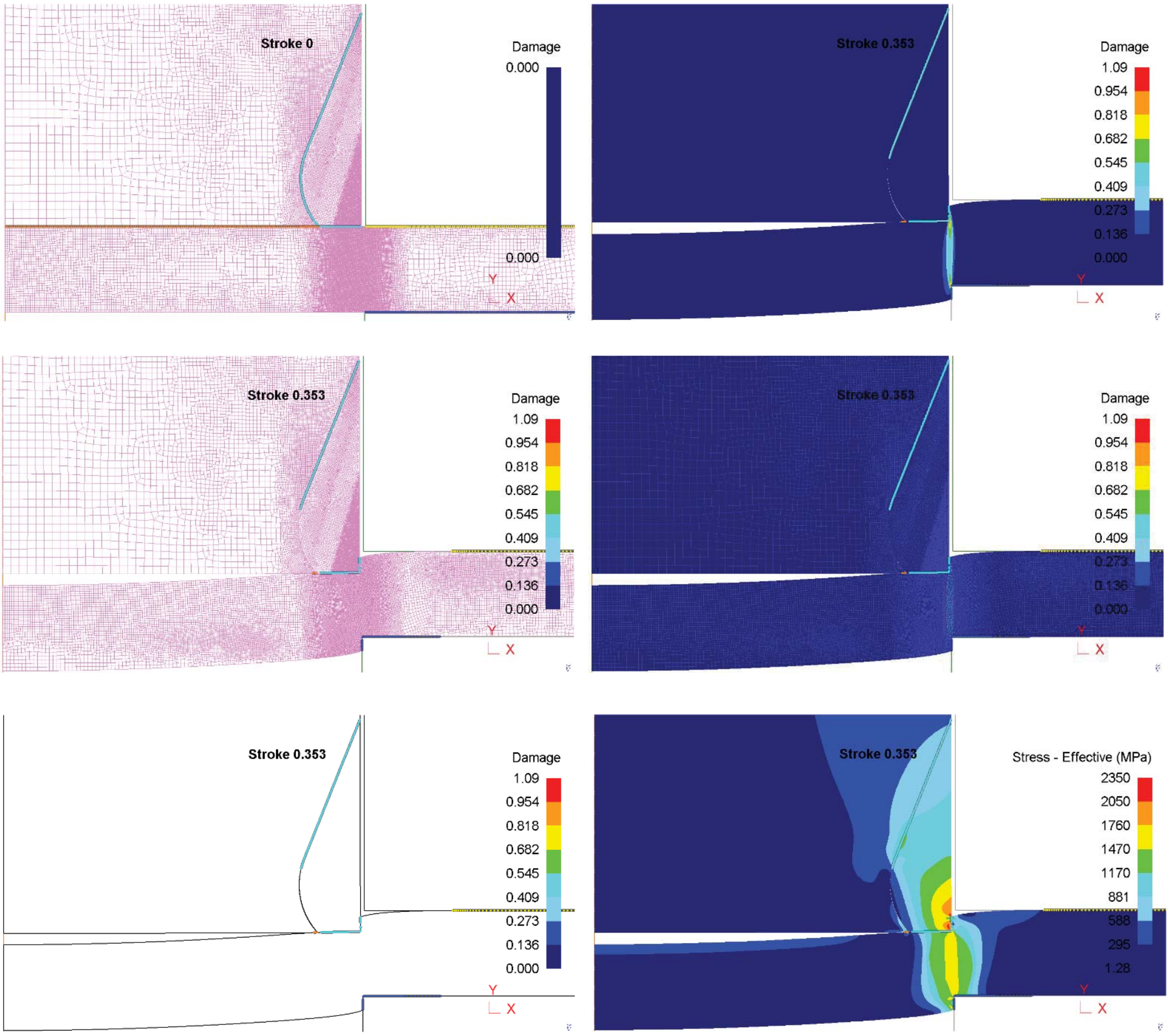

16. Top square-edge type

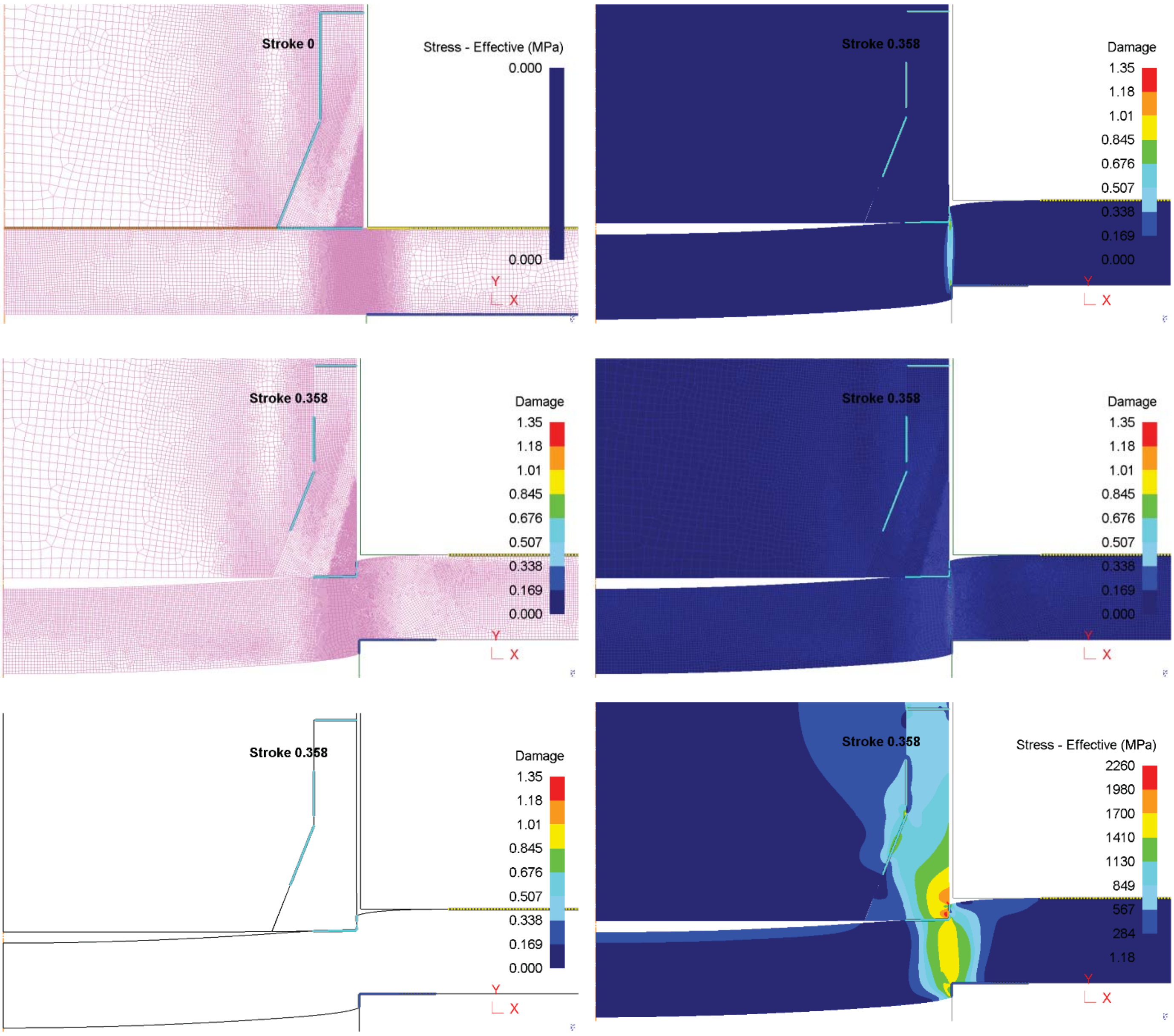

17. Regular triangle-edge type

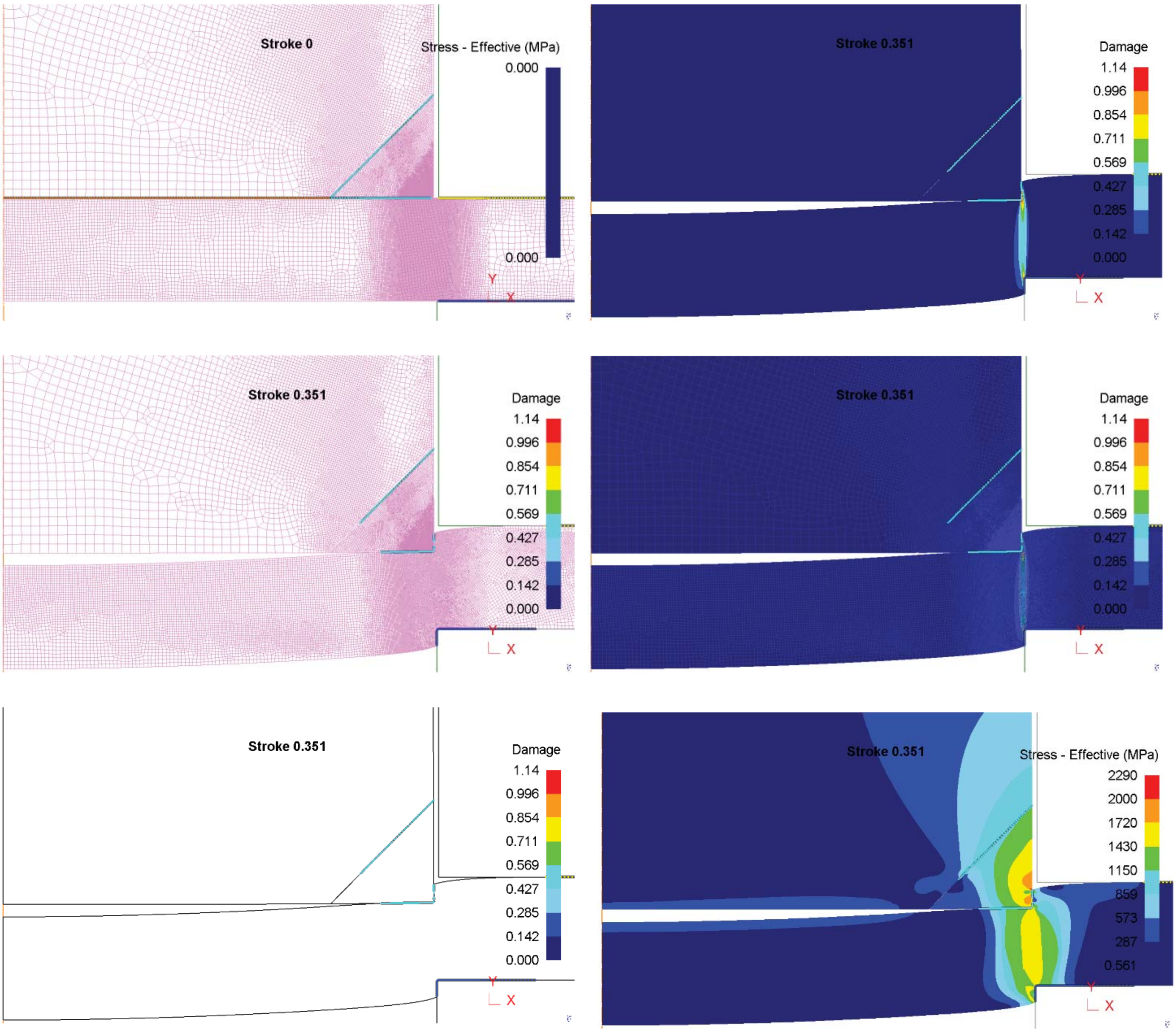

18. Sector edge type

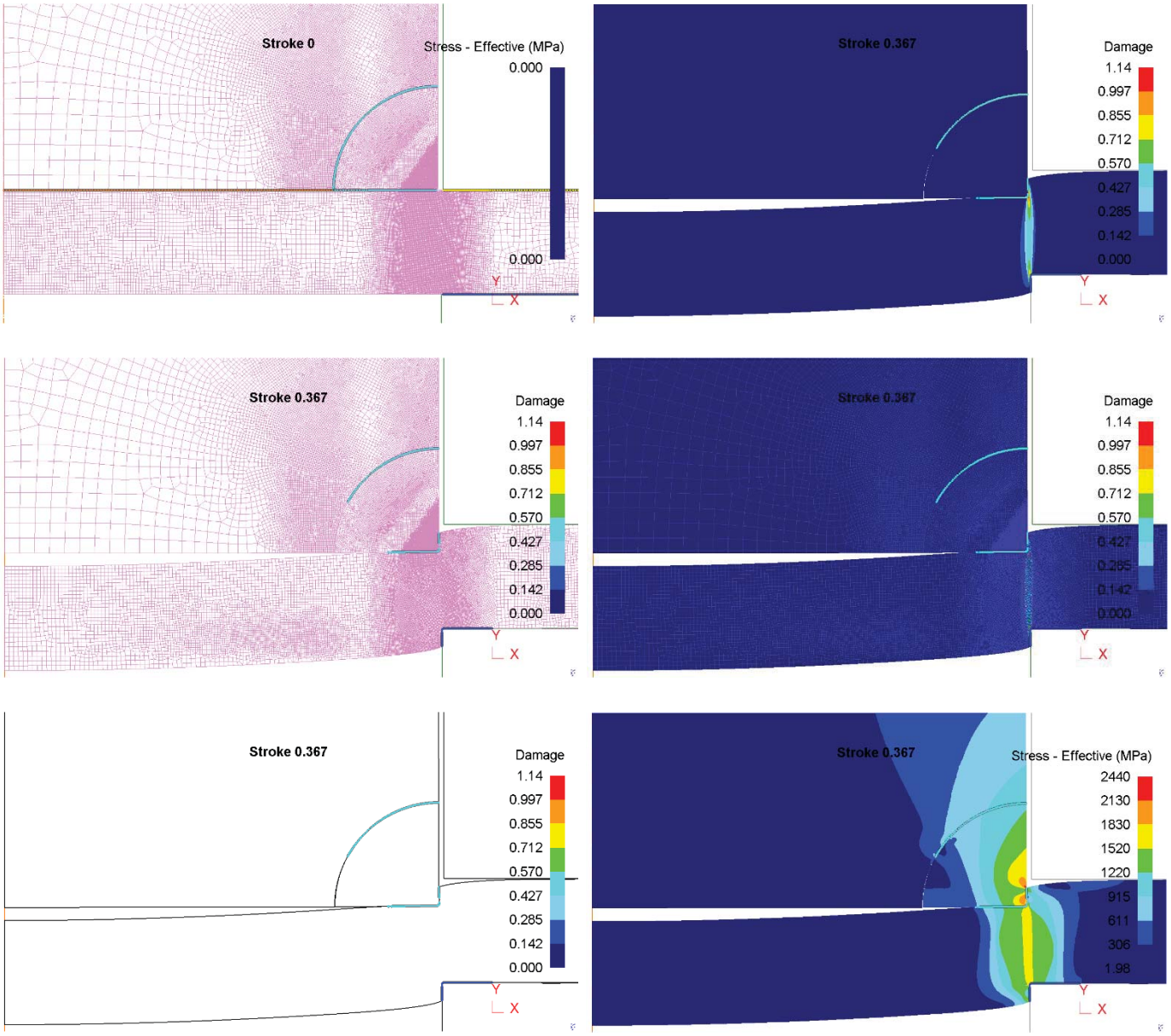

19. Gull shape-edge type

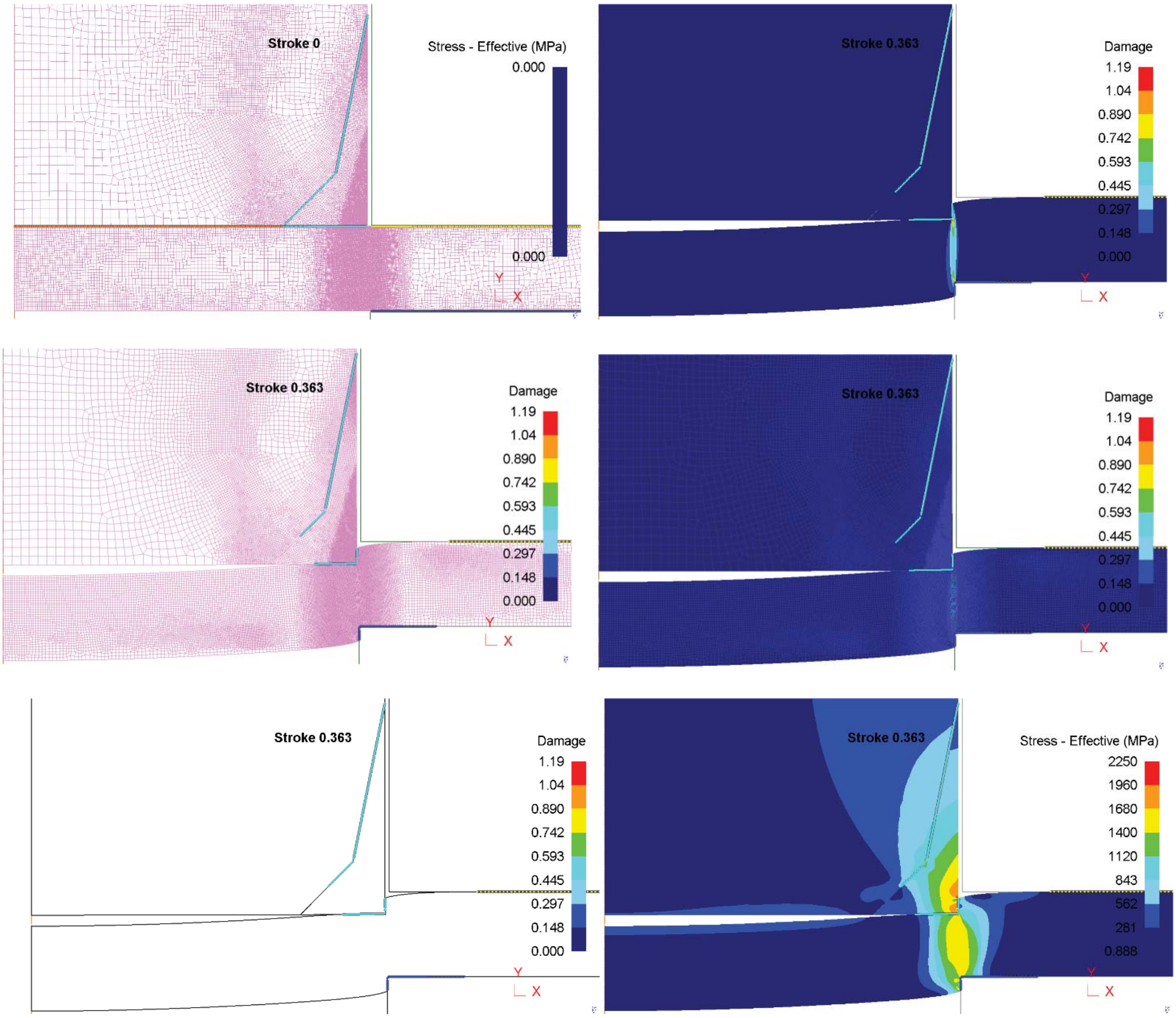

20. Top triangle-bottom ladder type

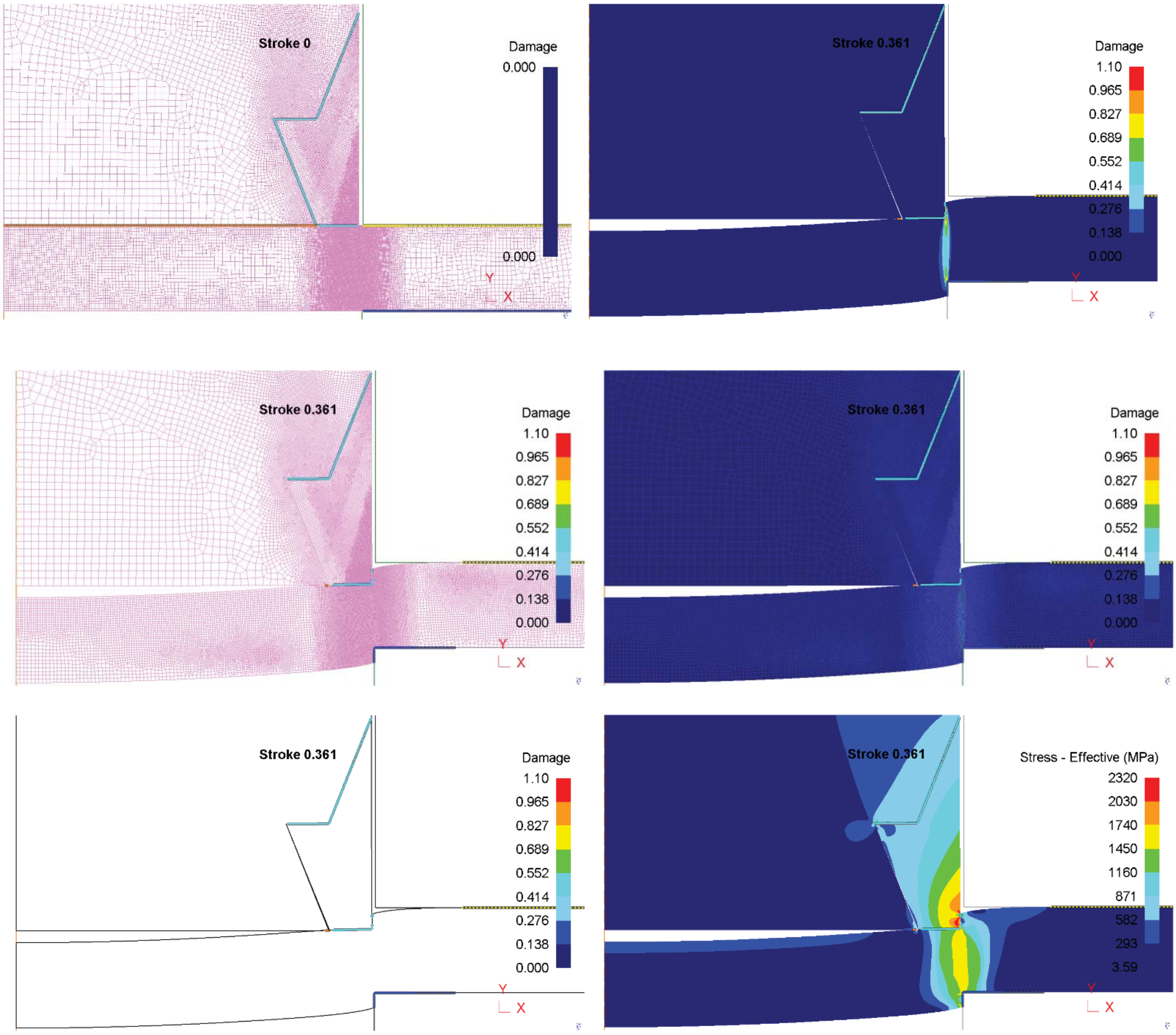

CONFERENCES

1. **KSME ULSAN2018; A Study on the Optimization of Punch Edges Shape for Enhancing Functional Part of Piercing Punc h**

2. **ICMT 2018; A Study on Analytical Selection of the Semi-Add itive Range and Shape for Piercing-Punch Strengthening**

3. **KSME 2019; A Study on Improvement of Mechanical Toughn ess of High Alloy Tool Steel Powder Using Multi-layer AM T echnology of Heterogeneous materials**

JOURNAL

1. A Study on the Range Prediction and Optimization of Punch Edge Shape for Enhancing Piercing Punches Using 3D Printing AM Technology and the Partial Semi-Additive Method, Journal of Mechanical Science and Technology, 1738-494X (Print) 1976-3824 (Online), under review.

LIST OF PROJECT

번호	과제명	사업명	연구기간	참여기관
1	3D 프린팅 기법을 이용한 자동차 초고강도부품(1500MPa)용 컷팅 프로세스 및 핫스템핑 금형개발 기초연구	지역신산업선도 인력양성사업	2018.03.01 ~2019.08.31	엠디티㈜

KSME

우 수 논 문 상

논문제목 : A Study on Improvement of Mechanical Toughness of High Alloy Tool Steel Powder Using Multi-lay AM Technology of Heterogeneous Materials

저 자 : Shiliang Wang*, Yong Seok Kim, Tian Gou, Young Jin Yum(울산대), Won Jun Kim(MDT Co.), Soon Yong Yang(울산대)

대한기계학회 재료 및 파괴부문 2019년도 춘계학술대회에서 발표한 위 논문은 연구주체의 독창성은 물론이고 연구 내용도 우수하여, 학문과 기술의 발전에 크게 기여할 것으로 사료되어 재료 및 파괴부문(회장 : 장윤석)의 추천에 따라 우수논문상 수상논문으로 결정하고 포상합니다.

2019년 4월 12일

대한기계학회 회장 박 찬 일